MAGNETOHYDRODYNAMICS OF TURBULENT ACCRETION DISCS AROUND BLACK
HOLES

by

RALPH EGON PUDRITZ

B.Sc., University of British Columbia, 1973
M.Sc., University of Toronto, 1975

A THESIS SUBMITTED IN PARTIAL FULFILLMENT OF
THE REQUIREMENTS FOR THE DEGREE OF
DOCTOR OF PHILOSOPHY

in

THE FACULTY OF GRADUATE STUDIES
(Department of Physics)

We accept this thesis as conforming
to the required standard

The University of British Columbia

December, 1979

In presenting this thesis in partial fulfilment of the requirements for an advanced degree at the University of British Columbia, I agree that the Library shall make it freely available for reference and study. I further agree that permission for extensive copying of this thesis for scholarly purposes may be granted by the Head of my Department or by his representatives. It is understood that copying or publication of this thesis for financial gain shall not be allowed without my written permission.

Department of _____PHYSICS_____

The University of British Columbia
2075 Wesbrook Place
Vancouver, Canada
V6T 1W5

Date __DEC 19 / 1979__

Abstract

The Cyg X-1 X-ray source is believed to be comprised of an accretion disc around a central black hole. We apply the methods of Mean Field Electrodynamics to the study of magnetic processes in such an accretion disc.

By decomposing the magnetic field in the disc into mean and fluctuating components, the observed X-ray properties of this system may be accounted for.

It is found that intense, short lived magnetic fluctuations may occur which give rise to solar-like flares on the surfaces of the accretion disc. The energy releases and time scales of such flares is found to provide a physical basis for the observed shot-noise like character of the X-ray emission from the system.

It is demonstrated that a rather strong, large scale magnetic field can be generated by turbulent dynamo action in the accretion disc. This result is the reason why magnetic fields may play a vital role in these systems. The long time averaged structure of the accretion disc is determined by the Maxwell-stress due to the mean field, and is in agreement with the "standard" cool accretion disc models.

We prove that on intermediate time and length scales, the Maxwell stresses due to the magnetic fluctuations remove the known instability of "standard" accretion disc models to ring-

like "clumping" and subsequent heating of the gas. This result shows that the hard X-ray emission of the Cyg X-1 source must arise from either a hot corona, or intense solar-type flares above the disc surfaces. If the hard X-ray emission arises from non-thermal electron populations accelerated in the flares, it is found that this emission must occur in a rapid "flash-phase" on submillisecond time scales. These flares occur well away from the inner disc boundaries so that we believe that submillisecond variations of the Cyg X-1 source need not be a test of the rotation of the central black hole.

Table Of Contents

List Of Tables

List Of Figures

Acknowledgement

First and foremost, I would like to express my most heartfelt gratitude to my supervisor, Prof. G. G. Fahlman. His fine physical intuition , his encouragement, and his emphasis on getting as close to the physical observations as the theory allows have all gone to make my work as his student a rewarding experience. I wish to thank him for all that he has done for me, and to express my deep respect for his scientific ability and his personal qualities.

I wish to thank my former supervisor Prof. M.H.L Pryce for so many different things. Conversation with him led me to work on accretion problems. His financial support aided me for the first two years of this work and discussions with him saved me from making some idiotic errors.

I thank Dr. John Gilliland for many stimulating conversations about dynamo theory and for introducing me to so many books and articles on the subject. This interaction saved me much thrashing about. I thank him for valuable comments on the first draft of this work.

I thank the staff and students of the Department of Geophysics and Astronomy, where most of this work was carried out, for their hospitality and friendship. In particular, I thank Dr. Serge Pineault and John Davies for many interesting discussions, and Prof. J. Auman for valuable considerations

about flare models.

I am particularly grateful to Patricia Monger for her help with the actual physical production of this thesis.

Finally, I acknowlege an NRC Postgraduate Scholarship on which two years of the work was carried out and a research assistantship from Prof. Fahlman over the last six month period.

List Of Symbols

Hydrodynamics

$\tilde{u}$ — Root mean square velocity fluctuation

c_s — Speed of sound

M_x — Mass of central compact object associated with X-ray source

$\dot{M}$ — Mass transfer rate to accretion disc

M_t — Turbulent Mach number

$V_k = (GM_x/r)^{1/2}$ — Keplerian speed (toroidal)

$R = V_k r/\nu > 10^8$ — Reynolds number

$t_k = r/V_k$ — Keplerian time scale

$t_D = r/U^r$ — Radial drift time scale

τ_u — Correlation time for turbulent eddies

Σ — Surface density (vertically averaged gas density)

$W^{r\phi}$ — Vertically averaged component of stress tensor giving rise to outward radial transport of angular momentum in an accretion disc

z_0 — Half-thickness of accretion disc

Magnetohydrodynamics

$\tilde{b}$ — Root mean square magnetic fluctuation

$\underline{\xi} = \overline{\underline{u}' \times \underline{b}'}$ — Mean EMF arising from correlation of fluctuating velocity and magnetic fields

α — Pseudoscalar arising in non-mirror symmetric turbulence and which gives rise to regeneration of the mean magnetic field

η_T — Turbulent diffusivity for mean magnetic field

η Ambient diffusivity for magnetic field

$\eta_T/\eta \gg 1$ High conductivity limit

$R_M = V_k r/\eta \sim 10^{10}$ Magnetic Reynolds number

$\gamma = \alpha/z\eta_T$ Ratio of regeneration due to dynamic action to dissipation for mean poloidal magnetic field

$\chi = V_k/r\eta_T$ Ratio of regeneration due to differential rotation to dissipation for mean toroidal magnetic field (Chap. 3)

$\beta = (\gamma/\chi)^{1/2}$ Measure of dynamo action to differential rotation (Chap. 3)

$\hat{r} = (\gamma\chi)^{1/4} r$ Dimensionless radial co-ordinate (Chap. 3)

$\hat{z} = (\gamma\chi)^{1/4} z$ Dimensionless vertical co-ordinate (Chap. 3)

$K^{1/2} \ll 1$ Dimensionless radial wavenumber for mean field modes (Chap. 3)

$\lambda = |\hat{z}|^{4/3}$ Dimensionless parameter; large when $M_t \ll 1$ and $|z| \sim z_0$

Σ^{ij} Maxwell stress due to mean magnetic field

$\overline{\sigma^{ij}}$ Maxwell stress due to auto-correlation of fluctuating magnetic fields

Chapter 1

Introduction

1. Observations Of X-ray Sources Associated With Binary Stellar Systems

Since the discovery of the first galactic X-ray source by Giaconi et al (1962), intensive observational and theoretical effort has brought us to the point where strong arguments can be made for the existence of a black hole. Many of these X-ray sources can be accounted for in terms of a hot gas spiralling into a white dwarf, neutron star, and in one case (the Cyg X-1 source), a black hole. These objects are themselves in close proximity to a more normal type of star.

This thesis analyzes the magnetohydrodynamics of a turbulent disc of hot gas (the so-called "accretion disc") around a central black hole. It is the contribution of this work to apply the methods of mean field electrodynamics (see Roberts (1971) and Moffat (1978) for reviews of this theory) to this problem. We intend to show that if the magnetic field in a turbulent accretion disc is regarded as having large-scale mean, and microscale fluctuating components; then the observed rapid variability of the X-ray output of the Cyg X-1 source can be explained in terms of solar-type flares arising from intense magnetic fluctuations and that the overall

structure of the accretion disc is controlled by the large-scale mean magnetic field. Other authors have concentrated only on the study of chaotic magnetic fields. Using our approach, it is shown that a large-scale mean magnetic field can be generated by turbulent dynamo action in the accretion disc and that an intimate connection exists between the mean and fluctuating magnetic fields. These types of results are not new to the theory of mean field electrodynamics, however, to our knowledge, they have never been considered within the physical framework of a turbulent accretion disc. It is our contention that the possibility of dynamo action in such a system makes the magnetic field a crucial element in the interpretation of the Cyg X-1 observations.

A more detailed outline of the thesis is presented in the last section of this chapter. The observations of the Cyg X-1 source are discussed in the remainder of this section. Section 2 outlines the basic physics of an accretion disc and how the gross observational features can be accounted for. Section 3 reviews previous work done on magnetic fields in accretion discs while section 4 presents ideas which motivated our own work.

The first important feature of these sources is their enormous power output, which for the Cyg X-1 source is of order 10^{37} erg s^{-1} which is ten thousand times the power of the sun.

There appears to be an upper limit of 10^{38} erg s^{-1} for the known sources. This is a suggestive observation because this is of the order of the "Eddington limit" of luminosity L_{cr} for an object of mass M (measuring M in units of solar mass $M_{\odot}$)

$$L_{cr} \simeq 10^{38} \left(M/M_{\odot} \right) \; erg \; s^{-1} \qquad (1.1)$$

which corresponds to the condition wherein the radiation pressure exerted on a gas equals the gravitational force of the object. We say more about this in section 2.

Of the nine optically identified X-ray sources, seven are known to be spectroscopic binaries. The fact that X-ray sources are members of binary systems provides a very important handle on the system, that is, its mass. The detailed analysis of mass determination for the observed star M_{obs} and of the unseen companion M_X is reviewed in Bahcall (1978). The allowed ranges of the masses M_X associated with the X-ray sources are listed in Table 1 (adapted from Bahcall (1978)).

Table 1. Masses M_X Associated With X-ray Sources

SOURCE	M_X (SOLAR MASS UNITS)
Vela XR-I	$1.0 \leqslant M_X \leqslant 3.4$
SMC X-I	$0.5 \leqslant M_X \leqslant 1.8$
Cen X-3	$0.7 \leqslant M_X \leqslant 4.4$
Her X-I	$0.4 \leqslant M_X \leqslant 2.2$
3U 1700-37	$0.6 \leqslant M_X$
Cyg X-I	$9 \leqslant M_X \leqslant 15$

The Cyg X-1 source stands out because of its high mass $M_X \geqslant 9 M_\odot$. The visible in this system is an OB supergiant with mass in the range 15-25 $M_\odot$, having an optical magnitude of 9. The binary period of the system is 5.6 days. The visible star varies by 0.07 magnitudes with a double peaked light curve which is evidence for tidal distortion since a tidally distorted star would present a changing area and hence an apparently changing luminosity with a frequency of twice the orbital-revolution frequency. A comprehensive discussion of the optical observations of the Cyg X-1 source may be found in

Bolton (1975).

We shall henceforth be considering only the Cyg X-1 source, and turn to a summary of the X-ray observations of this source.

X-ray Observations Of Cyg X-1.

This source, discovered by Boyer et al (1965) has a hard X-ray spectrum and is highly variable at all X-ray energies.

(1) X-ray Spectrum.

The Uhuru satellite observations in the 2-10 kev range have been extended into the 15-250 kev range by the OSO 8 satellite (see Dolan et al (1979)). One of the most intriguing aspects of the spectrum is that it undergoes transitions between two states: a high luminosity state with

$$L_{high} \approx 5.5 \times 10^{37} \; erg \; s^{-1}$$

and a low luminosity state with

$$L_{low} \approx 3.3 \times 10^{37} \; erg \; s^{-1}$$

assuming that the distance to the source is 2.5 kpc. The high state has an excess of energy in the 2-7 kev band and a lower amount of energy in the >7 kev domain as compared to the low state. Thus, a high to low transition was apparent in the Uhuru observations during March-April 1971 (see Sanford et al (1975)), while Dolan et al (1979) find a low to high transition occurring in Nov 1975.

Dolan et al find that over the 20-150 kev range of the X-

ray spectrum a power law of the form

$$\frac{dN}{dE} = C\left(E/E_0\right)^{-\delta} \text{ photons } cm^{-2} \ s^{-1} \ kev^{-1} \tag{1.2}$$

could be fitted.

They state that the spectra may all be represented by a single power law expression whose spectral index is different for the two intensity states. Their high state spectrum is reproduced in Fig. 1 while Fig. 2 shows five low state spectra they took. The best fit single power law parameters , over the 20-150 kev range are

low :

$\delta \approx 1.83 \pm 0.06$

$E_0 = 32.5 \ kev$

$C = 8.69 \pm 0.57$

high :

$\delta \approx 2.21 \pm 0.18$

$E_0 = 23.8 \ kev$ $\left(1.3\right)$

$C = 6.80 \pm 0.97$

Fig. 1 X-ray Spectrum Of Cyg X-1: High State (From Dolan Et Al (1979))
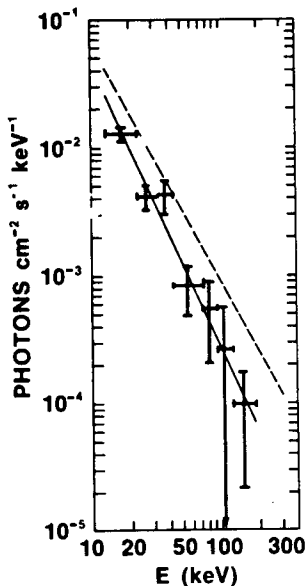
—Spectrum of Cyg XR-1 observed 1975 November 17, 0200 UT–1530 UT ($\Phi = 0.40$–0.50), when the source was in a high state. The values of α, C, and E_0 of the power law which best represents the data are given in Table 2; the power law is shown in the figure as the solid line. The dashed line is the power law which best represents the low-state spectrum shown in Fig. 2d.

Fig. 2 X-ray Spectrum Of Cyg X-1: Low State (From Dolan Et Al (1979)).
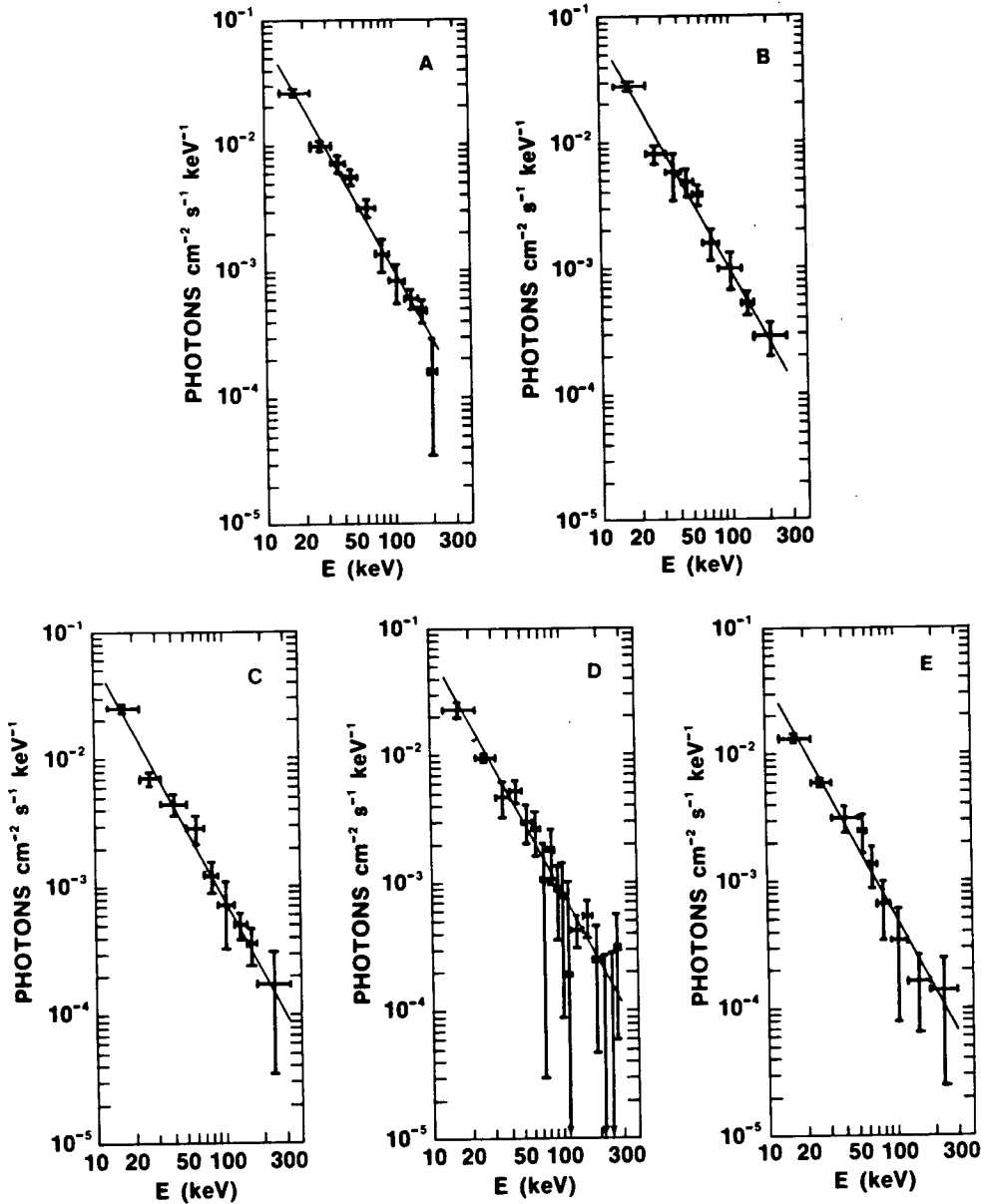
—Typical spectra of Cyg XR-1 observed by *OSO 8* when the source was in a low state as defined at lower energies. The straight line in each spectrum is the single power-law expression which gives an acceptable minimum χ^2 distribution about the observed intensities. The resultant values of α, C, and E_0 for each spectrum, as defined in eq. (1), are given in Table 2. (*a*) Spectrum observed 1977 November 13, 1050 UT–November 14, 0015 UT ($\Phi = 0.30$–0.40). (*b*) Spectrum observed 1977 October 22, 0115 UT–1445 UT ($\Phi = 0.30$–0.40). (*c*) Spectrum observed 1976, November 11, 1630 UT–November 12, 0600 UT ($\Phi = 0.80$–0.90). (*d*) Spectrum observed 1976 November 10, 0000 UT–1330 UT ($\Phi = 0.50$–0.60). (*e*) Spectrum observed 1975 November 14, 2000 UT–November 15, 0930 UT ($\Phi = 0.00$–0.10).

It is important to note that Dolan et al find that about one third of their spectra could also be well represented by a double power law in the 20-150 kev range with an increase in the spectral index of 0.5 or larger. The break-point between the two power laws occurred between 40 and 125 kev for different spectra.

Finally, Dolan et al considering their highest energy data points find evidence for an exponential cut-off in the spectra of both states somewhere between 150 and 200 kev.

The system seems to spend most of its time in the low state.

(2) Short Term X-ray Variability

For time profiles over the 1-50 kev range , the qualitative appearance is characterized by a continual aperiodic train of spiky variations with pulse sizes ranging up to a few times the average intensity on time scales of a fraction of a second (see Oda (1977) for a review).

As Oda points out, it appears that the pulses are a characteristic of the low state (greater predominance of hard X-ray component) and seems to get buried to some degree in soft X-ray emission during periods when the source is in the high state. This is a key point and is considered again in Chapter 4.

Terrell (1972) successfully simulated the time profile over periods of fractions to tens of seconds in terms of a

<u>shot</u> <u>noise</u> model comprised of a superposition of randomly occurring pulses (instantaneous rise and exponential decay) of constant amplitude and with characteristic times of fractions of a second.

In addition to the variations discussed Oda et al (1971) and Rotschild et al (1974) found evidence for millisecond bursts, which appear to occur in bunches. The energy of these bursts appears to be lower than the overall emission. The reality of these millisecond bursts has been questioned by Weisskopf and Sutherland (1978) who find that "spurious" millisecond bursts may arise as an artifact of the data analysis and may have nothing to do with the physical processes associated with the X-ray source.

We summarize the shot noise and millisecond burst parameters in Table 2 (see Rotschild et al (1977)).

Table 2. Summary Of Shot Noise And Millisecond Burst

Parameters

EVENT TYPE	SHOT NOISE	MILLISECOND BURST
ENERGY/EVENT	10^{36} ergs	10^{35} ergs
CHARACTERISTIC TIME	10^{-1} s	10^{-3} s
EVENTS/SECOND	8 s^{-1}	100 s^{-1}

The simplest explanation of the Cyg X-1 source is that of an accretion disc about a black hole of mass $M_X \approx 10 M_\odot$ with accretion rates of 10^{-9} $M_\odot yr^{-1}$ arising from mass outflow (Roche lobe overflow) from the visible star (see Bolton (1975)). The reader may consult Kellogg (1975) for a discussion of the viability of alternate models.

Henceforth, we shall only be considering these accretion disc models for the Cyg X-1 source.

2. The Basic Physics Of Accretion Discs

The observations suggest that the visible star is tidally distorted. This leads us to consider matter loss from the star

by Roche-lobe overflow.

We generate the so-called Roche equipotentials by going into the rotating frame of the binary system and drawing equipotentials of the gravitational and centrifugal potentials. Consider the case when the lower mass object M_X is compact and the larger mass star M_{obs} expands to fill its Roche-lobe (see Fig. 3). Matter may then leave its surface at the point of "zero gravity" (the inner Lagrangian point L_1) and flow over toward M_X. Such a gas stream will pick up angular momentum via the Coriolis forces and go into orbit around M_X rather than falling directly in (see numerical calculations of Flannery (1975) for a detailed examination of the hydrodynamics). The matter stream and the orbiting gas will stay in the orbital plane of the binary system. Viscosity of the gas will lead to the gradual spiralling of the gas in towards the central object M_X, thereby forming the so-called accretion disc.

Fig. 3 Mass Accretion By Roche Lobe Overflow (From Novikov And Thorne (1973))
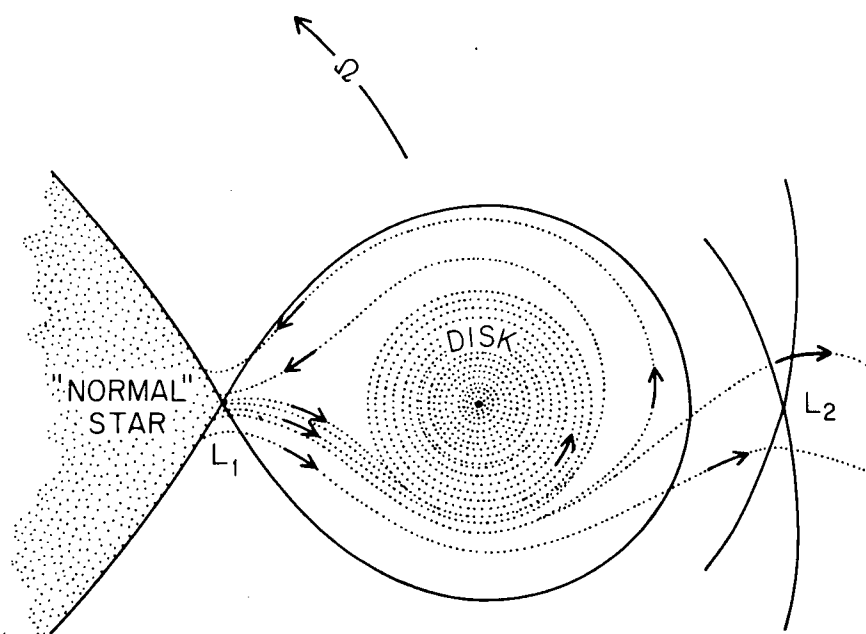
The basic physics of an accretion disc around a compact object was worked out by Prendergast (1960), Lynden-Bell (1969), Pringle and Rees (1972), and Shakura and Sunyaev (1973), and comprises the "standard model" of accretion discs.

Relativistic corrections are reviewed by Novikov and Thorne (1972).

The particles of an accretion disc moving in approximately Keplerian orbits about the central compact object, lose their angular momentum due to friction between adjacent rings of gas. These particles therefore gradually spiral towards the central object releasing gravitational potential energy. Part of this energy increases the kinetic energy of rotation so that at every radius the velocity is Keplerian to good approximation, and the other part is converted into thermal energy by the viscosity and subsequently radiated from the disc surface. The angular momentum is transported out to the outermost portion of the disc with the result that some of the matter arriving in the mass stream is flung away from the disc and escapes the system. For Cyg X-1, the outer radius of the disc is of order 5×10^5 km.

The angular momentum transport is provided by either the turbulence, the magnetic field (present in the matter that streams to the disc), or both. Modelling these stresses is one of the most important aspects of accretion disc theory, although for stationary discs, many of the basic observed properties of the system are independent of such models.

The action of the turbulent (Reynolds) stress and/or the magnetic (Maxwell) stress gives rise to a small inward

radial velocity by which matter matter slowly drifts into the inner regions of the disc. In the case where the central compact object is a black hole, general relativistic considerations show that the innermost stable, Keplerian-like orbit that can occur for a particle in orbit about a non-rotating hole occurs at

$$r_i = 3\, r_j = 6\, \frac{GM_x}{c^2}$$

where r_j is the Schwarzschild radius for a black hole of mass M_x. Matter will drop staight into the hole once it reaches this inner orbit. This radial infall from r_i to the event horizon will not liberate much energy in the form of heat. The Schwarzschild radius for $M=10 M_\odot$ is 30 km so the inner edge of the accretion disc is at 90 km. Keplerian orbital speeds at this innermost radius will be 1.0×10^{10} cm s^{-1} $\approx$ 1/3 c. General relativistic corrections to the flows are important only at this inner edge, and Newtonian gravity can be assumed in the disc to good approximation. For a rotating (Kerr) black hole, the innermost possible stable orbit is at the event horizon which for $M=10 M_\odot$ is at 15 km in this case.

The gravitational potential energy liberated as the particles traverse ever smaller orbits about the hole will be the binding enery in the last stable orbit. Hence, one expects energy releases of 0.057 mc^2 for the non-rotating case and 0.40 mc^2 for the rotating one. Thus, energy releases per

nucleon in an accretion disc about a central black hole rival or exceed (Kerr case) the efficiencies found in nuclear reactions.

The fluid picture of the gas is adopted which is described by the continuity equation, the conservation of angular momentum (Navier Stokes equations) and conservation of energy, where axial symmetry is assumed and cylindrical polar co-ordinates are employed.

If stationary conditions are assumed ($\partial/\partial t = 0$) one finds that most of the important disc properties are independent of a detailed model for the stress.

The continuity equation links the mass transfer through each annulus of given radius to the mass flow $\dot{M}$ (constant) arriving at the disc from the visible star. Thus, under stationary conditions,

$$\dot{M} = 2\pi \Sigma U^r r \qquad (1.4)$$

where Σ is the "surface density"

$$\Sigma \equiv \int_{-z_0}^{z_0} \rho(z) \, dz$$

with z_0 the half-thickness of the disc, and U^r the radial velocity.

For future reference, the vertical average of any quantity ψ is denoted $\langle \psi \rangle$ where

$$\langle \psi \rangle \equiv \int_{-z_0}^{z_0} \psi \, dz$$

Hydrostatic equilibrium between the z-component of the central object's gravitational force and the gas pressure $p = \rho c_s^2$ gives

$$\frac{z_o}{r} \approx \frac{c_s}{u^\phi} \tag{1.5}$$

where c_s is the sound speed and the toroidal velocity u^ϕ is Keplerian to good approximation.

$$u^\phi \approx V_K = \left(G M_x / r \right)^{\frac{1}{2}} \equiv \Omega_K \, r \tag{1.6}$$

We note that the self gravitation of the matter in the disc is negligible. Equation 1.5 shows that a thin disc ($z_o/r \ll 1$) implies the dominance of the Keplerian velocity in the problem.

The radial component of the Navier-Stokes equation (vertically averaged) gives, under stationary conditions

$$\Sigma \, u^r \frac{\partial}{\partial r} \left(u^\phi r \right) = -\frac{1}{r} \frac{\partial}{\partial r} \left(W^{r\phi} r^2 \right) \tag{1.7}$$

where $W^{r\phi}$ is the vertically averaged stress due to turbulence and/or magnetic fields. Application of 1.4 to this result gives,

$$W^{r\phi} = -\frac{\dot{M} \Omega_K}{2\pi} \left(1 - (r_i/r)^{\frac{1}{2}} \right) \tag{1.8}$$

where the boundary condition

$$W^{r\phi} \approx 0 \quad \text{at} \quad r = r_i$$

has been used. This condition insures that particles will drop

radially into the hole for $r<r_i$. Hence, the stress $W^{r\phi}$ has been determined independently of some prescribed 'viscosity' mechanism.

From the conservation of energy, we find that the energy flux per unit area is equal to the energy production by the shear stress $W^{r\phi}$. Thus after the vertical average is taken, we have

$$Q = \frac{W^{r\phi}}{2} \left(\nabla \underline{u} \right)_{r\phi} = -\frac{3}{4} \Omega_k W^{r\phi} \qquad (1.9)$$

where Q is the energy flux per unit surface area. From 1.8 we have

$$Q = \frac{3}{8\pi} \dot{M} \frac{G M_x}{r^3} \left(1 - (r_i/r)^{\frac{1}{2}} \right) \qquad (1.10)$$

which shows that a maximal energy flux is occurring at

$$r_Q = 1.36 \, r_i \approx 122 \, km$$

The total energy release is then

$$L = \int (4\pi r) \, Q(r) \, dr \approx \frac{1}{2} \frac{G M_x \dot{M}}{r_i} \qquad (1.11)$$

which gives for $M_x = 10 M_\odot$ a luminosity of

$$L \approx 4 \times 10^{45} \left(\frac{\dot{M}}{M_\odot \, yr^{-1}} \right) \, erg \, s^{-1}$$

Hence an observed luminosity of 4×10^{37} erg s^{-1} for the Cyg X-1

source is obtained with the deposition of $\dot{M}=10^{-8}M_{\odot}yr^{-1}$ onto the accretion disc.

The temperature and radiation spectrum are derived in a straightforward fashion. For a radiative flux Q, the radiation density is

$$\varepsilon = \frac{3}{4} \frac{Q}{c} \sigma \Sigma \qquad (1.12)$$

where σ is the opacity due to electron scattering. The two main types of scattering giving rise to X-rays are

(1) inverse Compton scattering by which a low energy photon scatters off an energetic electron gaining energy in the process

(2) bremsstrahlung in which X-rays are emitted from the acceleration of electrons in Coulomb fields.

In the first case, and for very low photon energies compared to electron energies we have the Thompson cross-section (independent of energy) giving the opacity

$$\sigma_T = 0.4 \ cm^2 \ gm^{-1} \qquad (1.13)$$

while for bremsstrahlung the opacity is

$$\sigma_{ff} = 0.11 \ T^{-7/2} \ n_e \ cm^2 \ gm^{-1} \qquad (1.14)$$

In the standard disc model thermodynamic equilibrium is assumed as well as the opticalthickness of the disc. Substitution of $\varepsilon = bT^4$ into 1.12 ($b=4\sigma/c=7.65\times10^{-15}erg \ cm^{-3} \ {}^{\circ}K^{-4}$

where σ is the Stefan-Boltzmann constant), and the use of the opacities 1.13 or 1.14 together with the equation of state for the gas and the radiation

$$P_g = \rho \, kT / m_P$$

$$P_r = \varepsilon / 3 \tag{1.15}$$

gives four equations (1.4, 1.5, 1.8, and 1.12) for 5 unknowns: $z_o(r)$, $\Sigma(r)$, $U^r(r)$, $T(r)$, and $W^{r\phi}(r)$. The detailed radial structure of the disc can be solved if we specify the stress $W^{r\phi}$ in terms of the other variables in the problem.

This specification of the stress is precisely the most difficult problem in turbulent hydrodynamics. By-passing these problems, the stress induced by turbulent motions (see Shakura and Sunyaev (1973) as an example) is modelled with a turbulent viscosity

$$\nu_T = \rho \, \tilde{u} \, l$$

where $\tilde{u}$ is the root mean square turbulent velocity and

$$W^{r\phi} = \nu_T \, r \, \frac{d\Omega}{dr} \approx -\rho \, U^\phi \, \frac{z_o}{r} \, \tilde{u} = -\left(\frac{\tilde{u}}{c_s} \right) \rho \, c_s^2$$

where equation 1.5 has been used. It is then assumed that the turbulent Mach number

$$M_t \equiv \tilde{u} / c_s \tag{1.16}$$

is a constant so that

$$W^{r\phi} \approx M_t \, P \tag{1.17}$$

Equation 1.17 now allows the solution of the radial disc structure. Solving equations 1.4, 1.5, 1.8, and 1.12; and using 1.6 in 1.8, one obtains expressions for z_0, ζ, U^r, and T in terms of three parameters: M_x, $\dot{M}$, and M_t. The solutions show that this optically thick disc is comprised of three zones:

A) inner zone; $P_r \gg P_g$, $\sigma_T \gg \sigma_{ff}$

B) middle zone; $P_g \gg P_r$, $\sigma_T \gg \sigma_{ff}$

C) outer zone; $P_g \gg P_r$, $\sigma_{ff} \gg \sigma_T$

Other general conclusions that may be drawn are (see Shakura and Sunyaev for an excellent analysis)

1) the dependence of T upon r is of power law form giving rise to a "non-thermal" looking power law X-ray spectrum

2) maximal temperatures are of order 10^8 °K

3) the half-thickness z_0 displays weak dependence on M_t and is of order 10^6 cm in the inner region to 10^8 cm in the outer region

4) Compton processes strongly affect the shape of the emitted spectrum in the inner disc region

5) exponential cut-off in spectrum for frequency range $h\nu \gg kT_{max}$ (characteristic for Compton process)

The main short-coming of the standard model is that it is too cool to explain the large X-ray power emitted in the 10-100 kev band of the spectrum.

Lightman and Eardley (1974) demonstrated that this

constant M_t model was unstable in the inner, radiation dominated zone and showed on this basis that this region would probably be extended, hot, and optically thin (this instability is considered again in Chapter 4). Shapiro, Lightman and and Eardley (1976) constructed a model, based on this observation, which gave electron temperatures $T_e \approx 10^9$ °K with much higher ion temperatures $T_i \approx 10^{11}$ °K (the so-called "two temperature" model). Soft photons from the cool ($T_e \approx 10^6$ °K) middle region scatter off energetic electrons in the extented hot inner region undergoing inverse Compton scattering. This accounts for the hard X-ray component. The spectrum has a power law form with an exponential cut-off at 150 kev, which is consistent with observations.

Transitions in the luminosity of Cyg X-1 (high and low states) are thought to arise from variations in the mass transfer rate M (see Alme and Wilson (1976)). A large increase in mass transfer would increase the low-energy photon flux from the outer regions of the disc which would account for a transition into the high state.

For a strictly hydrodynamic explanation of the rapid variability, Shakura and Sunyaev assume that if $M_t \approx 1$, strong convective turbulence might occur with the resultant emergence of hot clumps of plasma on the disc surfaces. These authors speculate that solar-type flares could occur in the disc if the field were built up enough.

3. Previous Work On Magnetic Processes In Accretion Discs

In a short early paper, Blumenthal and Tucker (1972) suggested that the X-ray pulsations from Cyg X-1 could be understood in terms of giant flare-like events in a region of high magnetic field. They proposed that in a flare, oscillations of the field would be set up leading to plasma heating in the flux tube and thermal emission. The hard X-ray component would arise from synchotron radiation from the high energy particles known to be emitted in such flares. They did not discuss how such fields could be generated.

Later work on magnetic processes focussed on the role of magnetic fields in transporting angular momentum in the disc. One feature of this work is that only fields at or below equipartition energies with the thermal energy are considered. Another feature is that the interaction between fluctuating velocity and fluctuating magnetic field was not considered. Such interactions however are known to give rise to very intense magnetic fluctuations as well as strong large scale "mean" fields under certain circumstances as much work on the theory of turbulent dynamo action shows.

Eardley and Lightman (1975) as an example discuss the angular momentum transport and disc structure arising from a chaotic magnetic field. Assuming that only a chaotic field can be present in the turbulent disc, these authors consider the growth of the b^ϕ component of the chaotic field at the expense

of the radial component by the shearing of the radial field lines in the Keplerian flow. They assume that dissipation on micro-scales is negligible so that the radial field $b^{'r}$ remains constant. With this picture, there is seemingly no limit to the growth of the chaotic field. Consequently field limitation by reconnection of the field lines comprising the "magnetic cells" of flux is invoked. Since the physics of reconnection events (known to be important in solar flares) is poorly understood, Eardley and Lightman write down a phenomenological equation for field limitation by reconnection, with a characteristic time for energy loss to the field as some fraction of the time required for an Alfvén wave to traverse the distance of the magnetic "eddy". Assuming stationarity and magnetohydrostatic balance, they then go on to compute the disc structure with the Maxwell stress due to the fluctuating fields providing the stress $W^{r\phi}$.

Ichimaru (1977) attacked the problem of angular momentum transport by fluctuating magnetic fields and theorized that the currents arising from reconnection of the "magnetic eddies" would induce an anomalous resistivity in the plasma. This anomalous resistivity arises from the scattering of these currents off of the magnetic fluctuations, and is very much a plasma theorist's point of view. Ichimaru then solves the induction equation for the fluctuating field and finds using his anomalous resistivity, that under stationary conditions

$$\frac{\langle \delta B^2 \rangle}{8\pi m T_i} = \frac{1}{6^{\frac{1}{2}} \nu} \left| r \frac{\partial \Omega}{\partial r} \right| \tag{1.18}$$

$$\frac{\chi}{4\pi m T_i} = \frac{1}{3\nu} r \frac{\partial \Omega}{\partial r} \tag{1.19}$$

where ν is given by

$$\nu = \left(\frac{\pi}{2}\right)^{\frac{1}{2}} \frac{\pi}{3} \left(\frac{T_i}{m}\right)^{\frac{1}{4}} / z_0$$

and χ is the ϕ-r component of the Maxwell stress due to the fluctuating magnetic fields.

The disc structure is now computed and it is found that the disc can exist in two physically distinct states for a given value of $\dot{M}$. If the radiative loss is small(large) compared to the rate of viscous heating near the outer disc boundary, the disc will exist in an optically thick (optically thin) geometrically thin (geometrically thick) configuration. The model has an optically thin, geometrically thick inner radiation dominated zone for both the states mentioned above which is similar to the two temperature regime found by Shapiro, Eardley, and Lightman. These states are identified with the high and low luminosity states discussed in section 1. Transitions between states is determined by the ratio $\dot{M}/T^2$ with the low state identified with a higher accretion rate and a lower temperature in the outer regions which corresponds to the optically thick, geometrically thin structure. Production of hard X-rays is as discussed in the two temperature model. Numerical calculations show that the outer regions are similar to the Shakura and Sunyaev optically thick solution. Although this is a very interesting explanation for the bimodal behaviour of the source, the explanation of the rapid

variations is not discussed.

The more recent work on magnetic phenomena in accretion discs concentrates on the idea of a magnetically confined hot corona as the agency which gives rise to the hard X-ray emission.

Liang and Price (1977) suggest that the accretion disc is likely to form a hot corona somewhat like the solar corona. They picture a sandwich like disc in which the middle layer is an optically thick, geometrically thin disc which generates the energy, surrounded by corona-like layers of much lower density which is pumped by energy from the inner disc. As in the sun, the optically thin corona has to reach high temperatures before radiative cooling is significant. They point to three advantages of such an idea:

(1) radiation produced at two temperatures (cool disc and hot corona)

(2) coronal X-ray emission occurs at much higher temperatures than for standard models

(3) corona expected to be highly dynamical and produce highly variable emission.

These authors suggest that a strong "disc wind" could be set up in these coronae. Specifically, a corona of temperature $T \geqslant 10^{11}$ °k gives rise to X-rays in the right range. In this picture, energy deposited in the corona is removed by either bremsstrahlung, Compton scattering, synchotron radiation or

wind cooling. Whether synchotron or Compton scattering is the dominant radiation mechanism is determined by the coronal magnetic field strength.

Finally Galeev, Rosner, and Viana (1979) work out a more detailed coronal model with the formation of loops of magnetic field (of scale 10^6 cm and equipartition field strength) protruding through the surface of the disc. They show that the reconnection of magnetic loops within the disc as imagined by the earlier work is too slow a process to prevent the amplification of the fields by shearing. They argue that regions of strong field are expected, and these emerge from the disc by magnetic buoyancy. They consider only a fluctuating field. The emergent loops of flux are strong enough to confine a coronal plasma which is heated to high temperatures when the loops undergo reconnections (flares). The hard X-ray emission then derives from the inverse Compton scattering of soft photons from the cool disc off the hot electrons in the corona. They show that such a process delivers flare like bursts of hard X-rays on time scales 1s and energies 10^{35}ergs s^{-1}, thereby giving a physical basis of Terrell's shot noise model.

We believe that this model has time variations that are slightly too slow and energy releases that are slightly too small to recover the shot noise model but that the idea that the main effect of the magnetic fluctuations is to give rise

to flares on the disc surface is correct.

It is important to try to track down the requirements for variability over the rapid time scales in terms of flaring mechanisms. In view of the lack of a theory of reconnection and flare activity that can account for both the enormous energy releases on short time scales for solar flares as an example, we turn to some experimental results for help.

4. Laboratory " Solar Flare " Experiments Scaled To Cyg X-1

Suppose we imagine that solar-like flares are occurring on the surface of the accretion disc model proposed for Cyg X-1. What constraints can be applied on the magnetic fields and their length scales in order that variabilities 10^{-1}s for the shot noise and 10^{-3}s for the millisecond bursts, with energy releases of 10^{36} ergs can be accounted for.

Solar flares (see Sweet (1969) for a review) typically involve the release of 10^{30}ergs in a period of 100s for moderate events and may range as high as 10^{32} ergs (solar luminosity is 10^{33} erg s^{-1}). The area of the flaring regions are 10^{17}-10^{20} cm^2, the emission region being as high as it is broad with a characteristic scale of 10^{9}cm. The overall "mean" field of the sun is 1-2 Gauss whereas the active regions may have 300-3,000 Gauss fields (exceeding local equipartition energies by two orders of magnitude in some cases). Flares originate near regions where the longtitudinal component of

the magnetic field changes sign (i.e near a neutral line of the field). Succeeding flares in an active region may occur with identical profiles and shapes suggesting that the flare configuration is determined by the local magnetic configuration. The time dependence and magnitude of X-ray emission are the same for a sequence of flares at a given site, but are strikingly different from site to site.

A series of beautiful experiments on magnetic field line reconnection were performed (see Bratenahl and Yeates (1970), and Baum et al (1973)) which were scaled to solar flares and found to be in good agreement with the observations (see Baum and Brahenahl (1976)). We outline the experiments and results and scale to conditions appropriate in Cyg X-1.

The laboratory experiments are done on a double inverse pinch device which creates a neutral line between two magnetic cells. The device consists of two insulation covered, current carrying rods which are parallel, 10cm apart , and carry current from discharging capacitor banks (see Fig. 4). Two cylindrical current sheets are driven radially outward from each rod by $\underline{J} \times \underline{B}$ forces, and merge upon collision leaving a neutral line in the centre of the assembly.

Fig. 4 Geometry Of The Field Line Reconnection Experiments

(From Baum Et Al (1973))
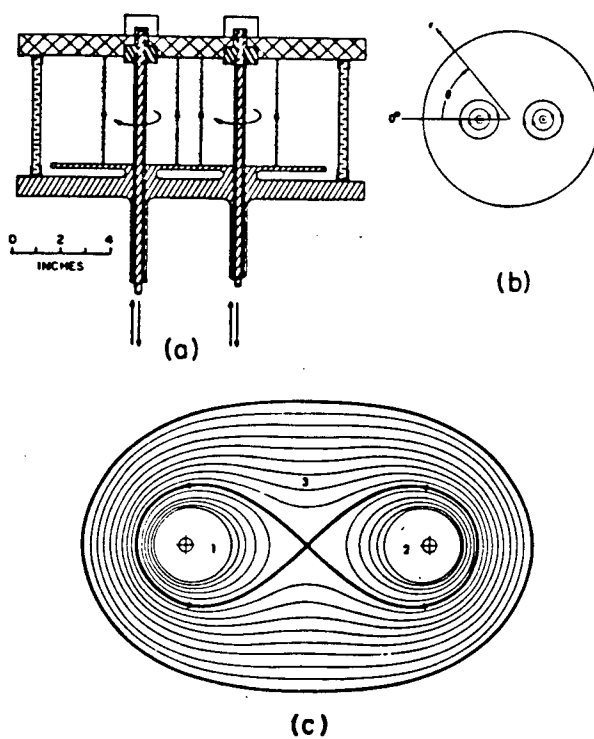
Double inverse pinch device chamber. (a) side, and (b) top view; (c) equipotential lines of the z component of the magnetic vector potential (curl-free magnetic field lines). The dark line is the separatrix which divides the flux into three regions. Region 3 is accessible from regions 1 and 2 by reconnection at the origin.

The main results of these experiments are:

(1) current density is a relative maximum along the neutral line

(2) the electric field along the neutral line grows as soon as the line is established with the current density increasing as well

(3) a discharge occurs during which the current drops abruptly, the electric field goes from 100 volts/cm →300 volts/cm (in 0.3 sec), and the resistivity jumps by a factor of 40

(4) X-ray production is observed which can be interpreted as thick target bremsstrahlung of energetic electrons impinging upon the anode in the immediate vicinity of the neutral line. The power law X-ray spectrum observed can be fitted with a power law electron spectrum. Thermal X-ray production is hard to estimate.

The most important aspect of these experiments for us is the fact that they scale correctly to moderate energy solar flares. From the experiments it is found:

(1) <u>flare duration:</u> $\Delta t_{lab} \approx 10^{-6}$ s

(2) <u>total energy release</u> $Q_{lab} = 1.6 \times 10^{8}$ erg

under conditions where the length scale and magnetic field were fixed in the experiment as :

(a) <u>length scale of reconnecting field:</u> $l_{lab} = 10$ cm

(b) <u>magnetic field:</u> $B_{lab} = 10^{4}$ Gauss

Baum and Bratenahl take the observed values L_{Sun}, B_{Sun} for the size of the reconnecting regions and their magnetic field strengths ($L_{Sun} = 10^9$ cm and $B_{Sun} = 10^3$ Gauss) and derive flare durations of 10^2 s and energy releases of 10^{30} erg, using the parameters above. The scaling relations they use, due to Parker, are

$$\Delta t_x = \left(\frac{L_x}{L_{lab}} \right) \Delta t_{lab} \qquad (1.20)$$

$$Q_x = Q_{lab} \left(\frac{B_x}{B_{lab}} \right)^2 \left(\frac{L_x}{L_{lab}} \right)^3 \qquad (1.21)$$

where Δt_x, l_x, and Q_x are the flare duration, flaring region size, and energy release.

The maximum cosmic ray energy possible from such flares can be estimated by integrating the electric field along the entire neutral line length. The scaling in this case is

$$V_x = V_{lab} \left(\frac{B_x}{B_{lab}} \right) \left(\frac{L_x}{L_{lab}} \right) \qquad (1.22)$$

where the measured voltage in the experiment $V_{lab} = 3 \times 10^3$ volts. For the solar parameters, $V_x = 30$ Gev in agreement with observations.

Assuming that "solar type" flares are responsible for the rapidly varying X-ray emission in Cyg X-1, we estimate the time scales and energy releases from the obervational data summarized in Table 2 for both the shot noise and millisecond

burst parameters. Using the scaling relations 1.20, 1.21, and 1.22 ; the laboratory parameters; and the time scales and energy releases for shot noise and millisecond bursts: we find the length scales, magnetic field, and maximal cosmic ray energies associated with flares on the disc. The results are given in Table 3.

Table 3. Characteristics Of Solar Type Flares In Cyg X-1

EVENT TYPE	SHOT NOISE	MILLISECOND BURST
L_x	10^6 cm	10^4 cm
B_x	$10^{10.5}$ Gauss	10^{13} Gauss
V_x	10^{15} ev	10^{15} ev

For the densities and temperatures in the standard cool disc model, equipartition fields in the disc are of order 10^8 Gauss. If the results of Table 3 are correct, one is

dealing with fields above equipartition energies. Such strong fields could not remain in the disc and would emerge from the disc surfaces and there undergo flaring.

The parameters for the shot noise are in agreement with what one would expect from the disc. The disc thickness varies from 10^6 cm to about 10^8 cm. In addition field strengths two orders of magnitude above equipartition strength are predicted which is similar to solar flares.

The bursts represent extreme conditions indeed. The largest astrophysical fields known are those for pulsars where 10^{12} Gauss fields have been observed. The results of Chapter 4 will show that the largest fields present are about $10^{10.5}$ Gauss, and give an alternative explanation of the millisecond activity if it is indeed real.

We note that the maximum cosmic ray energy observed to date is 10^{20} ev.

This analysis shows that in order to recover the rapid temporal variation of the Cyg X-1 source together with the massive energies associated with these variations, a solar type flare model requires intense (greater than equipartition energies if a standard underlying disc is assumed) magnetic fluctuations. A consistent MHD analysis should not therefore impose the condition of equipartition at the outset.

We turn to an outline of the remainder of the thesis.

5. Outline Of The Thesis

In Chapter 2, the full equations for a magnetized fluid are examined. The various fields are decomposed into mean and fluctuating components and the energy transfer between the various fields examined. The relations between the fluctuating velocity, temperature, and magnetic fields are developed using the methods of Mean Field Electrodynamics and a regime is identified where large magnetic fluctuations may occur. The magnitude of the mean magnetic field is found to be of central importance in assessing the structure of the various fluctuating fields.

In Chapter 3, a detailed analysis of the mean large-scale magnetic field is carried out. Since some assumptions about the disc structure and turbulence properties are required, we use the standard disc model as a basis for our calculations. Assuming steady conditions, these calculations determine a value for the turbulent Mach number independent of any other parameters. In the final section of the chapter, it is found that for appropriately large scales, the mean field can be generated by turbulent dynamo action.

In Chapter 4, the results of Chapters 2 and 3 are combined to give a coherent view of magnetic processes in the accretion disc. Arguments are made to show to what strength the mean field is expected to grow, which allows the magnitude of the magnetic fluctuations to be fixed, and a comparison

With the predictions of the scaling arguments of the previous section of this chapter to be made. A picture is built up wherein the mean magnetic field remains inside the disc at below equipartition strength and over the long time average is responsible for angular momentum transport in the disc. On intermediate time scale averages, it is shown that the Maxwell stress due to the fluctuations acts to supress the Lightman and Eardley instability so that the underlying accretion disc remains cool and thin. This result is important because it shows that the hard X-ray emission must derive from magnetic flare like processes. The magnetic fluctuations undergo flaring processes on time scales and with energy releases that explain the shot noise model of the X-ray variability. The hard X-ray emission is modelled in terms of a rapid, flash-phase subcomponent of the flares, in which non-thermal distributions of electrons account for the power-law X-ray spectrum.

Wherever possible, the mathematics has been relegated to a series of appendices. The entire analysis to be presented is non-relativistic. No major corrections to the results are expected for non-rotating black holes; however, interesting effects in addtion to those presented will arise for rotating black holes if the region immediately adjacent to the event horizon is considered. Appendix A reviews the ideas and results of Mean Field Electrodynamics required for this work.

Chapter 2

Magnetic Fluctuations In A Turbulent Accretion Disc

1. Introduction

The central aim of this chapter is to examine the properties of fluctuating velocity, magnetic and temperature fields in a turbulent accretion disc. As mentioned in the opening chapter, the assumption of stationarity allows solution of the disc equations without a detailed knowledge of the dissipation mechanisms operative in a turbulent disc. However the rapid variability of the disc's X-ray output down to millisecond time scales demands a careful examination of fluctuations in such a turbulent regime.

Let us first consider energy balance when magnetic fields are ignored. In a turbulent regime Reynolds stresses act to transfer energy out of the mean flow (in an accretion disc, this is basically a Keplerian velocity field) into the velocity fluctuations. Then pressure fluctuations and viscosity act to transfer energy out of the velocity fluctuations into internal energy. Stewart (1976) examined this process by using various scaling arguments applied to a coupled pair of equations for the fluctuating kinetic and internal energies. His techniques and results, briefly reviewed in section 2, will prove a useful starting point for

our analysis which includes magnetic fields.

When magnetic fields are included a host of new effects may arise. For the moment consider only the fluctuating fields. In addition to the effects described in the preceeding paragraph, energy is extracted from the velocity fluctuations by $E.J$ type interactions, and transferred into both the mean and fluctuating magnetic fields. Ohmic dissipation then transfers energy of the fluctuating magnetic into internal energy fluctuations. These processes are specified and examined in section 3.

Our object in section 4 is to solve for the kinetic, magnetic and internal energy fluctuations. Now in order to close this set of three equations for three unknowns it will be necessary to give a model for the ultimate value of the mean magnetic field. We will be using mean field theory to express the various correlations between the fluctuating velocity and magnetic fields in terms of the mean field. It is to be expected that the energy in the mean magnetic field will depend on the kinetic energy fluctuations. The specific model for this will specified in Chapter 4 and will enable us to close our coupled triplet of equations. Comparisons with Stewart's results will also be made in this section

As pointed out in Chapter 1, if we interpret the shot noise model for the X-ray output as due to solar type flares occurring on the surface of the accretion disc, large magnetic

fluctuations are required. In section 4 we show under what conditions such large fluctuations are possible, and discuss how they affect the overall disc structure. It will become apparent that in the regime that allows fluctuating fields on the order 10^{10} gauss, it is not possible to have a stationary accretion disc on time-scales $<10^{-1}$ sec. We believe that under the conditions mentioned, an accretion disc such as that believed to comprise the Cyg. X-1 X-ray source can be approximated as stationary only on time-scales$\sim$10 sec.

2. Stewart's Analysis Of Energy Balance In Turbulent Accretion Discs.

2.1 The Basic Equations

We begin with the equations of continuity, conservation of momentum and conservation of internal energy for a viscous fluid in the presence of an external gravitational field. Stewart adopts the use of a semicolon notation for covariant differentiation which facilitates the conversion into cylindrical polar co-ordinates (r, ϕ, z). The equations are

$$\dot{\rho} + \left(\rho u^\alpha\right)_{;\alpha} = 0 \tag{2.1}$$

$$\left(\rho \dot{u}^\alpha\right) + \left(\rho u^\alpha u^\beta\right)_{;\beta} = \rho \psi^{,\alpha} - p^{,\alpha} - t^{\alpha\beta}_{;\beta} \tag{2.2}$$

$$\left(\dot{\rho e}\right) + \left(\rho e u^\alpha\right)_{;\alpha} = -p u^\alpha_{;\alpha} - t^{\alpha\beta} e_{\alpha\beta} - q^\alpha_{;\alpha} \tag{2.3}$$

$$\frac{\partial}{\partial t} \equiv \dot{}$$

where ψ is the external gravitational potential, $t^{\alpha\beta}$ is the viscous stress tensor, $e_{\alpha\beta}$ is the symmetric strain tensor (i.e. $e_{\alpha\beta} = \frac{1}{2}\left(u_{\alpha;\beta} + u_{\beta;\alpha}\right)$), e is the internal energy, and q^{α} is the heat flux. The reader may consult Landau and Lifshitz (1959) for the detailed derivation of these equations.

In order to discuss turbulent processes, one now decomposes the fields into mean and fluctuating parts. Proceeding with this decomposition we write

$$u^{\alpha} = U^{\alpha} + u'^{\alpha}$$
$$\rho = \rho_0 + \rho'$$
$$p = P + p'$$
$$e = E + e'$$
$$q^{\alpha} = Q^{\alpha} + q'^{\alpha}$$

$$(2.4)$$

denoting the ensemble average of any quantity θ by $\bar{\theta}$, we have that $\overline{u^{\alpha}} = U^{\alpha}$, $\bar{\rho} = \rho_0$ etc. The ensemble average of the fluctuating quantities vanishes.

Let us introduce the decomposition 2.4 into the equations 2.1-2.3 and take their ensemble average. As a simple example, consider the continuity equation which becomes

$$\dot{\rho_0} + \left(\rho_0 U^{\alpha} + \overline{\rho' u'^{\alpha}} \right)_{;\alpha} = 0 \qquad (2.5)$$

Because density fluctuations ρ' are important we see that we pick up an extra term $\overline{\rho' u'^{\alpha}}$ in addition to the terms present when turbulence is absent. In order to make the

expressions compact, it is useful to define

$$\hat{u}^{\alpha} = u^{\alpha} + \frac{\overline{\rho' u'^{\alpha}}}{\rho_0} \tag{2.6}$$

which allows us to write 2.5 as

$$\dot{\rho_0} + (\rho_0 \hat{u}^{\alpha})_{;\alpha} = 0 \tag{2.7}$$

Stewart defines $\hat{u}^{\alpha}$ as the mass flow velocity. We introduce the $\wedge$ symbol in order to clearly distinguish this from the usual mean velocity $U^{\alpha} = \overline{u^{\alpha}}$. It is now natural to define

$$\hat{u}'^{\alpha} \equiv u'^{\alpha} - \overline{\rho' u'^{\alpha}}/\rho_0 \tag{2.8}$$

where we notice that $\hat{u}^{\alpha} + \hat{u}'^{\alpha} = U^{\alpha} + u'^{\alpha} = u^{\alpha}$.

Using the definitions 2.6 and 2.8 as well as the continuity equation 2.7 results in the equation of motion

$$\rho_0 \frac{D\hat{u}^{\alpha}}{Dt} = \rho_0 \psi'^{\alpha} - P'^{\alpha} + \hat{\tau}^{\alpha\beta}_{;\beta} \tag{2.9}$$

where

$$\frac{D}{Dt} \equiv \frac{\partial}{\partial t} + \hat{u}^{\alpha} \nabla_{\alpha}$$

and

$$\hat{\tau}^{\alpha\beta} \equiv -\overline{\rho \hat{u}'^{\alpha} \hat{u}'^{\beta}}$$

is the Reynolds stress. We have dropped the viscous stress in writing 2.9 because dissipation on the molecular level is negligible compared with the dissipation arising via the turbulent stresses.

The equation governing the dynamics of the mean flow energy is found by taking the dot product of eqation 2.9 with $\hat{u}_{\alpha}$ to give

$$\rho_0 \frac{D}{Dt} \left(\frac{\hat{u}^2}{2} \right) = \rho_0 \psi_{,\alpha} \hat{u}^{\alpha} + P \hat{u}^{\alpha}_{;\alpha} - \hat{\tau}^{\alpha\beta} \hat{E}_{\alpha\beta} + \tag{2.10}$$
$$+ \left[(\hat{\tau}^{\alpha\beta} - P\delta^{\alpha\beta}) \hat{u}_{\alpha} \right]_{;\beta}$$

where we have written

$$\hat{u}_{\alpha;\beta} = \frac{1}{2}\left[\hat{u}_{\alpha;\beta} + \hat{u}_{\beta;\alpha}\right] + \frac{1}{2}\left[\hat{u}_{\alpha;\beta} - \hat{u}_{\beta;\alpha}\right]$$

$$\equiv \hat{E}_{\alpha\beta} + \hat{R}_{\alpha\beta}$$

and $\hat{E}_{\alpha\beta}$ is the mean symmetric strain tensor.

The equation governing the dynamics of the fluctuating flow kinetic energy are found by dot producting the full equations of motion (using decompositions 2.4) by $\hat{u}'$ and taking the ensemble average resulting in

$$\rho_o \frac{D}{Dt}\left(\frac{\tilde{u}^2}{2}\right) = -\overline{p'^\alpha \hat{u}'_\alpha} + \overline{t^{\alpha\beta}\hat{e}'_{\alpha\beta}} + \hat{\tau}^{\alpha\beta}\hat{E}_{\alpha\beta} -$$

$$- \overline{\left[\left(t^{\alpha\beta} + \frac{1}{2}\rho\,\hat{u}'^\alpha\hat{u}'^\beta\right)\hat{u}'_\alpha\right]}_{;\beta} \qquad (2.11)$$

where $\tilde{u}^2 \equiv \overline{\rho\hat{u}'^\alpha\hat{u}'_\alpha}/\rho_o$ is the mean square velocity fluctuation.

The most important feature of these equations is that the Reynolds stress interacting with the mean strain ($\hat{\tau}^{\alpha\beta}\hat{E}_{\alpha\beta}$) transfers energy out of the mean flow and into the fluctuations. The first two terms in the right hand side of 2.11 represent the work done by pressure fluctuations and viscosity while the last term represents transport of fluctuating flow energy by the turbulent stresses. To maintain turbulence at all, some external agency (in this case the external gravitational field due to the central compact

object) must provide the strain $\hat{E}_{\alpha\beta}$.

Turning to the internal energy, defining the quantities:

$$\hat{E} \equiv E + \overline{\rho' e'}/\rho_0 \quad ; \quad \hat{e}' = e' - \overline{\rho' e'}/\rho_0 \qquad (2.12)$$

setting $e = c_v T$, (c_v constant) appropriate for a perfect gas so that $\hat{T} = \hat{E}/c_v$ and the temperature fluctuation $\hat{\theta}' = \hat{e}'/c_v$ the mean square thermal fluctuation $\tilde{\theta}^2 = \overline{\rho\, \hat{\theta}'^2}/\rho_0$ satisfies the equation

$$\frac{1}{2}\rho_0 c_v \frac{D}{Dt}(\tilde{\theta}^2) = -\overline{\hat{\theta}'\, p\, u^\alpha_{;\alpha}} - \overline{\hat{\theta}'\, t^{\alpha\beta}\, e_{\alpha\beta}} - \overline{q^\alpha_{;\alpha}\, \hat{\theta}'} -$$
$$- c_v\, T_{,\alpha}\, \overline{\rho\, \hat{\theta}'\, \hat{u}'^\alpha} - \frac{1}{2}\, \overline{(\rho c_v\, \hat{\theta}'^2\, \hat{u}'^\alpha)}_{;\alpha}$$

$$(2.13)$$

which may derived in the same manner as equation 2.11

2.2 Consequences Of The Mean Momentum Conservation Equation For Thin Discs

This section provides more of the details concerning the radial structure of accretion discs and provides some background for the discussion in Chapter 1. We apply the following four assumptions to the equations of motion 2.9 in cylindrical polar co-ordinates (see Stewart, p. 41)

A) the disc is thin with $z_0 \ll r$, where z_0 is the scale thickness,

B) the mean flow is almost toroidal with

$$|\hat{u}^\phi| \gg |\hat{u}^r| \gg |\hat{u}^z|$$

in fact we require

$$| \hat{u}^{\phi} | \gg \frac{r}{z_o} | \hat{u}^z |$$

where

$$u^{\phi} \equiv V \quad ; \quad u^r \equiv U \quad ; \quad u^z \equiv W$$

C) the mean flow is axisymmetric and symmetric about $z = 0$

D) the size of the largest eddies ℓ is of order z_o

1. The z-component of equation 2.9 is

$$\rho_o \left(\dot{W} + W_{,z} W + W_{,r} U \right) = - \rho_o \frac{V_k^2 z}{r^2} - P_{,z} + \hat{\tau}^{zz}{}_{,z} + \hat{\tau}^{zr}{}_{,r} \qquad (2.14)$$

so that assumption B) makes the left hand side negligible compared with the centripetal force. Using the thin disc approximation gives

$$\rho_o \frac{V_k^2 z}{r^2} \approx - P_{,z} + \hat{\tau}^{zz}{}_{,z} \qquad (2.15)$$

which is really an equation of hydrostatic balance. Then applying the estimates

$$P_{,z} \approx - \rho_o c_s^2 / z_o$$

$$\hat{\tau}^{zz}{}_{,z} \approx \rho_o \tilde{u}^2 / z_o \qquad (2.16)$$

where c_s is the speed of sound, gives the result

$$\left(\frac{z_o}{r} \right)^2 \approx \frac{c_s^2 + \tilde{u}^2}{V_k^2} \qquad (2.17)$$

Now in usual turbulence theory, the duration t_t of a turbulent eddy of size ℓ is

$$t_t \sim \ell / \tilde{u} \qquad (2.18)$$

so that equation 2.17 may be rewritten as (using assumption D)

$$t_t \sim t_k \left[1 + M_t^{-2} \right]^{\frac{1}{2}} \qquad (2.19)$$

where $M_t = \tilde{u} / c_s$ is the turbulent Mach number and $t_k = r/V_k$ is the Keplerian time scale. Equations 2.17 and 2.19 show that the Keplerian flow V_k is always supersonic and that the Keplerian time scale is the shortest time scale in the turbulent accretion disc problem (i.e. $t_t \geqslant t_k$). The time scales reflecting fluctuating proceses are tied to the Keplerian time scale in thin disc problems.

With reference to mean field theory (see Appendix A), the use of the first order smoothing approximation to simplify the solution of the fluctuating and mean magnetic field equations can be satisfied if we imagine the turbulence as a collection of random waves where if T_u is the correlation time for such a wave of wave-length ℓ

$$T_u \ll \ell / \tilde{u} \qquad (random \ waves) \qquad (2.20)$$

2. The r-component of equation 2.9 is

$$\rho_o \left(\dot{U} + U_{,z} W + U_{,r} U - \frac{V^2}{r} \right) = -\rho_o \frac{V_k^2}{r} - P_{,r} + \hat{\tau}^{rz}{}_{,z} + \hat{\tau}^{rr}{}_{,r} +$$

$$+ \frac{\left(\hat{\tau}^{rr} - \hat{\tau}^{\phi\phi} \right)}{r} \qquad (2.21)$$

where by assumption B) the largest term on the left is $-V^2\rho_0/r$ and from the result 2.17 the dominant term on the right is $-V_k^2\rho_0/r$ so that

$$V \approx V_k \left[1 + O\left(\frac{u}{V_k}\right) + \dots \right] \qquad (2.22)$$

which gives the mean toroidal flow as Keplerian to good approximation

3. The ϕ-component of equation 2.9 is

$$\rho_0 \left(\dot{V} + V_{,z} W + (rV)_{,r} \frac{u}{r} \right) = \hat{\tau}^{\phi z}_{,z} + \frac{(r^2 \hat{\tau}^{\phi r})_{,r}}{r^2} \qquad (2.23)$$

and using previous estimates gives

$$\rho_0 (rV_k)_{,r} \frac{u}{r} \approx \hat{\tau}^{\phi z}_{,z} + \frac{(r^2 \hat{\tau}^{\phi r})_{,r}}{r^2} \qquad (2.24)$$

Taking the vertical average (see Chapter 1, section 2) of these equations and noting that $\hat{\tau}^{\phi z}$ must vanish on a free surface the equation becomes

$$\langle \rho_0 u \rangle \frac{(rV_k)_{,r}}{r} = \frac{(r^2 \langle \hat{\tau}^{\phi r} \rangle)_{,r}}{r^2} \qquad (2.25)$$

which is equation 1.7.

2.3 Energy Balance For The Fluctuating Fields

Since the turbulence time scale $t_t \approx t_k$, the turbulence

will be well mixed in both the z and ϕ directions. However, long radial scale variation of mean quantities such as the mean strain will result in the radial variation of the turbulence. For thin discs then, the turbulence is statistically homogeneous in each annulus r=constant. We turn to the study of the fluctuation equations 2.11 and 2.13.

On the left hand side of these equations we have the appearance of the operator

$$\frac{D}{Dt} \equiv \frac{\partial}{\partial t} + \underline{u} \cdot \nabla$$

where $\partial/\partial t$ measures the rate of change at a point and $\underline{u} \cdot \nabla$ represents the advective rate of change following the mean flow. The D/Dt operator then measures the rate of change for a hypothetical point moving with the mean flow. For a steady flow $\frac{\partial}{\partial t} = 0$ and if we have homogeneity of turbulent quantities, i.e. they are independent of r, ϕ, and z, then $\underline{u} \cdot \nabla = 0$ as well.

A stationary disc requires $D\psi/Dt = 0$; where $\psi = \tilde{u}^2$ or $\tilde{\theta}^2$. Another approximation which is employed is to note that the divergence terms on the right hand side of the equations 2.22 and 2.23, which represent the spatial redistribution of energy vanish in the case that our turbulence is independent of z and ϕ. This can be seen by imagining that we integrate these terms over an annular volume with cross sectional dimension z_0 and then applying Gauss's theorem.

Equation 2.11 then reduces to

$$\hat{\tau}^{\alpha\beta} \hat{E}_{\alpha\beta} = \overline{p,_\alpha \hat{u}'^\alpha} - \overline{t^{\alpha\beta} \hat{e}'_{\alpha\beta}} \qquad (2.26)$$

In this equation, the left hand side represents the rate at which energy is being supplied to the turbulence via the reynolds stress interaction with the mean strain whereas the right hand side comprises the dissipation of energy by buoyancy and viscosity respectively. This type of relation is common to many analyses of turbulent processes (see Tennekes and Lumley (1972)). Equation 2.26 concentrates on those features of turbulence not directly related to spatial energy transport. The turbulence interacts with the mean flow and injects energy into the turbulence on the largest scale . The dissipation by viscosity (second term on right hand side) occurs at microscales however. As Tennekes and Lumley point out, all evidence suggests that the viscous dissipation at these microscales occurs at a rate dictated by the energy in the largest eddies. With an energy density in the largest scales of $\rho_o \hat{u}^2$ and a characteristic time $\ell/\hat{u}$, the viscous dissipation should occur at a rate $\rho_o \tilde{u}^3/\ell$, i.e.

$$- \overline{t^{\alpha\beta} \hat{e}'_{\alpha\beta}} \approx \rho_o \tilde{u}^3/\ell \qquad (2.27)$$

Denote the components of the fluctuating velocity by

$$\hat{\underline{u}}' \equiv (u', v', w')$$

in cylindrical polar co-ordinates. The main contribution to $\hat{E}_{\alpha\beta}$ is the $\phi-r$ component denoting the strain associated

with the Keplerian flow $V_K = r\Omega$. The left hand side is then

$$\widehat{\mathcal{T}}^{\alpha\beta} \widehat{E}_{\alpha\beta} \approx \rho_0 c_u \widetilde{u}^2 (-r\Omega') \tag{2.28}$$

where the correlation coefficient is $c_u \equiv \overline{u'v'}/\widetilde{u}^2$.

In the case of small pressure fluctuations the buoyancy term is approximately $\overline{P_{,\alpha} \widehat{u}'^\alpha}$. Now the gravitational force in the radial direction is balanced by the centripetal force (the gas is drifting radially at a much slower rate than its orbital period) so that the local gravity is mainly in the z direction. If we define $g_\alpha = \dfrac{P_{,\alpha}}{\rho_0}$ as the local gravity then the buoyancy term is

$$\overline{P_{,\alpha} \widehat{u}'^\alpha} \approx g \overline{\rho'w'} \tag{2.29}$$

where $g = (0,0,-g)$. Finally, assuming a perfect gas allows us to relate the density fluctuation ρ' with Θ

$$\frac{\rho'}{\rho_0} \approx -\frac{\widehat{\Theta}'}{\widehat{T}}$$

so that we have

$$\overline{P_{,\alpha} \widehat{u}'^\alpha} \approx -\frac{\rho_0 g}{\widehat{T}} c_\theta \widetilde{u} \widehat{\Theta} \tag{2.30}$$

with the velocity-temperature correlation coeficient $c_\theta \equiv \overline{\widehat{\theta}' \widehat{w}'}/\widetilde{\theta}\widetilde{u}$.

Combining equations 2.27 , 2.28 and 2.30 with 2.26 then gives

$$\left(-r\Omega'\right) c_u \tilde{u}^2 \simeq -\frac{g}{T} c_\theta \tilde{u} \hat{\theta} + \frac{\tilde{u}^3}{\ell_u} \qquad (2.31)$$

which shows that the buoyancy is coupling the velocity fluctuations to the thermal fluctuations, which we study next.

Using the same conditions that lead to equation 2.26, equation 2.13 becomes

$$\overline{\hat{\theta}' p u^\alpha_{;\alpha}} + c_v \hat{T}_{,\alpha} \overline{\rho \hat{\theta}' \hat{u}'^\alpha} = -\overline{q^\alpha_{;\alpha} \hat{\theta}'} \qquad (2.32)$$

where heating due to kinematic viscosity has been neglected. The left hand side is approximately

$$\rho_o g c_\theta \tilde{\theta} \tilde{u} + \rho_o c_v T_{,z} c_\theta \tilde{\theta} \tilde{u}$$

while the heat flux $\tilde{q}$ is divided up into its conductive and radiative parts with

$$\overline{q^\alpha_{;\alpha} \hat{\theta}'} \approx \rho_o c_v \left[-k \overline{\hat{\theta}' \nabla^2 \hat{\theta}'} + \frac{\tilde{\theta}^2}{t_r} \right]$$

where k is the thermal diffusivity and t_r is the time scale for radiative cooling. Introducing a thermal length scale ℓ_θ allows us to write 2.32 as

$$\left(T_{,z} + g/c_v \right) c_\theta \hat{\theta} \tilde{u} = -\frac{\tilde{\theta}^2 \tilde{u}}{\ell_\theta} - \frac{\tilde{\theta}^2}{t_r} \qquad (2.33a)$$

or

$$\widetilde{\theta} = - \frac{(T_{,z} + g/c_v)\, c_\theta\, \widetilde{u}}{(\widetilde{u}/\ell_\theta + 1/t_r)} \qquad (2.33\,b)$$

Equations 2.31 and 2.33 represent two equations in the unknowns $\widetilde{\theta}$ and $\widetilde{u}$. Using equation 2.33 (b), the equation for the velocity fluctuations becomes

$$(-r\Omega')\, c_u\, \widetilde{u}^2 = g\, \frac{(T_{,z} + g/c_v)}{(\widetilde{u}/\ell_\theta + 1/t_r)}\, c_\theta^2\, \widetilde{u}^2 + \frac{\widetilde{u}^3}{\ell_u} \qquad (2.34)$$

Stewart makes this equation more manageable by multiplying throughout by $\left[c_u^3\, \ell_u^2\, (-r\Omega')^2 \right]^{-1}$ and by defining the parameters

$$\beta \equiv c_\theta^2\, \ell_\theta / c_u^2\, \ell_u$$

$$\gamma \equiv \ell_\theta / c_u\, \ell_u\, (-r\Omega')\, t_r$$

$$R_i \equiv \frac{g}{T}\, (T_{,z} + g/c_v)\, \frac{1}{(-r\Omega')^2}$$

and the dimensionless turbulent intensity

$$x \equiv \widetilde{u} / c_u\, \ell_u\, (-r\Omega')$$

in terms of which equation 2.34 may be written as

$$1 = \frac{\beta R_i}{(x + \gamma)} + x \qquad (2.35)$$

The parameter R_i is the Richardson number but more insight into its role may be obtained if we note that using the equation of state for a perfect gas

$$p = \frac{R}{\mu} \rho T \qquad (2.36)$$

where R is the gas constant and μ the molecular weight and where $R/\mu = \frac{2}{3} c_v$ for a monatomic gas, we have $\rho = \frac{3}{2 c_v} \frac{p}{T}$. Taking the derivative with respect to z of this relation gives

$$-\frac{1}{\rho_0} \frac{\partial \rho_0}{\partial z} = \frac{1}{T} \left(T_{,z} + \frac{3}{2 c_v} \frac{1}{\rho_0} \frac{\partial p}{\partial z} \right)$$

so that the Richardson number in this approximation takes the form

$$R_i = -g \frac{1}{\rho_0} \frac{\partial \rho_0}{\partial z} \Big/ (-r\Omega')^2 \qquad (2.37)$$

In a stably stratified disc $\frac{\partial \rho_0}{\partial z} < 0$ so that $R_i > 0$ and consequently the buoyancy extracts energy from the turbulent kinetic energy. Conversely, an unstably stratified disc with $\frac{\partial \rho_0}{\partial z} > 0$ and $R_i < 0$ shows that energy is pumped into the turbulence via rising fluid elements. We shall assume a stably stratified disc where $R_i > 0$.

The frequency

$$f_B = \left(-g \frac{1}{\rho_0} \frac{\partial \rho_0}{\partial z} \right)^{\frac{1}{2}}$$

(the so-called Brunt-Väisälä frequency) represents the frequency of oscillation of a neutrally buoyant element in a stable density gradient and the Richardson number R_i given by 2.37 compares this frequency with the Keplerian frequency; the basic frequency in the problem.

Returning to equation 2.35 we define

$$f(x) = \frac{\beta R_i}{(x + \gamma)} + x$$

where f(x) is the ratio of the rate of energy dissipation to energy production. The condition f(x)=1 corresponds to stationary turbulence. If f(x)>1 as an example (not stationary), then we have greater dissipation than production so that the turbulence ultimately damps out.

Solving f(x)=1 entails nothing more than solving a quadratic equation in x. Two cases are interesting.

Case 1 $\gamma = 0$:

Here

$$x = \frac{1 \pm \sqrt{1 - 4\beta R_i}}{2}$$

so that stationary turbulence is possible only for $\beta R_i \leq \frac{1}{4}$ with damping (i.e. $f(x) > 1$) occurring when $\beta R_i > \frac{1}{4}$. Experimentally it is known that turbulence dies out when $R_i \gtrsim 0.2$ (Tennekes and Lumley p. 99) . Stewart goes on to argue that of the two roots, (assuming $\beta R_i < \frac{1}{4}$) the larger one is stable while the smaller root is unstable in that a fluctuation about this root may either lead to ultimate damping or increasing of the

turbulent intensity to the larger root. Since $\beta R_i \to 0$ as $z \to 0$

(i.e. $\frac{\partial \rho}{\partial z} = 0$ at $z = 0$) so that one always has a stationary

turbulence about the mid-plane of the disc with x=1. Using x=1

at z=0, together with the definition of x and $\tilde{u}=l_w/t_k$, shows

that the correlation c_u is $c_u=t_k/t_t$.

Case 2 $\gamma \neq 0$:

Again solving the quadratic equation for x shows that for

$$\gamma < \beta R_i < \frac{1}{4} \left(1 + \gamma^2 \right)$$

two stationary turbulent flows are possible only the flow

corresponding to the larger root being stable. For

$\beta R_i < \gamma$, one stationary flow is possible (i.e only one

root has x>0) and it is stable. Again we find that near z=0

(with $\beta R_i \to 0$) stationary turbulence is possible but near the

surface regions the relation of βR_i to γ is crucial.

When βR_i is large relative to γ these regions must have

a laminar flow because the turbulence damps out. Conversely,

for γ large relative to βR_i , the disc is turbulent right

to the surface. As Stewart points out, this is explained by

noting that large γ corresponds to rapid radiative cooling

which destroys the temperature fluctuations and hence

decreases the buoyancy effect.

In conclusion, it should be noted that in Stewart's

analysis $t_t \gg t_k$ with $t_t \approx t_k$ only when the turbulence is sonic or

supersonic. With Keplerian time scales of 10^{-3} sec. for the

inner region of an accretion disc with a rotating black hole and 10^{-2} sec. for a non-rotating hole (of mass $M_x \approx 10 M_\odot$), in order for the turbulence to be responsible for the rapid X-ray variation (hot blobs rising to surface as an example) Stewart's analysis would suggest a sonic or perhaps supersonic turbulence to be present. Our own work will show (Chapters 3 and 4) that energetic solar type flares may account for these rapid variations even in the case of subsonic turbulence in the disc.

We now turn to generalize the study of fluctuations in a turbulent accretion disc to the case that magnetic fields are included.

3. Equations Of Motion Including Magnetic Fields

3.1 The Basic Equations For A Fluid In A Magnetic Field

We now wish to study the dynamics of a turbulent, thin accretion disc when magnetic fields are included. To this end the complete set of equations describing a magnetic fluid are listed after which the decompostion of these fields (including the magnetic field) into mean and fluctuating parts will lead to the same type of analysis for the fluctuations as found in section 2.3.

For a magnetic fluid the continuity equation 2.1 is still valid. The Navier-Stokes equations 2.2 must now contain a

contribution on the right hand side from the Lorentz force.

$$\underline{f} = \underline{j} \times \underline{b} / c \quad = \left(\nabla \times \underline{b} \right) \times \underline{b} / 4\pi$$

This force may be written as the divergence of the Maxwell stress tensor, i.e

$$f^{\alpha} = \sigma^{\alpha\beta}{}_{;\beta} \tag{2.38}$$

where

$$\sigma^{\alpha\beta} = \left(b^{\alpha} b^{\beta} - \frac{1}{2} \left(b^i b_i \right) \delta^{\alpha\beta} \right) / 4\pi \tag{2.39}$$

and hence equation 2.2 becomes

$$\left(\rho \dot{u}^{\alpha} \right) + \left(\rho u^{\alpha} u^{\beta} \right)_{;\beta} = \rho^{\psi'\alpha} - p'^{\alpha} - t^{\alpha\beta}{}_{;\beta} + \sigma^{\alpha\beta}{}_{;\beta} \tag{2.40}$$

The electromagnetic fields in moving conductors are given by the equations

$$-\frac{1}{c} \frac{\partial \underline{b}}{\partial t} = \nabla \times \underline{e}$$

$$\nabla \times \underline{b} = 4\pi \underline{j} / c = \frac{4\pi\sigma}{c} \left[\underline{e} + \frac{\underline{u} \times \underline{b}}{c} \right]$$

where $\nabla \cdot \underline{b} = 0$ and where σ is the conductivity.

Solving for the electric field $\underline{e}$ in terms of $\underline{b}$ by the second equation, and substituting into the first, assuming that the conductivity is uniform (or nearly so) gives rise to the so-called induction equation of magnetohydrodynamics,

$$\frac{\partial \underline{b}}{\partial t} = \nabla \times \left(\underline{u} \times \underline{b} \right) + \eta \nabla^2 \underline{b} \tag{2.41}$$

where the magnetic diffusivity η is defined by $\eta = c^2/4\pi\sigma$. The use of this equation implies that the conductivity is independent of the magnetic field which requires that the mean free path of the electrons be small compared with the radius of curvature of their orbits in a magnetic field. This condition may break down in regions of sufficiently low density or high magnetic field strength. More details of the derivation may be found in Moffat's book (1978, Chapter 2).

Finally, the conservation of energy equation must be amended to include the magnetic field. The full equation is

$$\frac{\partial}{\partial t}\left[\left(\tfrac{1}{2}\rho u^2 + \rho \varepsilon - \rho \psi\right) + \frac{b^2}{4\pi}\right] = \nabla \cdot \left[\left\{\rho \underline{u}\left(\tfrac{1}{2}u^2 + \varepsilon + p/\rho - \psi\right) + \underline{u}\cdot\underline{\underline{t}} + \underline{q}\right\} + \right.$$
$$\left. + c\ \underline{e}\times\underline{b}/4\pi \right]$$

$$(2.42)$$

where the energy density $\widetilde{b}^2/8\pi$ contributed by the magnetic field has been included on the left hand side, and the energy flux density $\frac{c}{4\pi}\underline{e}\times\underline{b}$ (the Poynting vector) has been included on the right hand side. Writing $\underline{e}$ in terms of $\underline{b}$ again, the Poynting vector takes the form

$$\frac{c}{4\pi}\ \underline{e}\times\underline{b} = \frac{\eta}{4\pi}(\nabla\times\underline{b})\times\underline{b} - \frac{1}{4\pi}(\underline{u}\times\underline{b})\times\underline{b} \qquad (2.43)$$

which is then substituted into equation 2.42.

Equation 2.42 may be simplified by the same procedure

that leads from the conservation of total energy to equation 2.3. Specifically, we take the dot product of $\underline{u}$ with equation 2.4o (using the continuity equation for additional simplification), the dot product of $\underline{b}$ with equation 2.41, and subtract the resulting equations from 2.42 (with the substitution 2.43). After some algebra one finds

$$(\rho \dot{e}) + (\rho e u^\alpha)_{;\alpha} = p\, u^\alpha_{;\alpha} - t^{\alpha\beta}_{;\beta} - q^\alpha_{;\alpha} + \frac{1}{\sigma} j^\alpha j_\alpha \qquad (2.44)$$

where we recall $\underline{j} = \frac{c}{4\pi} \nabla \times \underline{b}$. Comparison of 2.44 with 2.3 shows that the equation for the internal energy is modified by the addition of the Joule heating term j^2/σ giving the rate of evolution of heat due to Ohmic dissipation. Equations 2.3, 2.40, 2.41 and 2.44 along with the equation of state $p = \rho c_s^2$ form the basic framework of our analysis.

3.2 Equations Governing The Mean And Fluctuating Fields

The decomposition of the various fields into mean and fluctuating components is now introduced where in addition to equation 2.4 we introduce $\underline{b} = \underline{B} + \underline{b}'$ with $\overline{\underline{b}} = \underline{B}$ (and hence $\overline{\underline{b}'} = o$) with

$$\Sigma^{\alpha\beta} \equiv \frac{1}{4\pi} \left[B^\alpha B^\beta - \frac{1}{2} B^2 \delta^{\alpha\beta} \right]$$

$$\sigma'^{\alpha\beta} \equiv \frac{1}{4\pi} \left[b'^\alpha B^\beta + B^\alpha b'^\beta - (b'^i B_i) \delta^{\alpha\beta} \right]$$

$$\sigma''^{\alpha\beta} \equiv \frac{1}{4\pi} \left[b'^\alpha b'^\beta - \frac{1}{2} b'^2 \delta^{\alpha\beta} \right]$$

(a) The Navier-Stokes Equation

The equation for the mean velocity field is

$$\rho_0 (\hat{u}^\alpha)^{\bullet} + \rho_0 \hat{u}^\beta (\hat{u}^\alpha)_{;\beta} = \rho_0 \psi^\alpha - p^{'\alpha} - T^{\alpha\beta}_{;\beta} + \hat{\tau}^{\alpha\beta}_{;\beta} + \left(\Sigma^{\alpha\beta}_{;\beta} + \overline{\sigma^{''\alpha\beta}}_{;\beta} \right) \tag{2.45}$$

where the last two terms are the effects due to the Maxwell stress.

To find the equation for the energy in the mean velocity field we take the dot product of $\hat{u}$ with equation 2.45 and find

$$\rho_0 \left(\frac{\hat{u}^2}{2} \right)^{\bullet} + \rho_0 \hat{u}^\beta \left(\frac{\hat{u}^2}{2} \right)_{;\beta} = \rho_0 \psi_{,\alpha} \hat{u}^\alpha + P \hat{u}^\alpha_{;\alpha} - \hat{\tau}^{\alpha\beta} \hat{E}_{\alpha\beta} -$$
$$- \left(\Sigma^{\alpha\beta} + \overline{\sigma^{''\alpha\beta}} \right) \hat{E}_{\alpha\beta} +$$
$$+ \left[\left(\hat{\tau}^{\alpha\beta} - P \delta^{\alpha\beta} + \Sigma^{\alpha\beta} + \overline{\sigma^{''\alpha\beta}} \right) \hat{u}_\alpha \right]_{;\beta} \tag{2.46}$$

where we see the Maxwell stresses interacting with the strain $\hat{E}_{\alpha\beta}$ of the mean velocity field to transfer energy out of the mean flow.

The energy in the fluctuating velocity field is found by taking the dot product of $\hat{u}'$ with the fully decomposed equation 2.10 and then averaging. The new term that arises as compared with the equation in the absence of magnetic fields (2.11) is

$$\overline{\hat{u}'_\alpha \left(\Sigma^{\alpha\beta}_{;\beta} + \sigma^{'\alpha\beta}_{;\beta} + \sigma^{''\alpha\beta}_{;\beta} \right)}$$

We manipulate this factor as follows:

$$\overline{\hat{u}'_\alpha \left(\Sigma^{\alpha\beta}_{;\beta} + \sigma'^{\alpha\beta}_{;\beta} + \sigma''^{\alpha\beta}_{;\beta} \right)} = \left(\overline{\hat{u}'_\alpha} \Sigma^{\alpha\beta}_{;\beta} + \overline{\hat{u}'_\alpha \sigma''^{\alpha\beta}_{;\beta}} \right) +$$

$$+ \overline{u'_\alpha \sigma'^{\alpha\beta}_{;\beta}}$$

We note that

$$\overline{\hat{u}'_\alpha \sigma'^{\alpha\beta}_{;\beta}} = \overline{u'_\alpha \sigma'^{\alpha\beta}_{;\beta}}$$

if the definition of $\hat{u}'^\alpha$ in terms of u'^α is used (equation 2.8). Using the definition of $\sigma'^{\alpha\beta}$ a rearrangement of this term gives

$$\overline{\underline{u}' \cdot \frac{1}{4\pi} \left[\left(\nabla \times \underline{B} \right) \times \underline{b}' + \left(\nabla \times \underline{b}' \right) \times \underline{B} \right]}$$

$$= -\frac{1}{4\pi} \left[\overline{\left(\underline{u}' \times \underline{b}' \right) \cdot \nabla \times \underline{B}} + \overline{\left(\underline{u}' \times \underline{B} \right) \cdot \nabla \times \underline{b}'} \right]$$

It is most instructive to introduce the electric fields induced by the presence of fluctuating velocities by the definitions

$$\underline{\mathcal{E}} \equiv \overline{\underline{u}' \times \underline{b}'} / c$$

$$\underline{\varepsilon}' \equiv \underline{u}' \times \underline{B} / c$$

(2.47)

If we remember $\underline{J} = \frac{c}{4\pi} \nabla \times \underline{B}$ and $\underline{j}' = \frac{c}{4\pi} \nabla \times \underline{b}'$, then

$$\overline{u'_\alpha \sigma'^{\alpha\beta}_{;\beta}} = - \underline{\mathcal{E}} \cdot \underline{J} - \overline{\underline{\varepsilon}' \cdot \underline{j}'}$$

(2.48)

The fluctuating kinetic-energy equation can therefore be

written as

$$\rho_0 \left(\frac{\tilde{u}^2}{2} \right)^{\cdot} + \rho_0 \, \hat{U}^\beta \left(\frac{\tilde{u}^2}{2} \right)_{;\beta} = - \overline{p'^\alpha \hat{u}'_\alpha} + \overline{t^{\alpha\beta} \hat{e}'_{\alpha\beta}} + \hat{\tau}^{\alpha\beta} \hat{E}_{\alpha\beta} -$$

$$- \overline{\left[\left(t^{\alpha\beta} + \frac{1}{2} \rho \hat{u}'^\alpha \hat{u}'^\beta \right) \hat{u}'_\alpha \right]_{;\beta}} +$$

$$+ \overline{\left(\Sigma^{\alpha\beta}_{\ \ ;\beta} + \sigma''^\alpha\beta_{\ \ ;\beta} \right) \hat{u}'_\alpha} - \mathcal{E}^\alpha J_\alpha - \overline{\varepsilon'^\alpha j'_\alpha}$$

$$(2.49)$$

with the new magnetic terms added on the last line. The term $\overline{\left(\Sigma^{\alpha\beta}_{\ \ ;\beta} + \sigma''^\alpha\beta_{\ \ ;\beta} \right) \hat{u}'_\alpha}$ has the same effect as $-\overline{p'^\alpha \hat{u}'_\alpha}$ in that it adds the pressure $\left(B^2 + \tilde{b}^2 \right)/8\pi$ to the fluid pressure p and hence contributes to the further damping of the turbulence by buoyancy processes as already discussed. In the absence of density fluctuations, the most important effects of the magnetic field are the terms $- \underline{\mathcal{E}} \cdot \underline{J} - \overline{\underline{\varepsilon}' \cdot \underline{j}'}$. Here the electric fields, induced by the interaction of the fluctuating velocity field and the magnetic field, do mechanical work on the system in the presence of currents. We will later confirm that these terms extract energy out of the velocity fluctuations and pump it into the mean and fluctuating magnetic fields respectively.

(b) The Induction Equation

Assuming the decomposition $\underline{b} = \underline{B} + \underline{b}'$ as already discussed, and using the same decomposition for the velocity,

equation 2.41 becomes after averaging

$$\frac{\partial \underline{B}}{\partial t} = \nabla \times \left(\underline{U} \times \underline{B} + \overline{\underline{u}' \times \underline{b}'} \right) + \eta \nabla^2 \underline{B} \qquad (2.50)$$

We notice that in turbulent fluids, the correlation of the fluctuating magnetic and velocity fields gives rise to an electromotive force $\overline{\underline{u}' \times \underline{b}'}$ not present when the flows are laminar. The counterpart of this term in the mean Navier-Stokes equation is the Reynolds stress. Here the similarity ends however because as Moffat (p. 248) points out the Navier-Stokes equations, being non-linear in $\underline{u}$ do not permit the ready calculation of $\overline{u'_i u'_j}$ in terms of mean quantities such as $\underline{U}$. Because the induction equation 2.41 is linear in the magnetic field however, it is possible to calculate $\overline{\underline{u}' \times \underline{b}'}$ in terms of mean field quantities such as $\underline{B}$ in a satisfactory manner. The detailed discussion of this theory is presented in Appendix A. It is important to note that the length and time scales over which the mean magnetic fields vary is assumed to be much larger than the scales involved for the fluctuating field $\underline{b}'$. This idea of separation of scales has been used in the development of the theory of equation 2.50 and has received some support from detailed computer simulations by Pouquet et al (1976).

Equation 2.50 will be studied in detail in the next chapter. The equation governing the energy in the mean

magnetic field may be found by taking the dot product of equation 2.50 with $\underline{B}/4\pi$. Making repeated use of the vector identity

$$\nabla \cdot (\underline{A} \times \underline{B}) = \underline{B} \cdot \nabla \times \underline{A} - \underline{A} \cdot \nabla \times \underline{B}$$

gives

$$\left(\frac{\dot{B^2}}{8\pi}\right) = -\underline{u} \cdot (\nabla \cdot \underline{\underline{\Sigma}}) + \overline{(\underline{u}' \times \underline{b}')} \cdot \frac{\nabla \times \underline{B}}{4\pi} + \frac{\eta}{4\pi} \underline{B} \cdot \nabla^2 \underline{B} +$$

$$+ \frac{1}{4\pi} \nabla \cdot \left[\left((\underline{u} \times \underline{B}) + \overline{(\underline{u}' \times \underline{b}')}\right) \times \underline{B} \right]$$

where recall $\nabla \cdot \underline{\underline{\Sigma}} = \frac{1}{4\pi}(\nabla \times \underline{B}) \times \underline{B}$. Further use of vector identities including

$$\underline{B} \cdot \nabla^2 \underline{B} = -\underline{B} \cdot \nabla \times \nabla \times \underline{B} = -\left[\nabla \cdot ((\nabla \times \underline{B}) \times \underline{B}) + (\nabla \times \underline{B})^2 \right]$$

allows the above equation to be written as

$$\left(\frac{\dot{B^2}}{8\pi}\right) = \underline{\underline{\Sigma}} : \underline{\underline{E}} + \overline{(\underline{u}' \times \underline{b}')} \cdot \nabla \times \underline{B}/4\pi - (\eta/4\pi)(\nabla \times \underline{B})^2 +$$

$$+ \nabla \cdot \left[\frac{(\underline{u}' \times \underline{b}') \times \underline{B}}{4\pi} + \left(\frac{(\underline{u} \times \underline{B}) \times \underline{B}}{4\pi} - \underline{u} \cdot \underline{\underline{\Sigma}}\right) - \eta \nabla \cdot \underline{\underline{\Sigma}} \right]$$

where $\underline{\underline{E}}$ is the symmetric strain tensor arising from $\underline{u}$. Now it is easily shown that

$$\frac{1}{4\pi} (\underline{u} \times \underline{B}) \times \underline{B} - \underline{u} \cdot \underline{\underline{\Sigma}} = -\left(\frac{B^2}{8\pi}\right) \underline{u}$$

so that with a little manipulation with this factor and use of the definition $\underline{\xi} = \overline{\underline{u}' \times \underline{b}'}/c$ gives

$$\left(\frac{\dot{B^2}}{8\pi}\right) + \underline{u} \cdot \nabla \left(\frac{B^2}{8\pi}\right) = -\left(\frac{B^2}{8\pi}\right) \nabla \cdot \underline{u} + \underline{\underline{\Sigma}} : \underline{\underline{E}} + \underline{\xi} \cdot \underline{J} - J^2/\sigma -$$

$$- \nabla \cdot \left[\frac{\eta}{4\pi} (\nabla \times \underline{B}) \times \underline{B} - \frac{c}{4\pi} \underline{\xi} \times \underline{B} \right] \qquad (2.51)$$

The right hand side of this equation contains the work done by the magnetic pressure $B^2/8\pi$, the interaction of the Maxwell stress with mean stress, our $\underline{E} \cdot \underline{J}$ term which here enters with a positive sign while in equation 2.49 it enters with a negative sign, the dissipation due to Ohmic heating, and the divergence of the electromagnetic energy flux which takes the form of the Poynting vector for a moving conductor. The appearance of $+ \underline{E} \cdot \underline{J}$ in equation 2.51 and $- \underline{E} \cdot \underline{J}$ in equation 2.49 for the fluctuations indicates that energy transfer from the fluctuating velocity field into the mean magnetic field is occurring. In order to have an advective term on the left hand side of $\hat{\underline{u}} \cdot \nabla (B^2/8\pi)$ we use $\underline{u} = \hat{\underline{u}} + \overline{\underline{u}'}$ with $\underline{E} = \hat{\underline{E}} + \hat{\underline{e}}'$ (using equations 2.6 and 2.8) to obtain, with a little rearrangement,

$$\left(\frac{B^2}{8\pi} \right)^{\cdot} + \hat{u}^\alpha \left(\frac{B^2}{8\pi} \right)_{;\alpha} = - \left(\frac{B^2}{8\pi} \right) \hat{u}^\alpha_{;\alpha} + \sum^{\alpha\beta} \left(\hat{E}_{\alpha\beta} + \hat{e}'_{\alpha\beta} \right) +$$

$$+ \; \underline{E}^\alpha J_\alpha \; - \; J^\alpha J_\alpha / \sigma \; -$$

$$- \left[\left(\frac{\eta}{4\pi} \left((\nabla \times \underline{B}) \times B \right)^\alpha - \frac{c}{4\pi} (\underline{E} \times \underline{B})^\alpha \right) + \frac{B^2}{8\pi} \overline{\hat{u}'^\alpha} \right]_{;\alpha}$$

$$(2.52)$$

The induction equation for the fluctuating magnetic field is found by decomposing the full induction equation 2.42 and subtracting the mean induction equation 2.50 to give

$$\frac{\partial \underline{b}'}{\partial t} = \nabla \times \left(\underline{u} \times \underline{b}' + \underline{u}' \times \underline{B} + \underline{G} \right) + \eta \nabla^2 \underline{b}' \qquad (2.53)$$

where

$$\underline{G} \equiv \overline{\underline{u}' \times \underline{b}'} - \overline{\underline{u}' \times \underline{b}'}$$

Neglect of the term $\nabla \times \underline{G}$ (the "first order smoothing approximation", see Appendix A.1) is possible when the turbulence is imagined to be a collection of random waves with $\tau_u \ll \ell_u / \widetilde{u}$. We shall be adopting this assumption in our calculations, and more about its role may be found in Appendix A.2. To find the equation for the energy in the magnetic fluctuations we take the dot product of equation 2.53 with $\underline{b}' / 4\pi$. Proceeding by exactly the manipulations we used to find equation 2.51, the result is:

$$\left(\frac{\dot{\overline{b'^2}}}{8\pi} \right) + \underline{u} \cdot \nabla \left(\frac{\overline{b'^2}}{8\pi} \right) = - \left(\frac{\overline{b'^2}}{8\pi} \right) \nabla \cdot \underline{u} + \overline{\underline{\underline{\sigma}''}} \cdot \underline{\underline{E}} + \overline{\underline{\varepsilon}' \cdot \underline{j}'} - \overline{\frac{j'^2}{\sigma}} -$$

$$- \nabla \cdot \left[\frac{1}{4\pi} \overline{(\nabla \times \underline{b}') \times \underline{b}'} - \frac{c}{4\pi} \overline{\underline{\varepsilon}' \times \underline{b}'} \right] \quad (2.53\,b)$$

analagous to equation 2.51. In this equation the fluctuating magnetic pressure $\overline{b'^2} / 8\pi$ is doing work, the fluctuating magnetic stress which transferred energy out of the mean flow is here acting as an energy source, the $\overline{\underline{\varepsilon}' \cdot \underline{j}'}$ term is transferring energy into $\overline{b'^2}$ from the fluctuating velocity field, Ohmic dissipation due to the fluctuating currents is dissipating energy as heat, and finally the divergence of the energy flux vector (which takes the form again of a Poynting vector in a moving conductor) is the last term in 2.53b. Again, in order to have the same type of advective term on the left hand side of 2.53b as Stewart has, we follow the same

procedure used in going from 2.51 to 2.52 to find

$$\left(\frac{\overline{b'^2}}{8\pi}\right)^{\cdot} + \hat{u}^\alpha\left(\frac{\overline{b'^2}}{8\pi}\right)_{;\alpha} = -\left(\frac{\overline{b'^2}}{8\pi}\right)\hat{u}^\alpha_{;\alpha} + \overline{\sigma''^{\alpha\beta}}\left(\hat{E}_{\alpha\beta} + \overline{\hat{e}'_{\alpha\beta}}\right) +$$

$$+ \overline{\varepsilon'^\alpha j'_\alpha} - \overline{j'^\alpha j'_\alpha}/\sigma -$$

$$- \left[\left(\frac{\eta}{4\pi}\overline{\left((\nabla\times\underline{b}')\times\underline{b}'\right)^\alpha} - \frac{c}{4\pi}\overline{\left(\underline{\varepsilon}'\times\underline{b}'\right)^\alpha}\right) + \frac{\overline{b'^2}}{4\pi}\overline{\hat{u}'^\alpha}\right]_{;\alpha}$$

$$(2.54)$$

(c) The Internal Energy Equation

The correction due to the magnetic fields is simply the addition of the Ohmic heating term appears in equation 2.44. If this equation is averaged (using the standard decomposition), we find that the mean internal energy equation for $\hat{E}$ has the terms $\left(J^2 + \overline{j'^2}\right)/\sigma$ as source terms on the right hand side of the equation indicating that the Ohmic dissipation J^2/σ of the mean field $\underline{B}$ and the Ohmic dissipation $\overline{j'^2}/\sigma$ from the fluctuating field $\underline{b}'$ are being transferred into the mean internal energy.

The equation for the mean-square thermal fluctuation is just

$$\frac{1}{2}\rho_0 c_v\left(\tilde{\theta}^2\right)^{\cdot} + \frac{1}{2}\rho_0 c_v\,\hat{u}^\alpha\left(\tilde{\theta}^2\right)_{;\alpha} = \overline{\hat{\theta}'\,p\,u^\alpha_{;\alpha}} - \overline{q^\alpha_{;\alpha}\,\hat{\theta}'} -$$

$$- c_v\,T_{,\alpha}\,\rho\,\overline{\hat{\theta}'\,\hat{u}'^\alpha} - \frac{1}{2}\overline{\left(\rho c_v\,\hat{\theta}'^2\,\hat{u}'^\alpha\right)_{;\alpha}} +$$

$$+ \eta\,\overline{\hat{\theta}'\,(\nabla\times\underline{b})^2}$$

$$(2.55)$$

It turns out that because the diffusivity η and not a turbulent magnetic diffusitivity appears in this last term, that it is negligible as far as the $\widetilde{\theta}$ fluctuations are concerned.

(d) Summary

The energy flow arising only from the new magnetic terms is summarized briefly. These effects are in addition to those discussed in section 2. Here we ignore the terms appearing as divergences ($\nabla \cdot [\quad]$) as discussed in section 2.

(1) Mean-flow Kinetic Energy: (equation 2.46)

1. Energy loss $-\left(\Sigma^{\alpha\beta} + \overline{\sigma''^{\alpha\beta}}\right)\widehat{e}'_{\alpha\beta}$ due to interaction of Maxwell stresses with the "mean" strain.

(2) Fluctuating Flow Kinetic Energy: (equation 2.49)

1. Energy loss $-\left(\Sigma^{\alpha\beta} + \overline{\sigma''^{\alpha\beta}}\right)\overline{\widehat{e}'_{\alpha\beta}}$ due to interaction of Maxwell stresses with strain $\overline{\widehat{e}'_{\alpha\beta}}$.

2. Energy loss $-\left(\mathcal{E}^{\alpha}J_{\alpha} + \overline{\mathcal{E}'^{\alpha}j'_{\alpha}}\right)$ due to the presence of fluctuating electric fields in a turbulent medium.

(3) Mean Magnetic Energy: (equation 2.53)

1. Energy gain $+\Sigma^{\alpha\beta}\left(\widehat{E}_{\alpha\beta} + \overline{\widehat{e}'_{\alpha\beta}}\right)$ which arises from the mean and fluctuating velocity fields respectively

2. Energy gain $+\mathcal{E}^{\alpha}J_{\alpha}$ which arise from the fluctuating

velocity field

    3. Energy loss $\quad - J^2/\sigma \quad$ which goes into the mean internal energy.

(4) <u>Fluctuating Magnetic Energy:</u> (equation 2.54)

    1. Energy gain $\quad + \overline{\sigma''^{\kappa\beta}} \left(\hat{E}_{\kappa\beta} + \widetilde{e}'_{\kappa\beta} \right)$ arising from the mean and fluctuating velocity fields respectively

    2. Energy gain $\quad \overline{\varepsilon'^{\kappa} j'_{\kappa}} \quad$ arising from the fluctuating velocity field

    3. Energy loss $\quad \overline{j'^2}/\sigma \quad$ which goes into the mean internal energy

    The next section will concern itself with the effect the magnetic fields have on the structure of the mean flow.

3.3 Consequences Of The Mean Momentum Conservation Equation (Including Magnetic Effects) For Thin Discs

    This section is entirely analagous to the analysis in section 2.2 except equation 2.45 (which includes the Maxwell stresses) is used instead of equation 2.9. We use exactly the same approximations (thin disc, axial symmetry, etc.) as given in section 2.2. In addition, and in conformity with the usual MHD assumptions,we add

    (E) the length scale $l_{b'}$ over which the magnetic fluctuations $\underline{b}'$ occur are of order of those over which the velocity fluctuates; $\quad \ell_{b'} \approx \ell_u$.

In the <u>low</u> <u>Mach</u> <u>number</u> regime; $M_t \ll 1$, we have $l_u \ll z_o$ (see Shakura et al (1978) and Chapter 3) and it is consistent from the "separation of scales" idea to imagine that the mean field varies on length scales $L \gtrsim z_o$.

In the <u>high</u> <u>Mach</u> <u>number</u> regime; $M_t \approx 1$, we have $l_u \approx z_o$ and the idea of a mean field is really only valid on scales $L \gg z_o$.

Chapter 3 will compute the structure of the mean magnetic field in the low Mach number regime, and in Chapter 4 it is shown that this regime produces magnetic fluctuations of a magnitude sufficient to explain the shot-noise model as has been discussed in Chapter 1.

1. The <u>z-component</u> of equation 2.45 gives with the assumptions given (compare with 2.15)

$$\rho_o \frac{V_k^2}{r^2} = -P_{,z} + \hat{\tau}^{zz}_{,z} + \sum^{zz}_{,z} + \overline{\sigma''^{zz}}_{,z} \qquad (2.56)$$

and using the estimates

$$\overline{\sigma''^{zz}}_{,z} \approx \overline{b'^2} / 8\pi l_u \qquad (M_t \ll 1)$$
$$\approx \overline{b'^2} / 8\pi z_o \qquad (M_t \approx 1)$$
$$\sum^{zz}_{,z} \approx B^2 / 8\pi z_o \qquad (M_t \ll 1)$$

$$\qquad (2.57)$$

shows that

$$\left(\frac{z_o}{r}\right)^2 \approx \frac{(c_s^2 + V_A^2) + (z_o/l_u)[\tilde{u}^2 + \tilde{v}_A^2]}{V_k^2} \qquad (M_t \ll 1)$$

$$\approx \frac{c_s^2 + \tilde{u}^2 + \tilde{v}_A^2}{V_k^2} \qquad (M_t \approx 1)$$

$$\qquad (2.58)$$

where the Alfven velocities

$$V_A^2 \equiv B^2/8\pi \rho_0 \qquad\qquad \tilde{v}_A^2 \equiv \overline{b'^2}/8\pi \rho_0$$

have been used. Thin discs then require that in addition to the requirements in section 2 that

$$V_A^2/V_K^2 \ll 1 \qquad ; \qquad \tilde{v}_A^2/V_K^2 \ll l_u/z_0 \qquad\qquad (M_t \ll 1)$$

$$\tilde{v}_A^2/V_K^2 \ll 1 \qquad\qquad (M_t \approx 1)$$

The previous inequalities are derived under the assumption that we are averaging the fluctuations over the large-scales and long-times characteristic for the mean flow. These scales may be identified as r for spatial variation and the drift time scale $t_0 = r/u^r \gg t_K$.

It is important to note that the possibility of intense fluctuations

$$\tilde{v}_A^2/V_K^2 \approx 1$$

on short length scales l_u and on very short time scales $\tau_u < t_K$ is not ruled out.

2. The <u>r-component</u> of equation 2.45 gives to lowest order

$$V \approx V_K$$

provided that the results for 2.58 with $z_0/r \ll 1$ hold.

3. The <u>ϕ-component</u> of equation 2.45 gives

$$\langle \rho_0 u \rangle \frac{(r V_K)_{,r}}{r} \approx \frac{\left(r^2 \langle \hat{P}^{\phi r} + \Sigma^{\phi r} + \overline{\sigma''^{\phi r}} \rangle\right)_{,r}}{r^2} \qquad\qquad (2.59)$$

More will be said about these Maxwell stresses in this chapter and in Chapter 4.

4. Energy Balance For The Fluctuating Fields (Including Magnetic Effects)

This section proceeds in similar fashion to section 2.3 except we have now three coupled equations for $\tilde{u}^2$, $\tilde{\theta}^2$ and $\tilde{b}^2$ instead of just two for $\tilde{u}^2$ and $\tilde{\theta}^2$. We assume stationarity (i.e. $D/Dt = 0$) and discard the terms in these equations involving divergences of quantites.

With these stated approximations and assumptions, and by splitting up the Maxwell stresses into diagonal (the magnetic pressure) and off-diagonal parts, the equations governing the fluctuations are from equation 2.49

$$-\overline{\left[p'^{\alpha} + \frac{(B^2 + \overline{b'^2})'^{\alpha}}{8\pi} \right] \hat{u}'_{\alpha}} + \overline{t^{\alpha\beta} \hat{e}'_{\alpha\beta}} + \hat{T}^{\alpha\beta} \hat{E}_{\alpha\beta} -$$

$$-\overline{(B^{\alpha}B^{\beta} + b'^{\alpha}b'^{\beta}) \hat{e}'_{\alpha\beta} \over 4\pi} - \mathcal{E}^{\alpha} J_{\alpha} - \overline{\mathcal{E}'^{\alpha} j'_{\alpha}} = 0 \qquad (2.60)$$

from equation 2.54

$$-\overline{\left(\frac{\overline{b'^2}}{4\pi}\right) \hat{U}^{\alpha}_{;\alpha}} + \overline{\frac{b'^{\alpha} b'^{\beta}}{8\pi}} \hat{E}_{\alpha\beta} + \overline{\mathcal{E}'^{\alpha} j'_{\alpha}} - \overline{j'^{\alpha} j'_{\alpha}}/\sigma = 0 \qquad (2.61)$$

and from equation 2.55

$$-\overline{\hat{\theta}' p u^{\alpha}_{;\alpha}} - c_v T_{,\alpha} \rho \overline{\hat{\theta}' \hat{u}'^{\alpha}} + \eta \overline{\hat{\theta}' (\nabla \times \underline{b})^2} - \overline{q^{\alpha}_{;\alpha} \hat{\theta}'} = 0 \qquad (2.62)$$

where in writing 2.60 the remaining term arising from the off

diagonal Maxwell stresses may be written as a divergence and hence ignored.

All of the purely hydrodynamic effects will remain unchanged from the estimates used in section 2.3 if we assume that the magnetic fields do not alter the underlying turbulence too much. This will be an assumption we shall employ throughout this thesis and justification for this procedure will be found in Chapter 4.

(1) <u>Analysis</u> <u>Of</u> <u>Equation</u> <u>2.60</u>

We note that the first term is approximately

$$- \left[\frac{\partial}{\partial z} \left(P + (B^2 + \overline{b'^2})/8\pi \right) \right] \frac{\overline{\rho' w'}}{\rho_0}$$

and from equation 2.56 which expresses magnetohydrostatic equilibrium we have

$$- \frac{1}{\rho_0} \frac{\partial}{\partial z} \left(P + (B^2 + \overline{b'^2})/8\pi \right) = g \tag{2.63}$$

so that

$$\overline{\left[P'^\alpha + (B^2 + \overline{b'^2})'^\alpha /8\pi \right] \hat{u}'_\alpha} \approx \frac{\rho_0 g}{T} c_\theta \tilde{u} \hat{\theta} \tag{2.64}$$

The next terms are the viscous dissipation and the energy source which are given by equations 2.27 and 2.28 respectively. In comparison to the first three terms, the term

$$\overline{\frac{\left(B^\alpha B^\beta + b'^\alpha b'^\beta \right)}{4\pi} \hat{e}'_{\alpha\beta}}$$

will be treated as negligible since only the small strain $\hat{e}'_{\alpha\beta}$ is involved.

Finally, we consider the terms $\underline{\varepsilon} \cdot \underline{J}$ and $\overline{\varepsilon' \cdot \underline{j}'}$. These terms are computed in Appendix B where we find (equations B.31 and B.34)

$$\overline{\varepsilon' \cdot \underline{j}'} \approx \frac{n_T}{\mathcal{L}_u^2} \, B^2 / 4\pi$$

$$\underline{\varepsilon} \cdot \underline{J} \approx \frac{n_T}{(L_z^B)^2} \, B^2 / 4\pi \left\{ \frac{L_z^B}{L_z} - 1 \right\} \qquad (2.65)$$

$$L_z^{-1} \equiv \rho_0^{-1} \, \partial \rho_0 / \partial z \qquad ; \qquad L_z^{B^{-1}} \equiv B^{-1} \, \partial B / \partial z$$

where the length scales for the mean density L_z and magnetic field L_z^B are defined and where the turbulent diffusivity n_T is

$$n_T \approx \tilde{u}^2 \, T_u \qquad (2.66)$$

As already discussed, $\overline{\varepsilon' \cdot \underline{j}'}$ and $\underline{\varepsilon} \cdot \underline{J}$ are the rates at which energy from the velocity fluctuations is being pumped into the fluctuating and mean magnetic fields respectively. From equation 2.65, we see that $\underline{\varepsilon} \cdot \underline{J}$ is positive only if the vertical scale of the mean field L_z^B is larger than the scale L_z for the vertical density profile. It is precisely under these conditions that the magnetic field is stable with respect to the magnetic buoyancy process (see discussion later in this section). When $L_z^B/L_z < 1$, the magnetic field cannot exist in a stable configuration and such a region of gas becomes buoyant.

The other important feature about equations 2.65 is that the ratio

$$\frac{\overline{\underline{\varepsilon}' \cdot \underline{j}'}}{\underline{\varepsilon} \cdot \underline{j}} \; > \; \left(\frac{L_z^B}{\ell_u}\right)^2 \; \gg \; 1$$

holds in the low Mach number regime $M_t \ll 1$. We see that energy is being transferred into the magnetic fluctuations at a rate $(L_z^B/\ell_u)^2$ faster than the rate into the large-scale mean magnetic field. If we approximate $L_z^B \approx z_o$ as an example, and denote ΔT_B as the growth time scale for the mean field , and $\Delta T_{\tilde{b}}$ as the growth time scale for the fluctuating magnetic field, then

$$\Delta T_B \; \approx \; \left(z_o/\ell_u\right)^2 \; \Delta T_{\tilde{b}} \; = \; M_t^{-2} \; \Delta T_{\tilde{b}}$$

We will assume that we are in the low Mach number regime for which $\overline{\underline{\varepsilon}' \cdot \underline{j}'} \gg \underline{\varepsilon} \cdot \underline{j}$.

Collecting all these approximations and substituting into equation 2.60 gives

$$\left(-r\Omega'\right) c_u \, \tilde{u}^2 \; \approx \; -c_\theta \frac{\tilde{u}\,\tilde{\theta}}{T} g \; + \; \frac{\tilde{u}^3}{\ell_u} \; + \; \frac{u_T}{\ell_u^2} \frac{B^2}{4\pi \rho_o} \qquad (2.67)$$

In this equation we find the energy source of the velocity fluctuations given by the Reynolds stress on the left hand side balanced by losses to the turbulent kinetic energy by buoyancy, viscosity, and energy transfer into the magnetic

fields.

Equation 2.67 shows that we must provide an analysis of the ultimate mean field energy $B^2/8\pi$ in terms of the turbulent kinetic energy if our equations are to be closed. This is a very difficult problem in general. If the mean field grows to equipartition strengths (via dynamo action) it must very strongly effect the turbulence in such a way that no further growth is possible. However, Malkus and Proctor (1975) have analyzed a mechanism by which the mean field growth is arrested at below equipartition strengths, a mechanism which involves the generation of large scale velocity fields instead of the suppression and alteration of the underlying turbulence. As already mentioned, this is discussed in Chapter 4 where it is shown that in line with Malkus and Proctor we estimate

$$B^2/4\pi\rho_0 \sim O\left(\Omega_k m_T\right) \qquad (2.68)$$

(2) Analysis Of Equation 2.61:

The use of equation 2.65 to approximate $\overline{\varepsilon' \cdot j'}$ yields

$$\left[-\frac{\overline{b'^2}}{4\pi}\frac{1}{r}\frac{\partial}{\partial r}(r \cdot u^r) + \overline{b'^\phi b'^r}(r\Omega')\right] + \left[\frac{m_T}{l_u^2}\frac{B^2}{4\pi} - \frac{\eta}{l_j^2}\frac{\overline{b'^2}}{4\pi}\right] = 0 \qquad (2.69)$$

where we have noted that $\underline{u}$ is axisymmetric and $u^r \gg u^z$ and where

$$\overline{j'^2}/\sigma = \eta\frac{\overline{(\nabla \times b')^2}}{4\pi} \approx \frac{\eta}{l_j^2}\frac{\overline{b'^2}}{4\pi}$$

in which ℓ_j is the relevant scale length for the fluctuating current. We have grouped the first two terms together because they represent magnetic interactions with the mean velocity field, whereas the last two terms represent processes on the microscales.

We first note that the Ohmic diffusion time scale is ℓ_u^2/η (see Moffat) so that we set $\ell_j \approx \ell_u$ *and hence

$$\left[-\overline{b'^2} \, \frac{1}{r} \frac{\partial}{\partial r} (r \, U^r) + \overline{b'^{\phi} b'^r} \, (r \Omega') \right] + \frac{1}{\ell_u^2} \left[\eta_T \, B^2 - \overline{b'^2} \, \eta \right] = 0$$
$$(2.70)$$

In the absence of a mean flow field, equation 2.70 reduces to

$$\overline{b'^2} = \frac{\eta_T}{\eta} \, B^2$$
$$(2.71)$$

which is exactly the result found by Krause and Roberts (1976) and their analysis is summarized in Appendix A.2. This important result shows that in astrophysical settings where $\eta_T \gg \eta$, the fluctuating fields can be much more powerful than the mean magnetic field. It is very important to note that this result (equation 2.71) does not violate the first order smoothing approximation (see Appendix A.2). As Krause and Roberts point out, the part of $\underline{b}'$ that is correlated with $\underline{u}'$ ($\underline{b}'_{corr}$) is of order

$$b'_{corr} \approx \left(\tau_u \, \tilde{u} / \ell_u \right) B \ll B$$
$$(2.72)$$

* This result is valid provided that $\tau_u \tilde{u}/\ell_u \ll 1$, an approximation valid for the sun and assumed valid for the accretion disc as well.

where the last inequality is a consequence of the first order smoothing approximation in which the turbulence is idealized as a collection of random waves with $\tau_u \tilde{u}/l_u \ll 1$.

We now consider the effect of a mean flow on the results of Krause and Roberts. These authors obtained the result 2.71 in the absence of a mean flow by solving the induction equation for the fluctuations

$$\frac{\partial \underline{b}'}{\partial t} - \eta \nabla^2 \underline{b}' = \nabla \times (\underline{u}' \times \underline{B})$$

as an inhomogeneous equation using the Green's function

$$G(\tau, \xi) = (4\pi \eta \tau)^{-3/2} \exp(-\xi^2/\eta\tau)$$

for the diffusion operator

$$\frac{\partial}{\partial t} - \eta \nabla^2$$

Krause and Roberts (1973) consider how these results are affected by the presence of mean flows. When we have a non-zero mean flow $\underline{U}$, the induction equation for the fluctuations may be written (taking $\nabla \cdot \underline{U} = 0$)

$$\frac{\partial \underline{b}'}{\partial t} + (\underline{U} \cdot \nabla \underline{b}' - \underline{b}' \cdot \nabla \underline{U}) - \eta \nabla^2 \underline{b}' = \nabla \times (\underline{u}' \times \underline{B})$$

Regarding $\underline{U}$ as a constant over the scales that $\underline{b}'$ varies then if we Fourier transform the above equation for $\underline{b}'$ the frequencies ω over which $\underline{b}'$ vary are Doppler shifted by the mean velocity $\underline{U}$ to

$$\omega \rightarrow \omega' = \omega - \underline{U} \cdot \underline{k}$$

so that the mean flow has a negligible effect on the result 2.71 provided

$$\frac{\underline{u} \cdot \underline{k}}{\omega} \ll 1$$

or in other words, if T is the time scale and r the length scale for $\underline{U}$,

$$\frac{\tau_u}{T} \ll \frac{\ell_u}{r} \qquad\qquad (2.72)$$

This same result is found using the Green's function approach if we note that the Green's function becomes roughly

$$G(\tau, \varsigma) \approx (4\pi \eta \tau)^{-3/2} \exp\left(-(\varsigma - U\tau)^2 / \eta \tau\right)$$

Hence, in the limit 2.72, we find that equation 2.71 holds so that from equation 2.70

$$\overline{b'^\phi b'^r} (r\Omega') - \overline{b'^2} \frac{1}{r} \frac{\partial}{\partial r}(r U^r) \doteq 0 \qquad\qquad (2.73)$$

In the small correlation time limit, and for $\tau_u \ll T$, the time scales over which the last two terms in equation 2.70 are in balance are much shorter that the time scales over which energy is being transferred out of the mean flow (the first two terms in 2.70).

The limit 2.72 may be regarded as the smallest time τ_u that gives the result 2.71 (and consequently 2.73). Equation 2.73 shows that on Keplerian time scales, the fluctuations

b'^{ϕ} are much larger than b'^{r}. This is understood by observing that on such time scales, the strong shear of the Keplerian flow is stretching the radial field lines of b'^{r} into toroidal field lines of b'^{ϕ}. Rearranging 2.73 slightly

$$\left| \frac{b'^{\phi} b'^{r}}{\tilde{b}^{2}} \right| \approx \left| \frac{u^{r}}{u^{\phi}} \right| = \left| \frac{u^{r}}{V_{\kappa}} \right| \ll 1 \tag{2.74}$$

where $\widetilde{b^{\phi}} \gg \widetilde{b^{r}}$ implies that $\tilde{b}^{2} \approx \overline{b'^{\phi 2}}$. Noting that

$$\overline{\sigma''^{\phi r}} \equiv \overline{b'^{\phi} b'^{r}} / 4\pi$$

we may write equation 2.74 in an interesting way:

$$\overline{\sigma''^{\phi r}} \approx \left[\frac{\tilde{b}^{2}/4\pi\rho_{0}}{u^{\phi 2}} \right] \rho_{0} u^{r} u^{\phi} \tag{2.75}$$

Now $\rho_{0} u^{r} u^{\phi}$ is the magnitude of the stationary stress as discussed in Chapter 1. On the long time $T \gg t_{\kappa}$, long scale $L \gg z_{0}$ magnetohydrostatic balance is maintained. Then from equation 2.58

$$\left(\tilde{b}^{2}/4\pi\rho_{0} \right)_{L,T} \ll V_{\kappa}^{2}$$

where we use L, T to denote these long scale averages. Thus from equation 2.75

$$\left(\overline{\sigma''^{\phi r}} \right)_{L;T} \ll \rho_{0} u^{r} u^{\phi}$$

so that the Maxwell stress due to the magnetic fluctuations is negligible and cannot determine the long scale structure of the accretion disc.

However, on short time and length scales, it is possible

to have magnetic fluctuations up to a maximum amplitude of

$$\tilde{b}^2 / 4\pi \rho_0 \lesssim u^{\phi\,2} \approx V_k^2 \tag{2.76}$$

For these scales, equation 2.73 shows that

$$\overline{\sigma''^{\phi r}} \approx \rho_0 \, u^r u^\phi$$

so that the Maxwell stress from the fluctuations, in small regions and for short times, are of order of the mean, long scale averaged stationary stress (of magnitude $\rho_0 u^r u^\phi$). We return to this point in Chapter 4.

We note that using the result 2.73, and examining the induction equation for $\underline{b}'$ using the assumptions of axial symmetry and disc thinness, that the limit 2.72 may be relaxed somewhat. The point here is that since the fluctuations b'^r are small compared to b'^ϕ, the equation for b'^ϕ shows that the terms involving the mean velocity are

$$\left(\underline{u} \cdot \nabla \underline{b}' - \underline{b}' \cdot \nabla \underline{u} \right)_\phi \approx \left(u^r b_r \right) b'^\phi - b'^r \frac{\partial u^\phi}{\partial r}$$

assuming that the fluctuations are independent of z and ϕ. If the fluctuations b'^r are small enough compared to b'^ϕ (as equation 2.73 shows) then the mean field terms for the predominant fluctuations b'^ϕ nearly cancel out. This implies that we may take the correlation time limit up to values $\tau_u \lesssim t_k$ without too seriously affecting the validity of 2.71 and 2.73.

Finally, it is important to note that when $\tilde{b}^2/4\pi\rho_0 > c_s^2$, the region wherein we find such a high field strength becomes buoyant and rises in the disc, a phenomenon first noted by Parker (1955a) and discussed more generally by Gilman (1970). Basically when the magnetic presure becomes large enough in a region, and assuming at least initially that we have pressure equalization, the gas pressure must drop and if $p \propto \rho$, we see that the density in this region decreases. Consequently, this region of high magnetic field strength floats upward in the gas (assuming $\frac{\partial \rho_0}{\partial z} < 0$). This phenomenon is called "magnetic buoyancy" (coined by Parker), and must of course transfer energy out of the turbulence and cool the region of gas in which this high magnetic fluctuation is prevalent. It is thought to occur in sunspot regions on the sun where very intense fields~10^{3^-} Gauss (much higher than equipartition strength) emerge from the solar surface.

We believe the same mechanism is operative here. The presence of intense magnetic fluctuations $\tilde{b}^2/4\pi\rho_0 \sim V_K^2$ does not violate the thin disc assumption because instead of bulging the disc so that $z_0 \sim r$, these fluctuations are associated with a buoyant region that rises up and eventually results in the emergence of these fields from the surface of the thin disc. We note that the rise time of these regions is roughly the Keplerian time scale. The condition that this magnetic buoyancy mechanism be operative is that the length scale of

the magnetic fluctuation be less that the density scale height, i.e that $\ell_b < z_o$.

The analysis leading to equation 2.73 leads to the result

$$\frac{\widetilde{b}^2}{4\pi} \approx \frac{M_T}{\eta} \frac{B^2}{4\pi} \lesssim \rho_o V_\kappa^2$$

As we have seen for maximal magnetic fluctuations $\widetilde{b}^2/4\pi\rho_o \approx V_\kappa^2$, the stresses induced are $\overline{\sigma^{''4r}} \sim \rho_o u^r u^\phi$. Since magnetohydrostatic equilibrium on time scales $\tau \approx \ell_u/V_\kappa$ is being violated we see that we have large fluctuations $O(\rho_o u^r u^\phi)$ in the stresses responsible for angular momentum transport outward (radially) and net radial inflow. Only if averaging is done on length scales $L \gg z_o$ or time scales $T \gg z_o/V_\kappa$ is it possible to discuss magnetohydrostatic equilibrium given by equation 2.59 or equivalently, equation 2.63. These large magnetic fluctuations then are to be considered as deviations from the mean magnetic fluctuations, which over time scales $T \gg z_o/V_\kappa$ will be of order $\widetilde{b}^2/4\pi\rho_o \lesssim c_s^2$.

(3) Analysis Of Equation 2.62

Using all the approximations that lead to equation 2.33 (a), equation 2.62 is

$$\left(T_{,z} + \frac{P_{,z}}{\rho_o C_v}\right) C_\theta \, \widetilde{\theta} \, \widetilde{u} \; - \; \frac{1}{\rho_o C_v} \, \eta \, \overline{\widetilde{\theta}'(\nabla \times \underline{b})^2} \; = \; - \frac{\widetilde{\theta}^2 \widetilde{u}}{\ell_\theta} \; - \frac{\widetilde{\theta}^2}{t_r}$$

Estimating the Ohmic dissipation term gives

$$\frac{\eta \, \overline{\widetilde{\theta}'(\nabla \times \underline{b})^2}}{\rho_o} \; \approx \; \frac{\eta \, C_\theta \, \widetilde{\theta}}{\ell_u} \left[\frac{\widetilde{b}^2}{4\pi\ell_u \rho_o} - \frac{1}{4\pi\rho_o} \, \widetilde{b} \, \frac{\partial B}{\partial z} \right]$$

$$\approx \; C_\theta \, \widetilde{\theta} \, \widetilde{u} \left(\frac{\eta}{\widetilde{u} \ell_u}\right) \left[\frac{\widetilde{b}^2/4\pi\rho_o}{\ell_u} + \frac{\widetilde{b} \, B/4\pi\rho_o}{z_o} \right]$$

Hence

$$\left(\left[T_{,z} + \frac{P_{,z}}{\rho_0 c_v} \right] - \frac{1}{c_v} \left(\frac{\eta}{\tilde{u}\,l_u} \right) \left[\frac{\tilde{b}^2/4\pi\rho_0}{l_u} + \frac{\tilde{b}\,B/4\pi\rho_0}{z_0} \right] \right) c_\theta\, \tilde{u}\, \tilde{\theta} \; = $$

$$= -\tilde{\theta}^2 \left[\frac{\tilde{u}}{l_\theta} + \frac{1}{t_r} \right] \qquad\qquad (2.77)$$

The important factor here, the turbulent magnetic Reynolds number $\left(R_M^t \right)^{-1} = \frac{\eta}{\tilde{u}\,l_u} \ll 1$ limits the role of Ohmic heating even in the case of maximal magnetic fluctuations. Equation 2.78 shows that because of Ohmic heating, the temperature fluctuations take a higher value than in the absence of magnetic fields.

Consider first the case where time scales are of order z_0/V_k with maximal fluctuations. With a mean field below equipartition we have

$$\left(\left(T_{,z} + \frac{P_{,z}}{\rho_0 c_v} \right) - \frac{1}{l_u c_v} \frac{B^2}{4\pi\rho_0} \right) c_\theta\, \tilde{u}\, \tilde{\theta} = -\tilde{\theta}^2 \left[\frac{\tilde{u}}{l_\theta} + \frac{1}{t_r} \right]$$

where we have used equation 2.77 and $\eta_T/\tilde{u}\,l_u \approx 1$. If the mean field is at equipartition strength $B^2/4\pi\rho_0 \approx c_s^2$, then the heating due to those large magnetic fluctuations is significant and acts to make regions containig the fluctuations hotter than in their absence. However, since we deal with mean fields below equipartition, this magnetic effect will be taken as ignorable.

For longer time scales where we have magnetohydrostatic equilibrium the magnetic terms are $< c_s^2/\ell_u$. Now since $\left(R_M^t\right)^{-1} \ll 1$, the magnetic effects are entirely negligible. We conclude that even for the largest magnetic fluctuations, as long as the mean field is below equipartion strength, the effects of Ohmic heating are negligible and that equation 2.33 (a) is still a good approximation to use for the magnitude of the thermal fluctuations. Hence

$$\tilde{\theta} \approx \frac{-\left(T_{,z} + \frac{1}{\rho_0 c_v} P_{,z} \right) c_\theta \tilde{u}}{\left(\tilde{u}/\ell_\theta + 1/t_r \right)} \qquad (2.78)$$

where we notice that g, given by equation 2.63, contains the magnetic pressure as well and that only the fluid pressure appears in equation 2.78.

We now combine equations 2.78 and 2.68 into equation 2.67 using the estimate 2.66 and where g is given by equation 2.63. We then obtain

$$\left(-r\Omega' \right) c_u \tilde{u}^2 \approx \frac{c_\theta^2 \, \tilde{u}^2 \, g}{T} \frac{\left(T_{,z} + \frac{1}{\rho_0 c_v} P_{,z} \right)}{\left(\tilde{u}/\ell_\theta + 1/t_r \right)} + \frac{\tilde{u}^3}{\ell_u} + \tilde{u}^4 \frac{T_u^2}{\ell_u^2} \Omega$$

$$(2.79)$$

If we note that $\tilde{u} \approx \ell_u/t_t$ and that the last term in equation 2.79 may be written $\tilde{u}^2 \Omega \left(T_u/t_t \right)^2$, the magnetic term adds an $\tilde{u}^2$ dependence which is the same dependence as

found for the Reynolds stress.

As in the analysis leading to equation 2.53, we multiply by $[c_u^3 \, \ell_u^2 \, (-r\Omega')^3]^{-1}$, and by using the definitions of β and γ, as well as equation 2.37 for the Richardson number (where g is given by equation 2.63) we have

$$f_{(x)} \equiv \frac{\beta R_i}{(x+\gamma)} + x + \zeta = 1 \qquad (2.80)$$

where

$$\zeta \equiv \frac{1}{c_u} \left(\frac{\tau_u}{t_t}\right)^2 \qquad (2.81)$$

and as before

$$x \equiv \tilde{u} / c_u \, \ell_u \, (-r\Omega') \approx \tilde{u} \, t_\kappa / c_u \, \ell_u$$

The last term in equation 2.80 represents the energy extracted from the turbulent kinetic energy by the term $\overline{\xi' \cdot f'} + \underline{\xi} \cdot \underline{f}$. As pointed out earlier, we feel the assignment $\tau_u \lesssim t_\kappa$ is appropriate in the disc so that we have

$$\zeta \approx \left(t_\kappa / t_t\right)^2 \frac{1}{c_u} \qquad (2.82)$$

As in section 2 we need only solve equation 2.80 in x. Again it is easier to split the analysis into two cases for convenience.

Case 1. $\gamma = 0$:

Here

$$x = \frac{(1-\zeta) \pm \sqrt{(\zeta-1)^2 - 4\beta R_i}}{2}$$

so that stationary turbulence is only possible provided

$$\beta R_i \leq (1-\zeta)^2 / 4$$

with of course the requirement that $\zeta < 1$. As $\zeta \rightarrow 1$; $\beta R_i \rightarrow 0$, so that turbulence in the whole disc is shut off. If $\zeta = \left(\dfrac{t_\kappa}{t_t}\right)^2 \dfrac{1}{c_u}$, we see that this corresponds to the limit of supersonic turbulence if c_u is estimated as t_κ / t_t. This begins to defy the validity of the theory we have used to derive these results, however, and the situation for $\zeta \rightarrow 1$ is probably considerably more complicated.

Case 2 $\quad \gamma \neq 0$:

Here we find that for

$$\gamma (1-\zeta) < \beta R_i < \frac{1}{4} \left[\gamma + (1-\zeta) \right]^2$$

two stationary turbulent flows are possible, only the flow corresponding to the larger root being stable. For

$$\beta R_i < \gamma [1-\zeta]$$

only one stationary flow is possible and it is stable.

Comparing these results with those found by Stewart in the absence of magnetic fields, shows that for small Mach numbers $M_t \ll 1$, the extraction of energy from the turbulent

kinetic energy by the magnetic fluctuations makes buoyancy a more effective agent in damping the turbulence (i.e. βR_i is restricted to small values if we are to have stationary turbulence). Furthermore, local extreme magnetic fluctuations $\tilde{b}^2/4\pi\rho_o \gg c_s^2$ cause large local values for βR_i which as we see above results in the shutdown of the turbulence in the region.

Our analysis may be put into perspective if we restrict ourselves to low Mach numbers $M_t \ll 1$, wherein $t_k/t_t \ll 1$. The first order smoothing assumption is valid provided we are considering time scales for turbulent disturbances $\tau_u \ll t_t = \frac{\ell_u}{\tilde{u}}$. Since the Keplerian time scale seems to be the fastest one in the problem, by focussing on the time scale $\tau_u \lesssim t_k$, the first order smoothing assumption is being satisfied for $M_t \ll 1$. On this time scale, equation 2.71 holds even in the presence of mean flows and hence large magnetic disturbances can occur. These are to be thought of as local strong perturbations of the overall fluid. Our scenario suggests that as the energy is being transferred into the local fluctuating magnetic field, the turbulence is damped out, the fluid cools and the magnetic field rises to the surface of the disc on times t_k for the largest fluctuation $\tilde{b}^2/4\pi\rho_o \approx V_k^2$ by some magnetic buoyancy type process. These loops of intense field escape from the disc by undergoing reconnection with a neighbouring loop in the manner described in Chapter 1. We leave to Chapter 4 the calculation of the strength of these local intense fields.

We turn now to investigate under what conditions a mean field can be generated by turbulent dynamo action in the accretion disc.

<u>Chapter 3</u>

<u>Solution Of The Induction Equation For The Mean Field B</u>

1. Introduction

As has been pointed out in Chapter 2 and Appendix A, additional terms appear in the induction equation for the magnetic field in a turbulent conductor as contrasted with one in which only laminar flow is occurring. When only a mirror-symmetric turbulence is present, a turbulent diffusivity η_T is added to the usual molecular diffusivity η of the mean magnetic field, and in conditions of high magnetic Reynolds numbers (as usually found in astrophysical flows), $\eta_T \gg \eta$. This indicates that the idea of "frozen- in" field lines of mean magnetic field is incorrect for strongly turbulent flows. When the turbulence possesses helicity, a mean current $\underline{J}$ parallel or anti-parallel to $\underline{B}$ arises and has the effect of regenerating the mean field. Steenbeck, Krause, and Rädler (1966) were able to show that the presence of local rotation and a density gradient induces helicity in the turbulence, thereby providing a mechanism by which dynamo action (self excitation of the mean field at the expense of turbulent kinetic energy) could sustain mean fields (the so-called "α -effect").

When the mean field remains weak (i.e much below equi-

partition with the energy in the turbulence) the Lorentz-force arising from these fields appearing in the Navier-Stokes equation may be regarded as negligible. Consequently, in this situation, prescription of the flow and the turbulence characteristics allows the calculation of $\underline{\mathcal{E}} = \overline{\underline{u}' \times \underline{b}'}$ in terms of $\underline{B}$ and various quantities arising from averaging over turbulent velocity fluctuations. The solution of the induction equation for the mean field (equation 2.50) is then possible if an appropriate set of boundary conditions for the problem on hand is provided.

For sufficiently vigorous helical turbulence, an initially weak mean field of sufficiently large scale will be amplified by dynamo action as has been shown in work on terrestial, solar , and galactic magnetic fields (see Moffat (1978)). Ultimately the field becomes strong enough so that a back-reaction on the flows occurs thereby preventing further growth. The magnetic field can act to suppress or alter the turbulence or induce large scale " mean " flows, both of which arrest further growth of the field.

The importance of the large scale mean magnetic field for accretion problems is three fold:

1. <u>Generation Of Magnetic Fluctuations.</u> The previous chapter has shown that the fluctuation magnetic field energy density is related to the mean magnetic field energy density by $\widetilde{b}^2 = \dfrac{M_T}{\eta} B^2$. The reason for this is understood if the induction

equation for the fluctuating magnetic field is considered (equation 2.53). A velocity fluctuation $\underline{u}'$ interacts with the mean field $\underline{B}$ and over a length scale l_u and time scale τ_u twists up the field line and creates a fluctuating magnetic field $\underline{b}'$ on these same length and time scales. Consequently, information about the amplitude and orientation of $\underline{B}$ allows us to estimate what type of magnetic fluctuations are to be expected.

2. Transport Of Angular Momentum. It was shown in Chapter 2 that the fluctuating Maxwell stress $\overline{\sigma''^{\phi r}}$ was significant only in those localized regions where fluctuations $\tilde{b}^2/4\pi \rho_\circ \sim V_k^2$ occur. Over sufficiently long time scales, these local intense fluctuations are unimportant so far as angular momentum transport in the disc is concerned. However, the mean Maxwell stress $\Sigma^{\phi r}$ contributes to the overall stresses (again on sufficiently long time scales) and hence is important in determining the disc structure.

3. The Presence Of A Magneto-sphere. The intense magnetic fluctuations emerge through the upper and lower surfaces of the accretion disc , and in our picture, engage in subsequent reconnections giving rise to solar type flares. The region exterior to the disc is expected to be of low density. If it is imagined to be a vacuum as an example (an idealization of course) , then the requirement that the exterior vacuum fields match continuously to the interior disc field at the upper and

lower surfaces of of the disc implies the presence of a large-scale, current-free magneto- sphere when large-scale mean fields are present in the disc. The strength and structure of such a large scale vacuum field is important for determining the trajectories that energetic particles leaving the disc region would take and the radiation that they would emit as they spiral along the field lines. More specifically, Blandford (1976) assuming a force-free magneto-sphere and Lovelace (1976), assuming a current free magneto-sphere have tried to construct models of double radio- sources resulting from the presence of magnetized accretion discs around a central compact object. Their work however does not discuss in detail how a large-scale magnetic field may be generated and maintained in the disc. It is felt that the work to be presented here can act as a first step towards a more comprehensive treatment of such theories.

With the previous arguments as a motivation, it will be the object of this chapter to solve the mean field induction equation under conditions appropriate to an accretion disc. It will be the assumption of this chapter that the mean field is initially weak. The mean flow will be taken to be Keplerian and the assumptions made about the turbulence as discussed in chapters 1 and 2 will be employed. Hence, we shall determine on what length and time scales we may expect the mean magnetic field to grow in a prescribed hydrodynamic setting.

In section 2, we begin with equation 2.50 and simplify it as much as possible using the approximations under which the disc structure was solved in the absence of magnetic fields. In particular, it will be assumed that the disc is thin, the mean flow is Keplerian, and that the mean field is axisymmetric. As discussed in Appendix A, it will be assumed that the underlying turbulence is mildly anisotropic so that helicity is present.

It will be necessary to specify the vertical density profile and the disc half-thickness z_0 at all radii. The density is approximately Gaussian in the gas-pressure dominated zone and this permits solution by analytical methods. The parameter z_0 however, depends on r and this is very difficult to deal with when matching to an exterior solution for the magnetic field. We will assume that z_0=const for the purpose of the analysis. As long as the radius of curvature R_0 is large, this defect can be corrected by a perturbation procedure involving a power series expansion in z_0/R_0.

Section 3 is devoted to the solution of the induction equation after the simplifications discussed in section 2 have been applied. In particular, the vertical structure of the mean field will be analyzed extensively. The point of the analysis will be to determine accurately the behaviour of the field near $|z| = z_0$ so that matching with an external vacuum

field can be accomplished. It will be assumed in this section that dynamo action and dissipation exactly balance one another so that stationary conditions prevail. When $M_t \ll 1$, the problem can be solved analytically.

In section 4 we match the disc solutions to an external vacuum field assuming stationarity (on long time-scales). This procedure will result in a relation between the turbulent Mach number M_t and the radial wavenumber of the field.

The final section attacks the same problem again assuming non-stationary conditions. Small deviations from equilibrium are assumed so that the dynamo action and dissipation are very nearly in balance. The procedure results in a dispersion relation linking the complex growth time scale to the turbulent Mach number and the radial wave-number.

It is important to point out that the entire theory being discussed is non-relativistic so that the study of the mean fields at the innermost edge of the disc is not considered. In particular, the electromagnetic boundary conditions at the event horizon are not considered. Recently Znajek (1978) has shown that the boundary conditions satisfied by the electromagnetic fields at the horizon of a Kerr hole may be interpreted in terms of equal electric and magnetic conductivities of such an object. In addition, Blandford and Znajek (1977) showed that electromagnetic fields could extract energy from a rotating hole (Kerr). Various idealizations

about the fields were made in this work, and we believe that the presence of a turbulent disc (not a perfect conductor) could considerably complicate the physics.

2. Analysis Of The Induction Equation For The Mean Field

2.1 Simplifications Arising From The Assumptions Of A Thin Disc And Axisymmetric Field.

We recall the induction equation for the mean field is

$$\frac{\partial \underline{B}}{\partial t} = \nabla \times \left(\underline{U} \times \underline{B} + \underline{\mathcal{E}} - \eta \nabla \times \underline{B} \right)$$

where $\underline{\mathcal{E}} = \overline{\underline{u}' \times \underline{b}'}$ and where we shall be working in cylindrical co-ordinates (r, ϕ, z).

The mean flow $\underline{U}$ is assumed to be $\underline{U} \approx (0, V_k(r), 0)$ which is valid provided that the disc is thin. This differential rotation of the gas contains shearing motions on the length scale r, which is important in the analysis of $\underline{\mathcal{E}}$. Specializing to cylindrical co-ordinates, defining

$$\underline{\mathcal{E}}' \equiv \underline{\mathcal{E}} - \eta \nabla \times \underline{B} \tag{3.1}$$

and assuming axial symmetry

$$\underline{B} = \left(B_r(r, z, t), B_\phi(r, z, t), B_z(r, z, t) \right) \tag{3.2}$$

gives

$$\frac{\partial B_r}{\partial t} = - \frac{\partial}{\partial z} \mathcal{E}'_\phi \tag{3.3}$$

$$\frac{\partial B_\phi}{\partial t} = \frac{\partial}{\partial z} \left[V_k B_z + \mathcal{E}'_r \right] - \frac{\partial}{\partial r} \left[-V_k B_r + \mathcal{E}'_z \right] \tag{3.4}$$

$$\frac{\partial B_z}{\partial t} = \frac{1}{r} \frac{\partial}{\partial r} \left(r \mathcal{E}'_\phi \right) \tag{3.5}$$

Since $\nabla \cdot \underline{B} = 0$, the assumption of axial symmetry for the field $\underline{B}$ allows us to use the representation

$$\underline{B} = \left(-\frac{\partial P}{\partial z} \, , \quad T \, , \quad \frac{1}{r} \frac{\partial}{\partial r} (r P) \right) \tag{3.6}$$

in which P and T are arbitrary functions of r, z, and t, and which will be fixed by substitution of equation 3.6 into equations 3.3-3.5. Equations 3.3 and 3.5 are then entirely equivalent so that only the coupled set 3.3 and 3.4 need be considered. Hence, these equations become, respectively,

$$\frac{\partial P}{\partial t} = \mathcal{E}_\phi' \tag{3.7}$$

$$\frac{\partial T}{\partial t} = \frac{\partial}{\partial z} \left[V_k \frac{1}{r} \frac{\partial}{\partial r} (rP) + \mathcal{E}_r' \right] - \frac{\partial}{\partial r} \left[V_k \frac{\partial P}{\partial z} + \mathcal{E}_z' \right] \tag{3.8}$$

Equation 3.8 may be simplified by noting $V_k = const / r^{1/2}$ so that

$$\frac{\partial T}{\partial t} = \frac{3}{2} \frac{V_k}{r} \frac{\partial P}{\partial z} + \left(\frac{\partial \mathcal{E}_r'}{\partial z} - \frac{\partial}{\partial r} \mathcal{E}_z' \right) \tag{3.9}$$

To proceed, it is necessary to calculate $\underline{\mathcal{E}}$, which is done in Appendix B using the following approximations:

1. Contributions to the helicity are taken to arise from the interaction of the antisymmetric component of the mean strain tensor ($R_{\alpha\beta} = \frac{1}{2} \left(U_{\alpha;\beta} - U_{\beta;\alpha} \right)$) with the density gradient $\rho_0^{-1} \nabla \rho_0$.

2. Gradients of the turbulent intensity $\tilde{u}^2$ are ignored. As discussed in Chapter 2, we expect the turbulent

coefficients to depend only on r (the turbulence is homogeneous in z and ϕ at each radius).

Appendix B shows that

$$\mathcal{E}_r = \alpha \left[B_r - \frac{\epsilon}{4} B_z - \frac{15}{8} L_z \frac{\partial B_z}{\partial r} \right] - \eta_T (\nabla \times \underline{B})_r \qquad (3.10)$$

$$\mathcal{E}_\phi = \alpha B_\phi - \eta_T (\nabla \times \underline{B})_\phi \qquad (3.11)$$

$$\mathcal{E}_z = \alpha \left[\frac{B_z}{2} - \frac{\epsilon}{4} B_r - \frac{15}{8} L_z \frac{\partial B_z}{\partial z} \right] - \eta_T (\nabla \times \underline{B})_z \qquad (3.12)$$

where

$$\underline{L}^{-1} \equiv \rho_0^{-1} \nabla \rho_0 = \rho_0^{-1} \left(\frac{\partial \rho_0}{\partial r}, 0, \frac{\partial \rho_0}{\partial z} \right) \qquad (3.13)$$

$$\eta_T \approx \tilde{u}^2 \tau_u \qquad (3.14)$$

$$\alpha = - \frac{\tilde{u}^2 \tau_u^2}{L_z} \frac{V_k}{r} \left(\frac{2}{5\pi} \right) \qquad (3.15)$$

and where $\epsilon \equiv \frac{\partial \rho_0}{\partial r} / \frac{\partial \rho_0}{\partial z}$ is the ratio of the density scales in the r and z directions. We emphasize that first order smoothing is assumed in these calculations ($Q \equiv \tilde{u} \tau_u / \ell_u \ll 1$) as well as the high conductivity limit $\eta_T / \eta \gg 1$.

For a thin disc, $\epsilon \ll 1$. In addition equation 3.15 shows that

$$\left| \frac{\alpha}{V_k} \right| = Q^2 \frac{\ell_u^2}{r L_z} \qquad (3.16)$$

so even if we relax the small correlation time limit (i.e say $Q \approx 1$) then $\alpha/V_k \approx \ell_u^2/L_z r$, so that $\alpha/V_k \ll 1$ for thin discs. We shall have more to say about this result after we substitute the equations 3.10 - 3.12 into 3.7 and 3.9.

Before we do this we note that

$$\mathcal{E}_r = \alpha \, B_r - m_T \, (\nabla \times \underline{B})_r$$

for thin, axisymmetric discs. Equation 3.12 shows that if the magnetic field length scales are of the same order as the density length scales, then all the terms multiplied by α should be of the same order of magnitude. However, since $\mathcal{E}_r$ and $\mathcal{E}_z$ enters into equation 3.9 in the combination $\frac{\partial \mathcal{E}_r}{\partial z} - \frac{\partial \mathcal{E}_z}{\partial r}$, we estimate that

$$\frac{\partial \mathcal{E}_r}{\partial z} - \frac{\partial \mathcal{E}_z}{\partial r} \approx \frac{\partial}{\partial z}(\alpha \, B_r) - m_T \left[\frac{\partial}{\partial z} (\nabla \times \underline{B})_r - \frac{\partial}{\partial r} (\nabla \times \underline{B})_z \right] \tag{3.17}$$

a result valid only for thin discs.

Noting that the representation 3.6 implies

$$\nabla \times \underline{B} = \left(-\frac{\partial T}{\partial z} , -\Delta P , \frac{1}{r}\frac{\partial}{\partial r}(rT) \right) \tag{3.18}$$

where

$$\Delta \equiv \left\{ \frac{\partial^2}{\partial r^2} + \frac{1}{r}\frac{\partial}{\partial r} - \frac{1}{r^2} + \frac{\partial^2}{\partial z^2} \right\} \tag{3.19}$$

substitution of equations 3.10 - 3.12 into 3.7 and 3.9 gives , using the approximation 3.17

$$\frac{\partial P}{\partial t} = \alpha \, T + (m_T + \eta) \, \Delta P \tag{3.20}$$

$$\frac{\partial T}{\partial t} = \frac{3}{2}\frac{V_k}{r}\frac{\partial P}{\partial z} - \alpha \frac{\partial^2 P}{\partial z^2} + (m_T + \eta) \, \Delta T \tag{3.21}$$

In the limit of high turbulent magnetic Reynolds number, $R_M^t \equiv \frac{\tilde{u}\ell_u}{\eta} \gg 1$ we have $\eta_T \gg \eta$ so that $\eta_T + \eta \approx \eta_T$. Let us rearrange equations 3.20 and 3.21 as (using $\eta_T \gg \eta$)

$$\frac{\partial P}{\partial t} - \eta_T \Delta P = \alpha T \qquad (3.22)$$

$$\frac{\partial T}{\partial t} - \eta_T \Delta T = \frac{3}{2}\frac{V_K}{r}\frac{\partial P}{\partial z} - \alpha \frac{\partial^2 P}{\partial z^2} \qquad (3.23)$$

The first thing to note about these equations is the appearance of the diffusion operator $\frac{\partial}{\partial t} - \eta_T \Delta$ on the left hand sides. It is untenable to assume that the the mean field remains frozen-in to the gas since $\eta_T \gg \eta$. In a sufficiently vigorous turbulence, η_T is so large that the mean fields quickly damp out in the absence of sources. The source terms for the poloidal and toroidal fields have been written on the right hand sides of the equations.

The source for the regeneration of the poloidal field P is the toroidal field T. Dynamo action is generating the poloidal field at the expense of toroidal field. If $\alpha = 0$, (i.e absence of helicity) the poloidal field has no source and hence decays exponentially with a time constant z_0^2/η_T which is not much longer that the Keplerian time scale t_K . With a damped out poloidal field, it is not possible to sustain the toroidal field by differential rotation, and so, very quickly, the entire mean field is dissipated.

There are two sources available for the regeneration of the toroidal field T. The first term on the right hand side of equation 3.23 is a term involving the interaction of the shearing of the toroidal flow ($\frac{\partial V_\kappa}{\partial r}$) with the radial field B_r ($= -\frac{\partial P}{\partial z}$). This term is absent for pure rotation ($\frac{d}{dr}\left(\frac{u_\phi}{r}\right) = 0$). Physically what is happening can be seen in terms of the radial field lines being stretched out in the ϕ direction by the differential rotation, thereby creating toroidal field T. The second source term again represents the effect of helical turbulence, this time resulting in the creation of toroidal field from poloidal field.

The source terms involving $\propto$ are best understood by Parker's (1955b) arguments. Consider an almost uniform long scale field $\underline{B}$ in the r-ϕ plane, in the presence of a vertical density gradient (see Fig. 5). Imagining that small-scale upwellings of fluid occur the field lines will be bent into horseshoe shaped loops. If, in addition, a local rotation is present, these horseshoes get twisted out of their initial planes. Averaging over all of these small-scale twisted horseshoe shaped loops, we see that an initially toroidal mean field should give rise to a radial component of the field (source term in equation 3.22) and an initially radial mean field should give rise to a toroidal component of the field (second source term in equation 3.23). These arguments explain why $\propto$ is dependent on both $\nabla \rho_0$ and $\nabla \times \underline{u}$ and why the

toroidal and poloidal field dependences arise in the source terms as they do.

Fig. 5 The α-Effect In Turbulence With Helicity
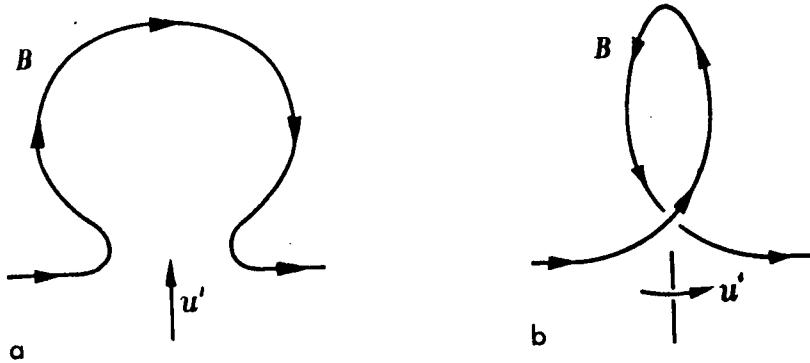
When the term proportional to α in equation 3.23 dominates the term arising from differential rotation, we see that the α-effect is responsible for regenerating both components of the field, a situation called the " α^2-dynamo ". When the differential rotation dominates the α term in 3.23, we have a " $\alpha\omega'$-dynamo ".

We have already noted that $\alpha/V_k \ll 1$ in the case of thin discs. Writing the right hand side of equation 3.23 as

$$\frac{3}{2} \frac{V_k}{r} \frac{\partial P}{\partial z} \left[1 - \frac{\alpha}{V_k} r \frac{\partial^2 P/\partial z^2}{\partial P/\partial z} \right]$$

and estimating

$$\frac{\partial^2 P/\partial z^2}{\partial P/\partial z} \approx -\frac{1}{L_z^\delta}$$

we see that the differential rotation dominates the α-effect source provided $\frac{\alpha}{V_k} \frac{r}{L_z} \ll 1$. Using the estimate 3.15 for α we see that this condition becomes $Q^2 \left(\frac{l_u}{L_3}\right)^2 \ll 1$. Since consistency

of our whole analysis requires use of the small correlation time limit ($a^2 \ll 1$) the differential rotation will act as the major mechanism for converting B_r to B_ϕ. If the limit $a^2 \ll 1$ is relaxed, our condition is that the turbulent eddies should be of a scale $\ell_u \ll L_z \approx z_o$.

The previous discussion indicates that our set of equations for the fields becomes

$$\frac{\partial P}{\partial t} - \eta_T \Delta P = \alpha T \qquad (3.24)$$

$$\frac{\partial T}{\partial t} - \eta_T \Delta T = \frac{3}{2} \frac{V_\kappa}{r} \frac{\partial P}{\partial z} \qquad (3.25)$$

these equations show that toroidal field gives rise to poloidal field by the α -effect while poloidal field gives rise to toroidal field by differential rotation, i.e.

$$P \underset{\alpha}{\overset{\omega'}{\rightleftarrows}} T$$

If the strength of these sources is sufficient to overcome the dissipation due to η_T, the fields will be amplified. Energy is being extracted from the turbulent kinetic energy in order to run the α -effect source for P while the Keplerian flow is the source of energy necessary to regenerate T.

Further progress requires that we specify the vertical density distribution and the expression of turbulent coefficients in terms of mean field quantities.

2.2 <u>Vertical Density Profile And The Calculation Of</u> α <u>And</u> η_T

In the standard model of accretion discs, Shakura and Sunyaev (1973) showed that in the regions where the gas pressure dominates the radiation pressure, the gas density ρ_0 may be written,

$$\rho_0(r,z) = \rho_c(r) \, e^{-(z/z_0)^2} \qquad (3.26)$$

For $|z| > z_0$, the density falls off exponentially at a faster rate. As we shall imagine the disc to have a discrete boundary at $|z| = z_0$, we use equation 3.26 as the density profile in the gas pressure dominated zones. Hence

$$L_z^{-1} = \frac{1}{\rho_0} \frac{\partial \rho_0}{\partial z} = -\frac{2z}{z_0^2} \qquad (3.27)$$

Their paper showed that if effects of turbulence are ignored, the inner, radiation-pressure dominated zone has a density profile independent of z. This result would imply that regeneration of the field by dynamo action would occur here, although in our case, additional difficult matching problems arise.

More recent work by Shakura et al (1978) shows that convective turbulence should occur in this radiation dominated zone which alters the vertical energy transport in such a way that the vertical density profile is no longer independent of z. For $\partial S/\partial z < 0$ and assuming a polytropic relation between pressure and density they show that

$$\rho_0(r,z) = \rho_c(r) \left[1 - \left(\frac{z}{z_0}\right)^2 \right]^m \qquad (3.28)$$

where n ranges from n=0.85 for M_t=1 to n=1.17 as $M_t \rightarrow 0$. The vertical density profile is then

$$L_z^{-1} (\text{rad. dom.}) = -\frac{2z}{z_o^2} n \left[1 - \left(\frac{z}{z_o}\right)^2 \right]^{-1} \qquad (3.29)$$

For $|z| < z_o$ the density profiles 3.29 and 3.27 are the same whereas in the surface regions the density in the radiation dominated zone falls off more quickly than in the gas dominated zone. We shall adopt the Gaussian profile 3.27 throughout the entire disc.

With the vertical density profile specified, we turn to calculate the turbulent coefficients $\propto$ and η_T. Shakura et al show that the velocity amplitude of the convective turbulence (dominant in the radiation zone) and the shear turbulence (dominant in the gas dominated zone) are of the same order of magnitude. Specifically

$$\tilde{u} / c_s = M_t \approx \ell_u / z_o \qquad (3.30)$$

so that $M_t \ll 1$ requires $\ell_u / z_o \ll 1$. So for low Mach numbers, we see that the discussion leading to equation 3.25 means that the shearing dominates the $\propto$ -effect regeneration of the toroidal field T even when the assumption of first order smoothing is relaxed.

Turning to the expressions 3.14 and 3.15 for η_T and $\propto$, we see that we would like to represent $\tilde{u}$ and T_u in terms of mean flow quantities. We adopt the assumption used in the standard disc models that M_t =const. It has already been

shown that hydrostatic equilibrium in the disc implies $c_s/V_k \approx z_o/r$ for $M_t \ll 1$. Consequently we write

$$\tilde{u} = M_t \left(\frac{z_o}{r}\right) V_k \qquad (3.31)$$

where for the theory we want to pursue $M_t \ll 1$ and $z_o = $ const.

First order smoothing theory is valid if we restrict ourselves to short correlation times,

$$Q = \tau_u \tilde{u}/l_u = \tau_u/t_t \ll 1 \qquad (3.32)$$

Now in the limit of small Mach numbers equation 2.19 shows that

$$t_t \approx t_k/M_t \qquad (3.33)$$

Putting 3.33 and 3.32 together gives

$$Q = M_t \tau_u/t_k \ll 1 \qquad (3.34)$$

so that if $\tau_u \lesssim t_k$, the assumption $M_t \ll 1$ delivers $Q \ll 1$. Therefore as long as $M_t \ll 1$, restriction of the correlation time to $\tau_u \lesssim t_k$ shows that $Q \approx M_t \ll 1$ and hence the mean field analysis is internally consistent.

Combining results, in the limit $M_t \ll 1$ and for $\tau_u \sim t_k$, expressions 3.14 and 3.15 for $\mathcal{M}_T$ and α become

$$\mathcal{M}_T(r) \approx \frac{M_t^2 \, z_o^2}{t_k} \qquad (3.35)$$

$$\alpha(r,z) \approx 2\left(\frac{z}{5\pi}\right) M_t^2 \frac{z}{t_k} \qquad (3.36)$$

where recall $t_k = r/V_k$. Here $\mathcal{M}_T$ has the dimensions $cm^2 \; s^{-1}$ and α the dimensions of a velocity $cm \; s^{-1}$. We note for future

reference the property

$$\alpha(r,z) = -\alpha(r,-z)$$

The simplifications arising from these assumptions are considered in the next subsection.

2.3 The Equations In Dimensionless-Form

Dividing 3.24 and 3.25 by M_T, and using the results 3.35 and 3.36 gives

$$\frac{2}{3} \chi \, t_\kappa \, \frac{\partial P}{\partial t} - \left\{ \frac{\partial^2}{\partial r^2} + \frac{1}{r} \frac{\partial}{\partial r} - \frac{1}{r^2} + \frac{\partial^2}{\partial z^2} \right\} P = \gamma_z \, T \qquad (3.37)$$

$$\frac{2}{3} \chi \, t_\kappa \, \frac{\partial T}{\partial t} - \left\{ \frac{\partial^2}{\partial r^2} + \frac{1}{r} \frac{\partial}{\partial r} - \frac{1}{r^2} + \frac{\partial^2}{\partial z^2} \right\} T = \chi \, \frac{\partial P}{\partial z} \qquad (3.38)$$

where

$$\gamma = \frac{2}{z_0^2} \left(\frac{2}{5\pi} \right)$$

$$\chi = \frac{3/2}{M_t^2 \, z_0^2} \qquad (3.39)$$

We note that γ_z is the ratio α/M_T and χ is the ratio $V_\kappa / r M_T$, and are measures of the strength of dynamo and shear processes which amplify the field with respect to the dissipation by M_T. Since both γ and χ are constants with dimension cm^{-2} we see that the quantity $(\chi\gamma)^{1/4}$ has dimension cm^{-1} and we use this to make the equations dimensionless. Thus

$$(\gamma\chi)^{1/4} = (6/5\pi)^{1/4} / M_t^{1/2} \, z_0 \qquad (3.40)$$

is a measure of the product of the two source terms ($\propto V_k/r$) divided by the square of the dissipation and is therefore a measure of overall source strength relative to the dissipation. This parameter is entirely analagous to the parameter k defined by Parker (1971) in his study of the galactic $\alpha\omega'$ dynamo.

It will prove convenient to solve the coupled equations 3.37 and 3.38 if we use B_r and B_ϕ instead of P and T. Thus

$$\frac{2}{3}\chi t_k \frac{\partial}{\partial t} B_r - \left\{\frac{\partial^2}{\partial r^2} + \frac{1}{r}\frac{\partial}{\partial r} - \frac{1}{r^2} + \frac{\partial^2}{\partial z^2}\right\} B_r = -\gamma\frac{\partial}{\partial z}(z B_\phi) \qquad (3.41)$$

$$\frac{2}{3}\chi t_k \frac{\partial}{\partial t} B_\phi - \left\{\frac{\partial^2}{\partial r^2} + \frac{1}{r}\frac{\partial}{\partial r} - \frac{1}{r^2} + \frac{\partial^2}{\partial z^2}\right\} B_\phi = -\chi B_r \qquad (3.42)$$

dividing both 3.41 and 3.42 by $(\gamma\chi)^{1/4}$ and defining the dimensionless variables

$$\hat{r} \equiv (\gamma\chi)^{1/4} r \qquad ; \qquad \hat{z} \equiv (\gamma\chi)^{1/4} z \qquad (3.43)$$

we have

$$\frac{t_k}{\bar{\beta}} \frac{\partial B_r}{\partial t} - \left\{\frac{\partial^2}{\partial\hat{r}^2} + \frac{1}{\hat{r}}\frac{\partial}{\partial\hat{r}} - \frac{1}{\hat{r}^2} + \frac{\partial^2}{\partial\hat{z}^2}\right\} B_r = -\beta\frac{\partial}{\partial\hat{z}}(\hat{z} B_\phi) \qquad (3.44)$$

$$\frac{t_k}{\bar{\beta}} \frac{\partial B_\phi}{\partial t} - \left\{\frac{\partial^2}{\partial\hat{r}^2} + \frac{1}{\hat{r}}\frac{\partial}{\partial\hat{r}} - \frac{1}{\hat{r}^2} + \frac{\partial^2}{\partial\hat{z}^2}\right\} B_\phi = -\frac{1}{\beta} B_r \qquad (3.45)$$

where

$$\beta \equiv (\gamma/\chi)^{1/2} = (8/15\pi)^{1/2} M_t = 0.41 M_t \qquad (3.46)$$

and $\bar{\beta} \equiv \frac{3}{2}\beta$. The quantity β is the ratio of source

strength due to dynamo action to the source strength due to differential rotation. In the limit $M_t \ll 1$, $\beta \ll 1$ which is showing the dominance of differential rotation over dynamo action in the small Mach number regime.

Equations 3.44 and 3.45 indicate that a natural choice for the dimensionless time co-ordinate would be $\hat{t} = \beta\, t / t_k$ which suggests that the temporal variation of the mean field should be roughly on scales $t_k / M_t \gg t_k$, assuming $M_t \ll 1$. The difficulty here is that $t_k \propto r^{3/2}$ so that equations 3.44 and 3.45 have the problem of inhomogeneity in the radial direction due to the radial dependence of M_T. This is in general a difficult problem but section 5 provides an analysis of a solvable regime.

In the next section, we assume that the dissipation and " $\propto \omega'$ " dynamo action are in balance so that the field is time independent.

3. Solutions To The Equations In The Stationary Case

We consider here the situation when $\frac{\partial B}{\partial t} = 0$; i.e the dissipation and dynamo action exactly compensate one-another. Equations 3.44 and 3.45 then become

$$\left\{ \frac{\partial^2}{\partial \hat{r}^2} + \frac{1}{\hat{r}} \frac{\partial}{\partial \hat{r}} - \frac{1}{\hat{r}^2} + \frac{\partial^2}{\partial \hat{z}^2} \right\} B_r = \beta \frac{\partial}{\partial \hat{z}} \left(\hat{z}\, B_\phi \right) \tag{3.47}$$

$$\left\{ \frac{\partial^2}{\partial \hat{r}^2} + \frac{1}{\hat{r}} \frac{\partial}{\partial \hat{r}} - \frac{1}{\hat{r}^2} + \frac{\partial^2}{\partial \hat{z}^2} \right\} B_\phi = \frac{1}{\beta} B_r \tag{3.48}$$

These equations admit separable solutions. Writing

$$B_r(\hat{r}, \hat{z}) = R(\hat{r}) Q(\hat{z})$$

$$B_\phi(\hat{r}, \hat{z}) = R(\hat{r}) U(\hat{z}) \tag{3.49}$$

and introducing the separation constant $-\kappa$ we find that R obeys the equation

$$\left\{ \frac{d^2}{d\hat{r}^2} + \frac{1}{\hat{r}} \frac{d}{d\hat{r}} + \kappa - \frac{1}{\hat{r}^2} \right\} R = 0 \tag{3.50}$$

while the z dependent factors are governed by the coupled equations

$$\left\{ \frac{d^2}{d\hat{z}^2} - \kappa \right\} Q = -\beta \frac{d}{d\hat{z}} (\hat{z} U) \tag{3.51}$$

$$\left\{ \frac{d^2}{d\hat{z}^2} - \kappa \right\} U = -\frac{1}{\beta} Q \tag{3.52}$$

Equation 3.52 gives

$$Q = -\beta \left\{ \frac{d^2}{d\hat{z}^2} - \kappa \right\} U$$

which is substituted into equation 3.51 to give a fourth order equation for U

$$\frac{d^4 U}{d\hat{z}^4} - 2\kappa \frac{d^2 U}{d\hat{z}^2} - \hat{z} \frac{dU}{d\hat{z}} + (\kappa^2 - 1) U = 0 \tag{3.53}$$

With κ real, $\kappa > 0$ results in solutions R being a linear combination of the Bessel functions $J_1(\kappa^{1/2}\hat{r})$ and $Y_1(\kappa^{1/2}\hat{r})$ whereas $\kappa < 0$ leads to a linear combination of the modified Bessel

functions $K_1\left((-\kappa)^{\frac{1}{2}}\hat{r}\right)$ and $I_1\left((-\kappa)^{\frac{1}{2}}\hat{r}\right)$. Matching to a vacuum with proper behaviour in the limit $z \to \infty$ and $r \to 0$, give $\kappa > 0$ and $R = J_1(\kappa^{\frac{1}{2}}\hat{r})$.

Equation 3.53 may most elegantly be solved by using an integral representation of the solution. Specifically, we seek a solution to equation 3.53 of the form

$$U(\hat{z}) = \int K(\hat{z}, t)\, v(t)\, dt \qquad (3.54)$$

Since the differential operator acting on U contains polynomials of only order one in $\hat{z}$, the choice of the Laplace kernel

$$K(\hat{z}, t) = e^{\hat{z}t} \qquad (3.55)$$

will require only the solution of a first order differential equation in t for the as yet unknown function v(t). This is carried out in Appendix C.1 where it is shown that U is given by

$$U(\hat{z}) = \int_C \frac{e^{-t^4/4 + \kappa t^2 + \hat{z}t}}{t^{\kappa^2}}\, dt \qquad (3.56)$$

where C is any contour for which the integrand vanishes at the end points. Of course there will be a number of different contours in the complex-t plane which accomplish this, and these will correspond to the different independent solutions of $\mathcal{L}_{\hat{z}}\{U\} = 0$. The appearance of the factor $t^{-\kappa^2}$ in equation 3.56 implies the presence of a branch cut in the complex-t plane.

Let us first consider the type of contours which are admissible. Consideration of the integrand shows that as $|t|$ → ∞, the factor $e^{-t^4/4}$ is the most important. If $Re(t^4) < 0$, the integral diverges as we integrate out to $|t| \to \infty$. Convergence of the integral occurs only in regions where $Re(t^4) > 0$. Writing $t = |t| e^{i\theta}$, this requirement becomes

$$\cos 4\theta > 0 \tag{3.57}$$

Solving the relation shows that there are four zones of convergence as diagrammed in Fig. 6. Therefore, our contours are most simply chosen to have as asymptotes the co-ordinate axes in the complex t plane. These contours are drawn in Fig. 6 where we also show the branch cut extending up the positive imaginary axis. The end points of these contours are at $|t| = \infty$ in the directions indicated, so that the requirement that the integrand vanish at the end points of the contour is satisfied.

Fig. 6. Contours Defining The Solutions $U_m(\hat{z})$
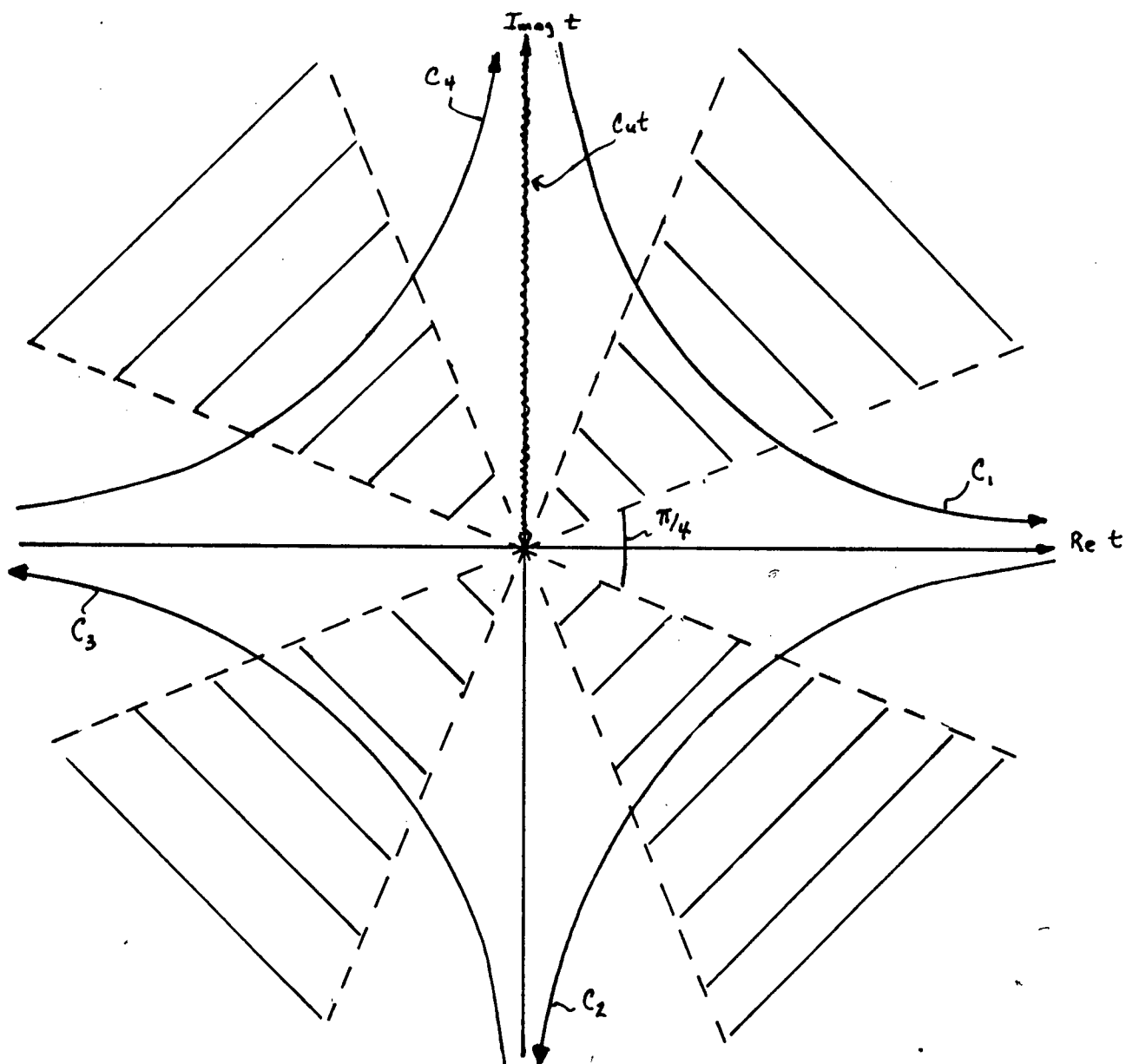
The presence of the branch cut implies that the four solutions

$$U_{\mu}(\hat{z}) = \int_{C_{\mu}} \frac{\exp\left[-t^4/4 + \kappa t^2 + \hat{z}t\right]}{t^{\kappa^2}} dt \qquad (3.58)$$

$$\mu = 1, 2, 3, 4$$

with the contours C_{μ} shown in Fig. 6 are linearly independent. It may readily be shown that the sum $\sum_{\mu=1}^{4} U_{\mu}(\hat{z}) \neq 0$. A phase shift is picked up due to the presence of the branch cut which insures that the sum is non-zero (see Appendix C.2).

The requirement that our disc solutions be matched continuously to an exterior vacuum solution at the upper and lower disc surfaces $z = \pm z_0$ demands the analysis of $U_{\mu}(\hat{z})$ as $z \longrightarrow \pm z_0$. It will be remembered that for $M_t \ll 1$, $|\hat{z}| \gg |$ as $z \longrightarrow \pm z_0$, so that we may use the asymptotic form for $U_{\mu}(\hat{z})$. The contintuity of the field throughout the disc will require matching conditions at $z = 0$. Consequently we must examine the behavoiur of $U_{\mu}(\hat{z})$ in the vicinity of $\hat{z} = 0$. These two tasks occupy the rest of this section.

It is important to point out that the assumption of separation of scales for the fluctuating and mean fields allows us to restrict attention to the limit $\kappa \ll 1$. This is readily seen by noting that $\kappa^{1/2}\hat{r} = (\kappa^{1/2}/M_t^{1/2}z_0)r$ so that the radial wavelength is $\lambda_r \simeq (M_t^{1/2}/\kappa^{1/2})z_0$. Since we require our mean field to vary on radial scales larger than z_0, we see that the limit $\kappa \ll 1$ focusses on the correct regime for analysis of the

mean fields. This observation will prove very helpful in simplifying the analysis to come.

We now digress to a discussion of the asymptotic analysis before going on with the problem of matching to the external vacuum field.

Asymptotic form of the solutions $U_m(\hat{z})$ as $\hat{z} \to \infty$.

In the limit $z \to z_0$, the limit $M_t \ll 1$ implies that $\hat{z} \gg 1$. It is convenient to define the variable τ as

$$t = |\hat{z}|^{1/3} \, \tau \tag{3.59}$$

and the real positive quantity λ by

$$\lambda \equiv |\hat{z}|^{4/3} = \left[\frac{(6/5\pi)^{1/4}}{M_t^{1/2}} \cdot \frac{z}{z_0} \right]^{4/3} \tag{3.60}$$

in terms of which the solutions 3.58 may be written

$$U_m(\kappa, \hat{z}) = \lambda^{(1-\kappa^2)/4} \int_{C_m} \frac{\exp\left[\lambda\left(-\tau^4/4 \pm \tau \right) + \lambda^{1/2} \kappa \tau^2 \right]}{\tau^{\kappa^2}} \, d\tau \tag{3.61}$$

where the positive sign is adopted for $\hat{z} > 0$ and the negative sign for $\hat{z} < 0$. Introducing the definitions

$$\chi(\tau) \equiv \tau^{-\kappa^2}$$

$$f(\tau) \equiv -\frac{\tau^4}{4} \pm \tau$$

$$g(\tau) \equiv \tau^2$$

allows us to write equation 3.61 in the form

$$U_m(\kappa, \hat{z}) = \lambda^{(1-\kappa^2)/4} \int_{C_m} \chi(\tau) \, e^{\lambda f(\tau) + \lambda^{1/2} \kappa g(\tau)} \, d\tau \tag{3.62}$$

We evaluate the integral in 3.62 in the limit $\lambda \to \infty$ (i.e $\hat{z} \to \infty$) by the method of steepest descents. This method is usually applied to integrals of the form

$$\psi(\lambda) = \int_c \chi(\tau) \, e^{\lambda f(\tau)} \, d\tau \qquad (3.63)$$

where if τ_0 is a saddle point (i.e where $f'(\tau) = 0$), and the contour may be deformed to pass through the saddle point onto the path of steepest descent (this must be justified by Cauchy's theorem), one finds that in the limit $\lambda \to \infty$, $\psi(\lambda)$ becomes

$$\psi(\lambda) \approx \chi(\tau_0) \, \frac{e^{\lambda f(\tau_0)} (2\pi)^{1/2} \, e^{i\alpha}}{|\lambda f''(\tau_0)|^{1/2}} \qquad (3.64)$$

where α is such that $f''(\tau_0) \, e^{2i\alpha}$ is real and negative.

This method requires extension in order to handle an integral such as that appearing in equation 3.61, where we have the appearance of an additional parameter . Physically we want to focuss on modes such that $\kappa \ll 1$, so that as Appendix D.1 shows, for $f(\tau)$ and $g(\tau)$ defined by 3.61, we have in the limit $\lambda \to \infty$, $\kappa < 1$;

$$\int_c \chi(\tau) \, e^{\lambda f(\tau) + \lambda^{1/2} \kappa g(\tau)} \, d\tau \approx \frac{\chi(\tau_0) \, e^{\lambda f(\tau_0)} (2\pi)^{1/2} \, e^{i\alpha} \, e^{-4/3 \kappa^2}}{|\lambda f''(\tau_0)|^{1/2}} \qquad (3.65)$$

where we more specifically require that $\kappa/\lambda^{1/2} \ll 1$.

The necessary mathematical details for the asymptotic analysis are found in Appendix D. The critical points of the

integrand are found in D.2 whereupon the paths of steepest descent from each saddle point is determined (section D.3). Our contours C_m are then deformed onto the paths of steepest descent , the contributions due to each saddle point picked up assessed, and the results summed to give the final asymptotic representation of $U_m(\kappa, \hat{z})$ (section D.4).

We find that the solutions U_m may be written, in the asymptotic limit $\hat{z} \to \infty$

$$U_m(\kappa, \hat{z}) \approx \frac{2\sqrt{\frac{2\pi}{3}} \; e^{-4/3 \kappa^2}}{\lambda^{(1+\kappa^2)/4}} \; \mu_m(\kappa, \hat{z}) \qquad (3.66)$$

where the functions μ_m are listed in Table 4.

Table 4. Asymptotic Analysis: The Functions $\mu_n(\kappa,\hat{z})$

	$\hat{z}>0$	$\hat{z}<0$
$\mu_1(\kappa,\hat{z})$	$e^{p\lambda}$	$e^{-\pi/3\,(\kappa^2+1)i}\, e^{q\lambda}$
$\mu_2(\kappa,\hat{z})$	$-e^{p\lambda}$	$-e^{\pi/3\,(\kappa^2+1)i}\, e^{q^*\lambda}$
$\mu_3(\kappa,\hat{z})$	$e^{2\pi/3\,(\kappa^2+1)i}\, e^{q\lambda}$	$e^{\pi(\kappa^2+1)i}\, e^{p\lambda}$
$\mu_4(\kappa,\hat{z})$	$-e^{-2\pi/3\,(\kappa^2+1)i}\, e^{q^*\lambda}$	$-e^{\pi(\kappa^2+1)i}\, e^{p\lambda}$

and where we recall that $|\lambda| = |\hat{z}|^{4/3}$. The numerical factors p, q, and q^* are

$$p = 3/4$$

$$q = -\frac{3}{8} - i\frac{3\sqrt{3}}{8}$$

$$q^* = -\frac{3}{8} + i\frac{3\sqrt{3}}{8}$$

$$(3.67)$$

These results show that two solutions (U_1 and U_2) grow exponentially for $z>0$ and exhibit exponentially damped oscillations in $z<0$. The solutions U_3 and U_4 behave conversely. The relation between $U_m(\kappa,z)$ and $U_m(\kappa,-z)$ found in the preceeding table are trivial applications of relations C.26-C.29.

We recall that the $\hat{z}$ dependence of B_r ($Q(\hat{z})$) is given

by equation 3.52 so that we must calculate $d^2U/d\hat{z}^2$. We shall also need to find $P(\hat{z})$ in order to evaluate $B_z(\hat{r},\hat{z})$. With the integral representation 3.58, this is easily done. Specifically

$$\frac{dU_n}{d\hat{z}} = \int_{C_n} t \frac{e^{-t^4/4 + \kappa t^2 + \hat{z}t}}{t^{\kappa^2}} dt \qquad (3.68)$$

$$\frac{d^2U_n}{d\hat{z}^2} = \int_{C_n} t^2 \frac{e^{-t^4/4 + \kappa t^2 + \hat{z}t}}{t^{\kappa^2}} dt \qquad (3.69)$$

Using the definitions 3.59 and 3.60 these integrals take the form

$$\frac{dU_n}{d\hat{z}} = \lambda^{(2-\kappa^2)/4} \int_{C_n} \tau^{1-\kappa^2} \exp\left[\lambda(-\tau^4/4 \pm \tau) + \lambda^{1/2}\kappa \tau^2\right] d\tau \qquad (3.70)$$

$$\frac{d^2U_n}{d\hat{z}^2} = \lambda^{(3-\kappa^2)/4} \int_{C_n} \tau^{2-\kappa^2} \exp\left[\lambda(-\tau^4/4 \pm \tau) + \lambda^{1/2}\kappa\tau^2\right] d\tau \qquad (3.71)$$

In the asymptotic regime $\lambda \to \infty$, making the same assumptions leading to the expression for U_n gives

$$\frac{dU_n(\kappa,\hat{z})}{d\hat{z}} \approx 2\frac{\sqrt{2\pi/3}\ e^{-4/3\kappa^2}}{\lambda^{\kappa^2/4}} \mu_n^{(1)}(\kappa,\hat{z}) \qquad (3.72)$$

where the functions $\mu_n^{(i)}(\kappa,\hat{z})$ are listed in Table 5,

Table 5. Asymptotic Analysis: The Functions $\mu_m^{(1)}(\kappa, \hat{z})$

	$\hat{z} > 0$	$\hat{z} < 0$
$\mu_1^{(1)}(\kappa, \hat{z})$	$e^{p\lambda}$	$e^{-\pi/3 \kappa^2 i} \, e^{q\lambda}$
$\mu_2^{(1)}(\kappa, \hat{z})$	$-e^{p\lambda}$	$e^{\pi/3 \kappa^2 i} \, e^{q^*\lambda}$
$\mu_3^{(1)}(\kappa, \hat{z})$	$e^{2\pi/3 \kappa^2 i} \, e^{q\lambda}$	$e^{\pi \kappa^2 i} \, e^{p\lambda}$
$\mu_4^{(1)}(\kappa, \hat{z})$	$e^{-2\pi/3 \kappa^2 i} \, e^{q^*\lambda}$	$-e^{-\pi \kappa^2 i} \, e^{p\lambda}$

And

$$\frac{d^2 U_m(k,\hat{z})}{d\hat{z}^2} = 2\sqrt{\frac{2\pi}{3}}\, e^{-\frac{4}{3}k^2}\, \lambda^{(1-k^2)/4}\, \mu_m^{(2)}(k,\hat{z}) \tag{3.73}$$

with the fuctions $\mu_m^{(2)}(k,\hat{z})$ listed in Table 6.

Table 6. Asymptotic Analysis: The Functions $\mu_m^{(2)}(k,\hat{z})$

	$\hat{z} > 0$	$\hat{z} < 0$
$\mu_1^{(2)}(k,\hat{z})$	$e^{p\lambda}$	$e^{-\pi/3(k^2-1)i}\, e^{q\lambda}$
$\mu_2^{(2)}(k,\hat{z})$	$-e^{p\lambda}$	$-e^{\pi/3(k^2-1)i}\, e^{q^*\lambda}$
$\mu_3^{(2)}(k,\hat{z})$	$e^{2\pi/3(k^2-1)i}\, e^{q\lambda}$	$e^{\pi(k^2-1)i}\, e^{p\lambda}$
$\mu_4^{(2)}(k,\hat{z})$	$-e^{-2\pi/3(k^2-1)i}\, e^{q^*\lambda}$	$-e^{\pi(k^2-1)i}\, e^{p\lambda}$

These results show that in the limit $\hat{z} \to \infty$,

$$\frac{dU}{d\hat{z}} \approx \lambda^{1/4} U \qquad ; \qquad \frac{d^2U}{d\hat{z}^2} \approx \lambda^{1/2} U$$

hence

$$Q = -\beta\left[\frac{d^2U}{d\hat{z}^2} - kU\right] \approx -\beta\left[\lambda^{1/2} - k\right]U = -\beta\left[1 - \frac{k}{\lambda^{1/2}}\right]\lambda^{1/2} U$$

Since $k/\lambda^{1/2} \ll 1$, we have

$$Q(\hat{z}) \approx -\beta\frac{d^2U}{d\hat{z}^2} \tag{3.74}$$

$$P(\hat{z}) \approx -\beta\frac{dU}{d\hat{z}} \tag{3.75}$$

We turn finally to the behaviour of $U_m(\hat{z})$ at $\hat{z}=0$.

Behaviour of $U_m(\hat{z})$ as $\hat{z} \to 0$.

The integral representation 3.58 allows the ready expansion of $U_m(\hat{z})$ about $\hat{z}=0$ since we only need to expand $e^{\hat{z}t}$ in a power series in $\hat{z}$, evaluating the integrals in t (the coefficients of the expansion) as we go. In order to facilitate the integrations, it is convenient to deform the contours C_m to run along the appropriate portions of the imaginary and real t axes. As an example, the contour C_1 is replaced by an integration running from $+i\infty$ to the origin, and form the origin out to $+\infty$. The coefficients are then proportional to integrals of the form

$$a_m(\kappa) \propto \int_0^\infty t^m \frac{\exp\left[-t^4/4 + \kappa t^2\right]}{t^{\kappa^2}} \, dt$$

which, with the variable $\tau = t^2$ can be written in general as

$$a_m(\kappa) \propto \int_0^\infty e^{-\beta\tau^2 - \gamma\tau} \tau^{\nu_m - 1} \, d\tau$$

where $\beta = \frac{1}{4}$ and $-\gamma = \kappa$ with $\nu_m \equiv (m+1-\kappa^2)/2$. This latter integral can be represented in terms of parabolic cylinder functions as (see Gradshteyn and Ryzhik (1965) p. 337, formula 3.462.1)

$$\int_0^\infty e^{-\beta\tau^2 - \gamma\tau} \tau^{\nu - 1} \, d\tau = (2\beta)^{-\nu/2} \Gamma(\nu) \exp\left(\frac{\gamma^2}{2\beta}\right) D_{-\nu}\left(\frac{\gamma}{\sqrt{2\beta}}\right)$$

$$(3.76)$$

where $Re\,\beta > 0$ and $Re\,\nu > 0$ and D_ν is the parabolic cylinder function. The condition $Re\,\nu_m > 0$ is easily met with our constraint that $\kappa \ll 1$.

The details are given in Appendix E. We only need the values of the expansions at $\hat{z}=0$ in order to do the matching problem of section 4. Defining

$$Q_m(\hat{z}) \equiv -\beta\left(\frac{d^2}{d\hat{z}^2} - \kappa\right) U_m$$

$$P_m(\hat{z}) \equiv \int Q_m(\hat{z})\, d\hat{z}$$

(3.77)

and taking the limit of $U_m(\kappa,\hat{z})$ as $\hat{z} \to 0^+$, we have

$$\lim_{\hat{z}\to 0^+} U_m(\kappa,\hat{z}) = \left[2^{(\nu_0-1)/2}\, e^{(\nu_0-1)\pi i/2}\, \sqrt{\pi}\, e^{\kappa^2/2}\right] \widetilde{U}_m(\kappa)$$

(3.78)

$$\lim_{\hat{z}\to 0^+} Q_m(\kappa,\hat{z}) = \left[2^{(\nu_2-1)/2}\, e^{(\nu_2-1)\pi i/2}\, \sqrt{\pi}\, e^{\kappa^2/2}\right] \widetilde{Q}_m(\kappa)$$

(3.79)

with $\widetilde{U}_m$ and $\widetilde{Q}_m$ given in Table 7

Table 7. Expansions About Z=0: The Functions $\widetilde{U}_n$ And $\widetilde{Q}_n$

n	$\widetilde{U}_n$	$\widetilde{Q}_n$
1	$D_{\nu_0-1}(x)$	$G_{\nu_0}(x)$
2	$e^{-\pi\nu_0 i}\, D_{\nu_0-1}(-x)$	$e^{-\pi\nu_2 i}\, G_{\nu_0}(-x)$
3	$e^{-2\pi\nu_0 i}\, D_{\nu_0-1}(x)$	$e^{-2\pi\nu_2 i}\, G_{\nu_0}(x)$
4	$e^{-3\pi\nu_0 i}\, D_{\nu_0-1}(-x)$	$e^{-3\pi\nu_2 i}\, G_{\nu_0}(-x)$

where

$$x \equiv -i\sqrt{2}\,K \tag{3.80}$$

$$\begin{cases} \nu_0 \equiv (1-K^2)/2 \\[4pt] \nu_1 \equiv \nu_0 + \frac{1}{2} \\[4pt] \nu_2 \equiv \nu_0 + 1 \end{cases} \tag{3.81}$$

$$G_\nu(x) \equiv D_\nu(x) - \frac{x}{2}\, D_{\nu-1}(x) \tag{3.82}$$

Writing

$$\lim_{\hat{z} \to 0^+} \left(\frac{dU_n}{d\hat{z}} \right) = \left[2^{(\nu_1-2)/2} \; e^{(\nu_1-1)\pi i/2} \; \sqrt{\pi} \; e^{\kappa^2/2} \right] \widetilde{U}'_n(\kappa)$$

(3.83)

$$\lim_{\hat{z} \to 0^+} \left(P_n \right) = -\beta \left[2^{(\nu_1-2)/2} \; e^{(\nu_1-1)\pi i/2} \; \sqrt{\pi} \; e^{\kappa^2/2} \right] \widehat{P}_n(\kappa)$$

(3.84)

we tabulate $\widetilde{U}'_n$ and P_n in Table 8.

Table 8. Expansions About Z=0: The Functions $\widetilde{U}'_n$ And $\widetilde{P}_n$

n	$\widetilde{U}'_n$	$\widetilde{P}_n$
1	$D_{\nu_1-1}(x)$	$G_{\nu_1-1}(x)$
2	$e^{-\pi\nu_1 i} D_{\nu_1-1}(-x)$	$e^{-\pi\nu_1 i} G_{\nu_1-1}(-x)$
3	$e^{-2\pi\nu_1 i} D_{\nu_1-1}(x)$	$e^{-2\pi\nu_1 i} G_{\nu_1-1}(x)$
4	$e^{-3\pi\nu_1 i} D_{\nu_1-1}(-x)$	$e^{-3\pi\nu_1 i} G_{\nu_1-1}(-x)$

The limits as $\hat{z} \to 0^-$ of the functions U_n, Q_n, $\frac{dU_n}{d\hat{z}}$, P_n may be found using the above results plus the

important symmetry relations

$$U_1(\kappa, -\hat{z}) = e^{\pi i (1-\kappa^2)} U_3(\kappa, \hat{z})$$

$$U_2(\kappa, -\hat{z}) = e^{\pi i (1-\kappa^2)} U_4(\kappa, \hat{z})$$

$$U_3(\kappa, -\hat{z}) = e^{-\pi i (1-\kappa^2)} U_1(\kappa, \hat{z})$$

$$U_4(\kappa, -\hat{z}) = e^{-\pi i (1-\kappa^2)} U_2(\kappa, \hat{z})$$

$$(3.85)$$

derived in Appendix C.2.

4. Matching To An External Vacuum-Solution.

We will suppose that outside the disc (i.e $|z| > z_0$) the gas is so tenuous that the region may be regarded as a vacuum. A vacuum cannot support currents so that we demand $\nabla \times \underline{B}^{VAC} = 0$, which together with $\nabla \cdot \underline{B}^{VAC} = 0$, requires that $\underline{B}^{VAC}$ be derivable from a potential ψ , with

$$\underline{B}^{VAC} = \nabla \psi \tag{3.86}$$

$$\nabla^2 \psi = 0 \tag{3.87}$$

If we assume axial symmetry of the vacuum field, and require that

$$\underline{B}^{VAC} \longrightarrow 0 \quad \text{as} \quad z \rightarrow \pm \infty$$

$$\underline{B}^{VAC} \text{ finite} \quad \text{as} \quad r \rightarrow 0 \tag{3.88}$$

then ψ may be written in separable form as

$$\psi_k(\hat{r},\hat{z}) = J_0(k^{1/2}\hat{r}) \begin{cases} e^{-k^{1/2}(\hat{z}-\hat{z}_0)} & : \quad \hat{z} > +\hat{z}_0 \\ e^{-k^{1/2}(\hat{z}+\hat{z}_0)} & : \quad \hat{z} < -\hat{z}_0 \end{cases}$$

$$(3.89)$$

which, using equation 3.86 gives in the region $\hat{z} > \hat{z}_0$

$$B_r^{VAC}(k;\hat{r},\hat{z}) = E(k) J_1(k^{1/2}\hat{r}) e^{-k^{1/2}(\hat{z}-\hat{z}_0)}$$

$$B_z^{VAC}(k;\hat{r},\hat{z}) = E(k) J_0(k^{1/2}\hat{r}) e^{-k^{1/2}(\hat{z}-\hat{z}_0)} \qquad (3.90)$$

and in the region $\hat{z} < -\hat{z}_0$

$$B_r^{VAC}(k;\hat{r},\hat{z}) = F(k) J_1(k^{1/2}\hat{r}) e^{k^{1/2}(\hat{z}+\hat{z}_0)}$$

$$B_z^{VAC}(k;\hat{r},\hat{z}) = -F(k) J_0(k^{1/2}\hat{r}) e^{k^{1/2}(\hat{z}+\hat{z}_0)} \qquad (3.91)$$

where

$$B_\phi^{VAC} = 0 \qquad (3.92)$$

everywhere in the vacuum and where $E(k)$ and $F(k)$ represent amplitudes to be fixed by the boundary conditions.

At the upper and lower surfaces of the disc $|z| = z_0$, we require that B_r, B_ϕ, and B_z be continuous, i.e.

$$[B_r] = [B_\phi] = [B_z] = 0 \qquad (at \ |z| = z_0) \qquad (3.93)$$

These requirements impose a set of six constraints.

At the plane z=0, we require continuity of the fields and their gradients, i.e

$$\left[B_r \right] = \left[B_\phi \right] = \left[B_z \right] = \left[\frac{\partial B_\phi}{\partial z} \right] = 0 \qquad (at \ z=0)$$

$$(3.94)$$

which are four more conditions totalling ten altogether.

Noting that $U(\kappa, \hat{z})$ is a superposition of the four independent solutions $U_n(\kappa, \hat{z})$, and writing the disc mean field components as

$$B_\phi(\kappa; \hat{r}, \hat{z}) = R(\kappa; \hat{r}) \sum_{n=1}^{4} C_n(\kappa) \ U_n(\kappa; \hat{z}) \qquad : \qquad \hat{z} > 0$$

$$(3.95)$$

$$B_\phi(\kappa; \hat{r}, \hat{z}) = R(\kappa; \hat{r}) \sum_{n=1}^{4} D_n(\kappa) \ U_n(\kappa; \hat{z}) \qquad : \qquad \hat{z} < 0$$

where the other components follow form equations 3.49, 3.52, and 3.6 the boundary conditions 3.93 and 3.94 give a set of ten equations for the ten unknowns E, F, C_n, and D_n (n=1,2,3,4). We use the results of the asymptotic analysis to evaluate U_n at $\pm z_0$ (specifically equations 3.66, 3.72, and 3.73 together with the results 3.74 and 3.75) in order that the conditions 3.93 can be met with the vacuum solutions (3.90 and 3.91) specified at $\pm z_0$. The constraints at z=0 require equations 3.78 - 3.84 together with the relations 3.85 to establish the form of the solutions in the limit $z \rightarrow 0^-$.

The radial behaviour of these solutions may be readily matched if we pick a vacuum mode with dimensionless wavenumber

$h^{\frac{1}{2}}$, $k > 0$; such that $k = \kappa$. With $\kappa > 0$ we see that

$R(\kappa; \hat{r}) = J_1(\kappa^{\frac{1}{2}}\hat{r})$.

As it stands, a set of ten simultaneous equations in ten unknowns must be solved. This set may be reduced to a set of five if we limit the discussion to modes in thich the dominant disc field B_ϕ is either an even or an odd funcion of $\hat{z}$ (see Parker (1971)). Turning to equations 3.24 and 3.25, and remembering that $\alpha(\hat{z}) = -\alpha(-\hat{z})$, we have that for <u>even</u> <u>modes</u> $U(\hat{z}) = U(-\hat{z})$, so that $P(\hat{z}) = -P(-\hat{z})$. Similarly, for <u>odd</u> <u>modes</u> $U(\hat{z}) = -U(-\hat{z})$ so that equations 3.24 and 3.25 are satisfied if $P(\hat{z}) = P(-\hat{z})$. For even modes then, the toroidal field B_ϕ will be an even function of $\hat{z}$, the radial field B_r will be an even function of $\hat{z}$, and the vertical field B_z will be an odd function of $\hat{z}$. Exactly the reverse is true for odd modes.

Consequently for even modes

$$P = \frac{dU}{d\hat{z}} = 0 \qquad (\text{at } \hat{z} = 0) \qquad (3.96)$$

and for odd modes

$$U = \frac{dP}{d\hat{z}} = 0 \qquad (\text{at } \hat{z} = 0) \qquad (3.97)$$

If the full matching conditions are written out, it is found that the choice

$$
\begin{aligned}
D_3 &= + e^{-\pi i (\kappa^2 - 1)} \, C_1 \\
D_4 &= + e^{-\pi i (\kappa^2 - 1)} \, C_2 \\
D_1 &= + e^{-\pi i (\kappa^2 - 1)} \, C_3 \\
D_4 &= + e^{-\pi i (\kappa^2 - 1)} \, C_4 \\
F &= + E
\end{aligned}
\qquad (3.98)
$$

satisfies equation 3.96 for even modes whereas the choice

$$D_3 = -e^{-\pi i (\kappa^2 - 1)} C_1$$

$$D_4 = -e^{-\pi i (\kappa^2 - 1)} C_2$$

$$D_1 = -e^{-\pi i (\kappa^2 - 1)} C_3 \qquad\qquad (3.99)$$

$$D_2 = -e^{-\pi i (\kappa^2 - 1)} C_4$$

$$F = -E$$

satisfies equation 3.97 for odd modes.

The analysis has therefore been reduced to the study of the five equations:

$$[B_r] = [B_z] = 0 \ ; \quad B_\phi = 0 \qquad (at\ z = z_0) \qquad (3.100)$$

together with 3.96 for even modes; and 3.100 together with 3.97 for odd modes. The limit $z \to 0^+$ is to be used in all results for z=0. Restriction to either even or odd modes has allowed us to consider only the z>0 region. We have five equations for the five unknowns $E(\kappa)$, $C_i(\kappa)$ where the other coefficients are given by either 3.98 or 3.99. These two sets of equations 3.98 and 3.99 are a direct consequence of the symmetry relations 3.85.

Written out in detail, equations 3.100 are for the radial component

$$\beta f(\kappa, \lambda_0) \left\{ C_1 e^{p\lambda_0} - C_2 e^{p\lambda_0} + C_3 e^{2\pi/3 (\kappa^2-1) i} e^{q\lambda_0} - C_4 e^{-2\pi/3 (\kappa^2-1) i} e^{q^* \lambda_0} \right\} = E$$

$$(3.101)$$

the ϕ component

$$\frac{1}{\lambda_o^{1/2}} f(\kappa,\lambda_o) \left\{ C_1 e^{p\lambda_o} - C_2 e^{p\lambda_o} + C_3 e^{\frac{2\pi}{3}(\kappa^2+1)i} e^{q\lambda_o} - C_4 e^{-\frac{2\pi}{3}(\kappa^2+1)i} e^{q^*\lambda_o} \right\} = 0$$

$$(3.102)$$

and the z component

$$-\beta \frac{\kappa^{1/2}}{\lambda_o^{1/4}} f(\kappa,\lambda_o) \left\{ C_1 e^{p\lambda_o} - C_2 e^{p\lambda_o} + C_3 e^{\frac{2\pi}{3}\kappa^2 i} e^{q\lambda_o} + C_4 e^{-\frac{2\pi}{3}\kappa^2 i} e^{q^*\lambda_o} \right\} = E$$

$$(3.103)$$

where from equation 3.60

$$\lambda_o \equiv |\hat{z}_o|^{4/3} = \left[\frac{(6/5\pi)^{1/4}}{M_t^{1/2}} \right]^{4/3} \qquad (3.104)$$

$$f(\kappa,\lambda_o) \equiv 2\sqrt{\frac{2\pi}{3}} e^{-\frac{4}{3}\kappa^2} \lambda_o^{(1-\kappa^2)/4} \qquad (3.105)$$

For even modes these equations are supplemented by the relations 3.96 which written out are

<u>Even Modes</u>

$$C_1 D_{y_i-1}(x) + C_2 e^{-\pi y_i i} D_{y_i-1}(-x) + C_3 e^{-2\pi y_i i} D_{y_i-1}(x) + C_4 e^{-3\pi y_i i} D_{y_i-1}(-x) = 0$$

$$(3.106)$$

$$C_1 G_{y_i-1}(x) + C_2 e^{-\pi y_i i} G_{y_i-1}(-x) + C_3 e^{-2\pi y_i i} G_{y_i-1}(x) + C_4 e^{-3\pi y_i i} G_{y_i-1}(-x) = 0$$

$$(3.107)$$

and for odd modes are supplemented by the relations 3.97 which

written out are

Odd Modes

$$C_1 D_{\nu_0-1}(x) + C_2 e^{-\pi\nu_0 i} D_{\nu_0-1}(-x) + C_3 e^{-2\pi\nu_0 i} D_{\nu_0-1}(x) + C_4 e^{-3\pi\nu_0 i} D_{\nu_0-1}(-x) = 0$$

$$(3.108)$$

$$C_1 G_{\nu_0}(x) + C_2 e^{-\pi\nu_2 i} G_{\nu_0}(-x) + C_3 e^{-2\pi\nu_2 i} G_{\nu_0}(x) + C_4 e^{-3\pi\nu_2 i} G_{\nu_0}(-x) = 0$$

$$(3.109)$$

where all these results follow from Tables 7 and 8.

These equations may be put in matrix form $\underline{\underline{A}}^{e,o}\underline{x} = 0$ where $\underline{\underline{A}}^{e,o}$ is the 5x5 matrix of coefficients of the above sets of equations and $\underline{x}$ is the column vector of the unknowns $C_\mu^{e,o}$, $E^{e,o}$. Specifically $\underline{\underline{A}}^e$ is the matrix of coefficients of equation 3.101 - 3.103 and 3.106 and 3.107; while for odd modes $\underline{\underline{A}}^o$ is the matrix of coefficients of equations 3.101 -3.103 and 3.108 and 3.109.

We require that

$$\det \underline{A}^{e,o} = 0$$

for non-trivial solutions. The point of this analysis will be to find a relation between $\lambda_0^{e,o}$ (i.e. $M_t^{e,o}$) and K , which are the only parameters appearing in the matrices.

Manipulation of the determinants shows that in both cases, the problem reduces to setting a 3x3 determinant equal

to zero. This arises because in both cases, $\det A^{e,o}$ takes the form

$$0 = \det A^{e,o} = \det \begin{pmatrix} \cdots\cdots & C^{e,o} \\ B^{e,o} & 0 \end{pmatrix}$$

$$= \det B^{e,o} \cdot \det C^{e,o}$$

where $B^{e,o}$ are 2x2 matrices and $C^{e,o}$ are 3x3 matrices. This being the case, the solution can be found quite easily. The coefficients of $B^{e,o}$ are dependent only on κ via the various parabolic cylinder functions we have defined, and $\det B^{e,o}$ vanishes only for $\kappa = 0$ in general.

Hence our conditions for even and odd modes become $\det C^{e,o} = 0$ where

$$C^e \equiv \begin{pmatrix} 2i \sin 2\pi/3 & 2i \sin 2\pi/3 & 1 \\[2em] \left(e^{2\pi i/3} - e^{-2\pi \nu_1 i} e^{-2\pi/3 k^2 i} e^{(p-q)\lambda_0} \right) & \left(-e^{-2\pi i/3} + e^{-2\pi \nu_1 i} e^{2\pi k^2 i/3} e^{(p-q^*)\lambda_0} \right) & 0 \\[2em] 1 - e^{2\pi i/3} & 1 + e^{-2\pi i/3} & \lambda_0^{1/4}/k^{1/2} \end{pmatrix}$$

$$(3.110)$$

$$C^o \equiv \begin{pmatrix} 2i \sin 2\pi/3 & 2i \sin 2\pi/3 & 1 \\[2em] \left(-e^{2\pi i/3} - e^{-2\pi \nu_1 i} e^{-2\pi/3 k^2 i} e^{(p-q)\lambda_0} \right) & \left(+e^{-2\pi i/3} + e^{-2\pi \nu_1 i} e^{2\pi k^2 i/3} e^{(p-q^*)\lambda_0} \right) & 0 \\[2em] 1 - e^{2\pi i/3} & 1 + e^{-2\pi i/3} & \lambda_0^{1/4}/k^{1/2} \end{pmatrix}$$

$$(3.111)$$

and where we note that $\nu_1 \equiv 1 - \frac{k^2}{2}$ and that the only difference between C^e and C^o is a sign difference in the second row.

After some algebraic manipulation, for even modes the requirement $\det C^e = 0$ gives

$$\left(\cos \psi + e^{-3/8 \lambda_0} \frac{}{2} \right) + i \left\{ -\left(\sqrt{3} \frac{\lambda_0^{1/4}}{k^{1/2}} + \frac{\sqrt{3}}{2} \right) \left(\cos \psi + e^{-3/8 \lambda_0} \frac{}{2} \right) - \frac{1}{2} \left(\sin \psi - e^{-3/8 \lambda_0} \frac{\sqrt{3}}{2} \right) \right\} = 0$$

$$(3.112)$$

and for odd modes the requirement $\det C^0 = 0$ gives

$$-\left(\cos\psi - \frac{e^{-3/8\,\lambda_0}}{2}\right) + i\left\{\left(\sqrt{3}\,\frac{\lambda_0^{1/4}}{k^{1/2}} + \frac{\sqrt{3}}{2}\right)\left(\cos\psi - \frac{e^{-3/8\,\lambda_0}}{2}\right) + \frac{1}{2}\left(\sin\psi + e^{-3/8\,\lambda_0}\frac{\sqrt{3}}{2}\right)\right\} = 0$$

$$(3.113)$$

where

$$\psi \equiv \frac{3\sqrt{3}}{8}\,\lambda_0 + \frac{\pi}{3}\,k^2 \qquad (3.114)$$

We note that equation 3.113 takes exactly the same form as 3.112 if for odd modes we take $\psi \to \tilde{\psi} = \psi - \pi$.

In each of equations 3.112 and 3.113, we demand that the real and imaginary parts vanish separately. We shall also take $e^{-3/8\,\lambda_0} \to 0$ since $\lambda_0 \to \infty$. Noting that $\frac{\lambda_0^{1/4}}{k^{1/2}} \gg 1$, we have from equation 3.112 for even modes

$$\cos\psi + i\left\{-\sqrt{3}\,\frac{\lambda_0^{1/4}}{k^{1/2}}\cos\psi - \frac{1}{2}\sin\psi\right\} = 0 \qquad (3.115)$$

with the equation for odd modes given by 3.115 where ψ is replaced by $\tilde{\psi}$, and $\psi \approx \frac{3\sqrt{3}}{8}\,\lambda_0$.

From the vanishing of the real parts, we have to first approximation for <u>even modes</u>

$$\cos\left(\frac{3\sqrt{3}}{8}\,\lambda_0\right) = 0 \qquad (3.116\,a)$$

and for <u>odd modes</u>

$$\cos\left(\frac{3\sqrt{3}}{8}\,\lambda_0 - \pi\right) = 0 \qquad (3.116\,b)$$

where for both cases we have from the vanishing of the imaginary parts

$$\tan\left(\frac{3\sqrt{3}}{8}\lambda_0\right) \approx -2\sqrt{3}\,\frac{\lambda_0^{1/4}}{\kappa^{1/2}} \tag{3.117}$$

We note that the sets of equations 3.116 (a) and 3.117 (for even modes) and 3.116 (b) and 3.117 (for odd modes) are compatible since we have with $\lambda_0 \gg 1$, $\cos\left(\frac{3\sqrt{3}}{8}\lambda_0\right) \approx 0$, and hence $\tan\left(\frac{3\sqrt{3}}{8}\lambda_0\right) \to \infty$. This is compatible with 3.116 since $\lambda_0^{1/4}/\kappa^{1/2} \to \infty$. Equation 3.117 should be regarded as a first order correction in $\kappa^{1/2}$ to equations 3.116.

To zeroth order in $\kappa^{1/2}$ then,

$$\frac{3\sqrt{3}}{8}\lambda_0 \approx \left(m-\frac{1}{2}\right)\pi \qquad m = 1, 2, 3, \cdots \tag{3.118}$$

for even modes and

$$\frac{3\sqrt{3}}{8}\lambda_0 \approx \left(m+\frac{1}{2}\right)\pi \qquad m = 1, 2, 3, \cdots \tag{3.119}$$

for odd modes. Substitution of these results into equation 3.116, and subsequent expansion in $\kappa^{1/2}$ gives the first order corrections,

Even Modes

$$\lambda_0 \approx \frac{8}{3\sqrt{3}}\left(m-\frac{1}{2}\right)\pi + \frac{1}{2\sqrt{3}}\,\frac{\kappa^{1/2}}{\left[\frac{8}{3\sqrt{3}}\left(m-\frac{1}{2}\right)\pi\right]^{1/4}} + \cdots \tag{3.120}$$

Odd Modes

$$\lambda_0 \approx \frac{8}{3\sqrt{3}}\left(m+\frac{1}{2}\right)\pi + \frac{1}{2\sqrt{3}}\,\frac{\kappa^{1/2}}{\left[\frac{8}{3\sqrt{3}}\left(m+\frac{1}{2}\right)\pi\right]^{1/4}} + \cdots \tag{3.121}$$

If we recall that $\lambda_o = \left[\dfrac{(6/5\pi)^{1/4}}{M_t^{1/2}} \right]^{4/3}$, and express λ_o in terms of M_t using 3.118 and 3.119, we find that M_t^e and M_t^o should fall in narrow ranges (governed by $\kappa^{1/2}$) about the values

$$M_{t,n}^e \approx 0.19 \big/ (2n-1)^{3/2} \qquad\qquad n=1,2,3,\cdots$$

$$M_{t,n}^o \approx 0.19 \big/ (2n+1)^{3/2} \qquad\qquad n=1,2,3,\cdots$$

$$(3.122)$$

where the first values are

$$M_{t,1}^e = 0.19 \quad , \qquad M_{t,2}^e = 0.04$$

$$M_{t,1}^o = 0.04 \quad , \qquad M_{t,2}^o = 0.02$$

$$(3.123)$$

The reader is cautioned that these results may change slightly if more precise information about the spectral energy density of the turbulence is available (see Appendix B).

Solving for the amplitudes $C_n(\kappa)$, and $E(\kappa)$ we find

$$C_1(\kappa) = C_2(\kappa) = \mp\, e^{-\pi\kappa^2 i}\, C_4(\kappa) \qquad \begin{bmatrix} - \text{ for even modes} \\ + \text{ for odd modes} \end{bmatrix}$$

$$C_3(\kappa) = e^{-2\pi/3\,(\kappa^2+1)i}\, e^{i\frac{3\sqrt{3}}{8}\lambda_o}\, C(\kappa)$$

$$C_4(\kappa) = e^{2\pi/3\,(\kappa^2+1)i}\, e^{-i\frac{3\sqrt{3}}{8}\lambda_o}\, C(\kappa) \qquad\qquad (3.124)$$

$$E(\kappa) = -i\beta\, \lambda_o^{(1-\kappa^2)/4}\, e^{-\frac{3}{8}\lambda_o}\, e^{-\frac{4}{3}\kappa^2}\, C(\kappa)$$

where $C(\kappa)$ is some complex amplitude to be determined by conditions on the radial behaviour of the solutions.

The relative strength of the vacuum field is from 3.124

$$\left| \frac{E(\kappa)}{C_M(\kappa)} \right| \sim \beta \lambda_0^{1/4} e^{-\frac{3}{2}\lambda_0} \propto M_t^{5/6} e^{-M_t^{-2/3}} \ll 1 \qquad (3.125)$$

where $\beta \sim M_t$, $\lambda_0^{1/4} \sim M_t^{-1/6}$, and $M_t \ll 1$. Hence the vacuum field is very weak compared to the field in the disc for the long-range " mean-field " modes. Powerful large scale vacuum fields definitely require conditions in the disc such that $M_t \approx 1$.

We now wish to write out the components of $\underline{B}$ for each mode κ in the regime $z \to z_0$. To do this we use the results 3.124 together with the asymptotic forms of the field components. For each mode κ , we shall have to sum all the contributions arising for each n, from $M_{t,M}^e$ and $M_{t,M}^o$, given by 3.122. Since $\lambda_{0,M} \propto M_{t,M}^{-2/3}$, the dominant contributions will arise from $M_{t,1}^e$ for even modes and $M_{t,1}^o$ for odd modes. The results 3.122 then show that the dominant field B_ϕ in a stationary setting will be even (i.e. B_ϕ will have "dipole symmetry" whereas B_z will be an odd function of z and so is of "quadrupole symmetry") since $M_{t,1}^e = 0.19 \gg M_{t,1}^o = 0.04$. The relative amplitudes of even to odd modes is approximately

$$\left| \frac{B^o}{B^e} \right| \approx \exp\left[-\frac{3}{8} \left[(6/5\pi)^{1/4} \frac{z}{z_0} \right]^{4/3} \left(\frac{1}{(M_{t,1}^o)^{2/3}} - \frac{1}{(M_{t,1}^e)^{2/3}} \right) \right] \approx e^{-1.5 (z/z_0)^{4/3}}$$

away from the centre plane of the disc.

Hence, we expect a toroidal field B_ϕ of "dipole symmetry" with $M_t \sim M_{t,1}^e = 0.19$ under stationary conditions. For even modes then, we find

$$B_r(k; \hat{r}, \hat{z}) \simeq \beta \, B(k) \, \lambda^{(1-\kappa^2)/4} \, e^{-\frac{3}{8}\lambda} \sin\left(\frac{3\sqrt{3}}{8}\left[\lambda_0 - \lambda\right] + \frac{2\pi}{3}\right) J_1(\kappa^{\frac{1}{2}}\hat{r}) \qquad (3.126)$$

$$B_\phi(k; \hat{r}, \hat{z}) \simeq B(k) \, \lambda^{-(1+\kappa^2)/4} \, e^{-\frac{3}{8}\lambda} \sin\left(\frac{3\sqrt{3}}{8}\left[\lambda_0 - \lambda\right]\right) J_1(\kappa^{\frac{1}{2}}\hat{r}) \qquad (3.127)$$

$$B_z(k; \hat{r}, \hat{z}) = -\beta \, B(k) \, \lambda^{-\kappa^2/4} \, e^{-\frac{3}{8}\lambda} \cos\left(\frac{3\sqrt{3}}{8}\left[\lambda_0 - \lambda\right] - \frac{2\pi}{3}\right) J_0(\kappa^{\frac{1}{2}}\hat{r}) \qquad (3.128)$$

where we have absorbed common factors into $B(k)$

$$B(k) \equiv i \, 4 \sqrt{\frac{2\pi}{3}} \, e^{-4\kappa^2/3} \, C(k)$$

and where

$$\lambda = \left[\frac{(6/5\pi)^{1/4}}{(M_{t,1}^e)^{1/2}} \frac{z}{z_0}\right]^{4/3}$$

with

$$\beta = (8/15\pi)^{1/2} M_{t,1}^e$$

We also note the vacuum amplitude is

$$E(k) \simeq -\beta \, B(k) \, \frac{1}{4} \sqrt{\frac{3}{2\pi}} \, \lambda_0^{(1-\kappa^2)/4} \, e^{-\frac{3}{8}\lambda_0}$$

Finally, the radial behaviour of our modes goes as $J_\nu(k^{1/2}\hat{r})$ where $\nu = 0$ or 1. Now

$$k^{1/2}\hat{r} = k^{1/2}\hat{z}_0 \frac{\hat{r}}{\hat{z}_0} = k^{1/2}\frac{\hat{z}_0}{z_0} r$$

noting that $\lambda_0 \equiv z_0^{4/3}$ we have

$$k^{1/2}\hat{r} = \frac{k^{1/2}\lambda_0^{3/4}}{z_0} r$$

so that the scale L of the modes is

$$L = \frac{1}{k^{1/2}\lambda_0^{3/4}} z_0 \tag{3.129}$$

Focussing on long scale modes $L \gg z_0$ requires from equation 3.129

$$k^{1/2} \ll \frac{1}{\lambda_0^{3/4}} \tag{3.130}$$

Equation 3.130 shows that to have scales $L \gg z_0$ for the mean field is equivalent to considering $k^{1/2}$ in the range

$$k^{1/2} \ll \lambda_0^{-3/4}$$

Having worked out the consequences of stationarity, we now investigate the situation when dynamo action and dissipation do not exactly compensate one another.

5. Small Deviations From Equilibrium

In this concluding section we shall assume $\frac{\partial B}{\partial t} \neq 0$ and

therefore investigate the possibility of having dynamo action dominating the dissipation. Returning to our full equations 3.44 and 3.45, we seek to define an appropriate dimensionless time co-ordinate $\hat{t}$. Noting that $t_k = r^{3/2}/A$ where $A = (GM_x)^{1/2}$ (M_x is the mass of the central object). Making r dimensionless (recall $\hat{r} = (\gamma x)^{1/4} r$) allows t_k to be written $t_k = \hat{r}^{3/2} / A \, (\gamma x)^{3/8}$ so that the choice

$$\hat{t} = \bar{\beta} \, t \, / \, T_k$$

$$T_k \equiv \frac{1}{A \, (\gamma x)^{3/8}} = \frac{M_t^{3/4}}{(6/5\pi)^{3/8}} \frac{z_o^{3/2}}{A} \tag{3.131}$$

results in the equations

$$\hat{r}^{3/2} \, \frac{\partial B_r}{\partial \hat{t}} - \left\{ \frac{\partial^2}{\partial \hat{r}^2} + \frac{1}{\hat{r}} \frac{\partial}{\partial \hat{r}} - \frac{1}{\hat{r}^2} + \frac{\partial^2}{\partial \hat{z}^2} \right\} B_r = -\beta \frac{\partial}{\partial \hat{z}} (\hat{z} \, B_\phi) \tag{3.132}$$

$$\hat{r}^{3/2} \, \frac{\partial B_\phi}{\partial t} - \left\{ \frac{\partial^2}{\partial \hat{r}^2} + \frac{1}{\hat{r}} \frac{\partial}{\partial \hat{r}} - \frac{1}{\hat{r}^2} + \frac{\partial^2}{\partial \hat{z}^2} \right\} B_\phi = -\frac{1}{\beta} B_r \tag{3.133}$$

Again, these equations are separable assuming a time dependence

$$\underline{B} (\hat{r}, \hat{z}, t) = B(\hat{r}, \hat{z}) \, e^{\gamma \hat{t}} \tag{3.134}$$

where γ is a complex constant. We should remember that the $\hat{r}^{3/2}$ factor arises because our turbulent diffusivity $M_T \propto r^{-3/2}$. Introducing 3.134 into equations 3.132 and 3.133, we may again seek separable solutions in r and z with a

separation constant $-k$ to find that $R(\hat{r})$ now obeys

$$\left\{ \frac{d^2}{d\hat{r}^2} + \frac{1}{\hat{r}} \frac{d}{d\hat{r}} + (k - \gamma\hat{r}^{3/2}) - \frac{1}{\hat{r}^2} \right\} R(\hat{r}) = 0 \qquad (3.135)$$

and with $Q(\hat{z})$ and $U(\hat{z})$ obeying equations 3.51 and 3.52 as before. Since we will be matching to external vacuum solutions, we take k as real and positive. We may regard $\Gamma(\hat{r}) = \gamma \hat{r}^{3/2}$ as an effective dimensionless, square, radial wave-number (complex in general). Introducing

$$k'(\hat{r}) = k - \Gamma(\hat{r}) \quad ; \quad \Gamma(\hat{r}) = \gamma\hat{r}^{3/2} \qquad (3.136)$$

we investigate the two extremes:

(1) $|k| \gg |\Gamma|$, Then $k' \sim k$ and $R(\hat{r}) \approx J_1(k^{1/2}\hat{r})$

(2) $|k| \ll |\Gamma|$, Then $k' \sim \Gamma(\hat{r})$ which results in the equation

$$\left\{ \frac{d^2}{d\hat{r}^2} + \frac{1}{\hat{r}} \frac{d}{d\hat{r}} - \gamma\hat{r}^{3/2} - \frac{1}{\hat{r}^2} \right\} R(\hat{r}) = 0 \qquad (3.137)$$

This equation may be solved exactly. In the case where $\gamma = -\gamma_0$ ($\gamma_0 > 0$ and real) we find decaying fields and from Abramowitz and Stegun ((1968) formula 9.1.53) the solution is

$$R(\hat{r}) = J_{4/7} \left(\frac{4}{7} \gamma_0^{1/2} \hat{r}^{7/4} \right)$$

which using definition 3.136 is

$$R(\hat{r}) = J_{4/7}\left(4/7\left(\Gamma_0(a)\right)^{1/2}\hat{r}\right)$$

<div align="right">(3.138)</div>

which supports the claim about $\Gamma(\hat{r})$ made above.

Restriction to the case $|\kappa| \gg |\Gamma|$ amounts to studying slowly varying temporal variations of the mean field, and as we will see, the analysis will follow along the lines as given in sections 3 and 4. The second limit $|\kappa| \ll |\Gamma|$, corresponding to rapid variations of the mean field, greatly complicates the mathematics. In particular, we have modes of radial dependence $R_{4/7}\left(\Gamma^{1/2}\hat{r}\right)$ in the disc (R symbolizing the appropriate Bessel function) whereas the vacuum modes have a radial dependence going as $J_1(\kappa^{1/2}\hat{r})$. The matching of disc and vacuum solutions then is complicated. On short enough time scales, the mean disc field is strongly influenced by the inhomogeneity introduced by a radially varying turbulent diffusivity η_T . The mathematical problems introduced by rapid time variations are probably best handled by a boundary-layer type analysis, where we note with Braginskii (1965) that in general, when matching to an exterior vacuum solution, a boundary layer of thickness $\delta \ll z_0$ is expected about $z = \pm z_0$.

The previous chapter showed that the disc is not stationary on time scales $\leq 10 t_\kappa$ so that a rapidly varying mean field on these time scales could not develop. in

stationary conditions. We shall therefore only concern ourselves with slow temporal variations of the mean field in the limit $|\kappa| \gg |\Gamma|$. In this limit, we may think of the background hydrodynamic setting as stationary. In addition, no new mathematical procedures need to be introduced.

Concentrating on the $|\kappa| \gg |\Gamma|$ limit then, we seek solutions to our disc equations and match to an external vacuum solution as we did before. For $\gamma \neq 0$; this will result in a dispersion relation which relates γ to κ and other constants. To deal with our radial inhomogeneity, we note with Whitham (1974) that in working with non-uniform media, the dispersion relation to first approximation is the dispersion relation for a uniform medium provided that the typical periods and wavelengths over which the medium varies are long compared to the waves being considered. In these cases, the procedure is to compute the dispersion relation in the case where the various parameters in equation are taken to be constant, and then to reinsert their spatial and temporal dependences when the relation has been established.

Therefore, we will regard $\theta \equiv \Gamma/\kappa$ to be a small parameter, and to regard the variations of Γ with $\hat{r}$ as negligible in order to determine the dispersion relation to lowest order. Beginning with the $e^{\gamma \hat{t}}$ time dependence in the manner already discussed, we write

$$\left\{ \frac{\partial^2}{\partial \hat{r}^2} + \frac{1}{\hat{r}} \frac{\partial}{\partial \hat{r}} - \frac{1}{\hat{r}^2} \right\} B_r = \left[-\left(\frac{\partial^2}{\partial \hat{z}^2} - \Gamma \right) B_r + \beta \frac{\partial}{\partial \hat{z}} (\hat{z} B_\phi) \right]$$

$$\left\{ \frac{\partial^2}{\partial \hat{r}^2} + \frac{1}{\hat{r}} \frac{\partial}{\partial \hat{r}} - \frac{1}{\hat{r}^2} \right\} B_\phi = \left[-\left(\frac{\partial^2}{\partial \hat{z}^2} - \Gamma \right) B_\phi + \frac{1}{\beta} B_r \right]$$

with the intent now of introducing the separation constant
$-\kappa$, with Γ regarded as constant and with $|\kappa| \gg |\Gamma|$. We
then find, using 3.49 that $R(\hat{r})$ satisfies equation 3.50 while
equations 3.51 and 3.52 become

$$\left\{ \frac{d^2}{d\hat{z}^2} - \bar{\kappa} \right\} Q = -\beta \frac{d}{d\hat{z}} (\hat{z} U) \qquad (3.139)$$

$$\left\{ \frac{d^2}{d\hat{z}^2} - \bar{\kappa} \right\} U = -\frac{1}{\beta} Q \qquad (3.140)$$

where

$$\bar{\kappa} \equiv \kappa + \Gamma$$

with the understanding that $|\kappa| \gg |\Gamma|$. Equations 3.139 and
3.140 are exactly those we dealt with before except that

$$\kappa \to \bar{\kappa} \equiv \kappa + \Gamma$$

With our vacuum field assumed to have $e^{\gamma \hat{t}}$ time
dependence, the matching procedure in section 4 may again be
used, along with the various forms of the solutions $U_n(\kappa, \hat{z})$
etc where in all cases we replace κ with $\bar{\kappa} = \kappa + \Gamma$. Since
we assume $|\kappa| \gg |\Gamma|$, our solutions are negligibly affected by
any complex component introduced by Γ .

Our strategy is to expand the relations $\det C^{e,o} = 0$ to
first order in $\theta = \Gamma/\kappa$, and then to solve for θ . We

stress that Γ will be complex in general. The dispersion relation $\det C^{e,o} = 0$ derived from the matrices 3.110 and 3.111 is in general form

$$\left(T_1 T_2 - T_3 T_4 \right)^{e,o} = 0 \qquad (3.141)$$

where for even modes

$$T_1^e = \left(e^{2\pi i/3} - e^{i\bar\psi} \, e^{3/8 \lambda_o} \right)$$

$$T_2^e = \left(i \left(2 \sin\tfrac{2\pi}{3} \, \frac{\lambda_o^{1/4}}{k^{1/2}} + \sin 2\bar{\tfrac{\pi}{3}} \right) - \left(1 + \cos\tfrac{2\pi}{3} \right) \right)$$

$$T_3^e = \left(- e^{-2\pi i/3} + e^{-i\bar\psi} \, e^{3/8 \lambda_o} \right) \qquad (3.142)$$

$$T_4^e = \left(i \left(2 \sin\tfrac{2\pi}{3} \, \frac{\lambda_o^{1/4}}{k^{1/2}} + \sin\tfrac{2\pi}{3} \right) - \left(1 - \cos\tfrac{2\pi}{3} \right) \right)$$

and for odd modes

$$T_1^o = \left(- e^{2\pi i/3} - e^{i\bar\psi} \, e^{3/8 \lambda_o} \right)$$

$$T_3^o = \left(+ e^{-2\pi i/3} + e^{i\bar\psi} \, e^{3/8 \lambda_o} \right) \qquad (3.143)$$

$$T_2^o = T_2^e \qquad \text{and} \qquad T_4^o = T_4^e$$

where

$$\psi = \frac{3\sqrt{3}}{8} \lambda_o + \bar{\tfrac{\pi}{3}} \, \bar{k}^2$$

$$\bar{k} = k + \Gamma$$

Noting that

$$\bar{K}^2 = K^2 \left[1 + 2\theta + \theta^2 \right]$$

$$\bar{K}^{-\frac{1}{2}} = K^{-\frac{1}{2}} \left[1 - \frac{\theta}{2} + \cdots \right]$$

we expand 3.141 to first order in θ using 3.142 for even modes and 3.143 for odd modes. Multiplying the resulting equations by $e^{-\frac{3}{8}\lambda_o}/2$ then gives the equations for even and odd modes

$$\left(T_{real}^{e,o} + i\, T_{imag}^{e,o} \right) + \theta^{e,o} \left[F + i\, G \right] = 0 \qquad (3.144)$$

where T_{real}^e and T_{imag}^e are the real and imaginary parts of equation 3.112 and T_{real}^o and T_{imag}^o are the real and imaginary parts of equation 3.113. Note that $\theta = 0$ gives back our original dispersion relations. The factors F and G are the same for both even and odd modes and are

$$F = -\frac{2\pi}{3} K^2 \sin\psi \qquad (3.145)$$

$$G = \frac{\sqrt{3}}{2} \frac{\lambda_o^{\frac{1}{4}}}{K^{\frac{1}{2}}} \left(\cos\psi + \frac{e^{-\frac{3}{8}\lambda_o}}{2} \right) + \frac{2\pi}{3} K^2 \left(\sin\psi \left[\sqrt{3} \frac{\lambda_o^{\frac{1}{4}}}{K^{\frac{1}{2}}} + \frac{\sqrt{3}}{2} \right] - \frac{1}{2} \cos\psi \right) \qquad (3.146)$$

Before we proceed, let us analyze the relative magnitudes

of the terms in F and G. The first term in G is

$$G_1 \approx \frac{\lambda_0^{1/4}}{\kappa^{1/2}} \cos \psi$$

while the second term is of order

$$G_2 \approx \kappa^2 \sin \psi \frac{\lambda_0^{1/4}}{\kappa^{1/2}}$$

Taking the ratio

$$\left| \frac{G_1}{G_2} \right| \approx \frac{1}{\kappa^2 |\tan \psi|} \qquad (3.147)$$

Near equilibrium, we may use equation 3.117 in both even and odd cases to give

$$\left| \frac{G_1}{G_2} \right| \approx \frac{1}{\kappa^{3/2} \lambda_0^{1/4}} \qquad (3.148)$$

Since we will want to focuss on long radial scale mean fields, equation 3.130 shows that for $L \gg z_0$

$$\frac{1}{\kappa^{1/2} \lambda_0^{3/4}} \gg 1$$

together with our usual limit

$$\frac{\kappa^{1/2}}{\lambda_0^{1/4}} \ll 1$$

gives $\left| G_1 / G_2 \right| \gg 1$. Hence, for near equilibrium conditions and focussing on long radial scale modes gives

$$G \approx \frac{\sqrt{3}}{2} \frac{\lambda_0^{1/4}}{\kappa^{1/2}} \cos \psi$$

$$\qquad (3.149)$$

$$G \gg F$$

Using all these approximations it may be shown from equation 3.144 that

$$\theta^{e,o} = -\frac{1}{F^2 + G^2} \left\{ \left(T_{real}^{e,o} F + T_{imag}^{e,o} G \right) + i \left(T_{imag}^{e,o} F - T_{real}^{e,o} G \right) \right\}$$

$$\approx \frac{1}{G} \left\{ -T_{imag}^{e,o} + i T_{real}^{e,o} \right\} \tag{3.150}$$

Assuming $e^{-3/8 \lambda_o}$ terms are negligible we find from 3.150

$$\theta^e = \frac{1}{\sqrt{3}} \frac{K^{1/2}}{\lambda_o^{1/4}} \left\{ \left(\frac{2\sqrt{3} \lambda_o^{1/4}}{K^{1/2}} + \tan\psi \right) + 2i \right\} \tag{3.151}$$

where

$$\theta^o = -\theta^e \tag{3.152}$$

The result 3.152 shows that for the same λ_o, frequencies in the odd modes are exactly the negative of those for the even modes. We comment on this later.

Noting that $\theta = \Gamma/K$, equation 3.151 gives for even modes

$$\Gamma_{real}^e = \frac{1}{\sqrt{3}} \frac{K^{3/2}}{\lambda_o^{1/4}} \left(2\sqrt{3} \frac{\lambda_o^{1/4}}{K^{1/2}} + \tan\psi \right) \tag{3.153}$$

$$\Gamma_{imag}^e = \frac{2}{\sqrt{3}} \frac{K^{3/2}}{\lambda_o^{1/4}} \tag{3.154}$$

For growing modes to occur one must have $\Gamma_{real}^{e,o} > 0$, which for even modes gives

$$\frac{2\sqrt{3} \lambda_o^{1/4}}{(-\tan\psi)} > K^{1/2}$$

We have already seen that under equilibrium conditions $\tan \psi < 0$ for both even and odd modes. Hence, we see that a critical dimensionless wavenumber $K_c^{1/2}$ enters the problem so that when $K^{1/2}$ is small enough so that

$$K_c^{1/2} > K^{1/2} \qquad (3.155)$$

$$K_c^{1/2} \equiv 2\sqrt{3} \, \lambda_o^{1/4} / |\tan \psi| \qquad (3.156)$$

then exponential growth of the field takes place. Those modes $K^{1/2}$ such that $K^{1/2} > K_c^{1/2}$ will decay. Using the result 3.129 for the scale of the mean field components, we see that even modes of scale

$$L^e > L_c \equiv \frac{z_o \, |\tan \psi|}{2\sqrt{3} \, \lambda_o} \qquad (3.157)$$

will grow exponentially while scales of $L < L_c$ will decay. We recall that $\psi = \frac{3\sqrt{3}}{8} \lambda_o$ with λ_o a function of the turbulent Mach number M_t (see 3.104) and that with $L \gg z_o$; $|\tan \psi| \gg \lambda_o$.

The mode $K_+^{1/2}$ for which $d\Gamma / d(K^{1/2}) = 0$ is found to be

$$K_+^{1/2} = \frac{2}{3} K_c^{1/2} \qquad (3.158)$$

and this mode is the most rapidly amplified component in the spectrum.

The relation 3.153 may be written in more suggestive form as

$$\Gamma_{real}^e = 2K \left[1 - \frac{K^{1/2}}{K_c^{1/2}} \right] \qquad (3.159)$$

For consistency, we note that when $|\Gamma| \approx \kappa$ the analysis can no longer be applied. From 3.159 the range of dimensionless wavenumbers considered here is therefore

$$\tfrac{1}{2} \kappa_c^{1/2} < \kappa^{1/2} < \tfrac{3}{2} \kappa_c^{1/2}$$

Within this range, the fastest decaying mode occurs at $\kappa_-^{1/2} = \tfrac{3}{2} \kappa_c^{1/2}$, which gives a faster decay rate than the rate at which the mode $\kappa_+^{1/2} = \tfrac{2}{3} \kappa_c^{1/2}$ is growing. Specifically, we find that when $\Gamma_{real}^e > 0$,

$$\Gamma_{real,+}^e \equiv max\left\{ \Gamma_{real}^e \right\} = \left(\tfrac{2}{3}\right)^3 \kappa_c \qquad (at\ \kappa = \kappa_+) \tag{3.160}$$

and when $\Gamma_{real}^e < 0$ then

$$-\Gamma_{real,-}^e \equiv max\left\{ -\Gamma_{real}^e \right\} = \left(\tfrac{3}{2}\right)^2 \kappa_c \qquad (at\ \kappa = \kappa_-) \tag{3.161}$$

These growth rates correspond to the scales

$$L_+ = \tfrac{3}{2} L_c$$

for the growing mode κ_+ and to

$$L_- = \tfrac{2}{3} L_c$$

for the decaying mode κ_- where we demand $\tfrac{2}{3} < \tfrac{L}{L_c} < 2$.

The result 3.154 shows that one necessarily has an

oscillatory dynamo at work here, whose frequency increases as we go to smaller and smaller scales.

Using the result 3.152, we see that for odd modes

$$\Gamma^{o}_{real} = -2K\left[1 - \frac{K^{1/2}}{K_c^{1/2}}\right] = -\Gamma^{e}_{real}$$

$$\Gamma^{o}_{imag} = -\frac{2}{\sqrt{3}}\frac{K^{3/2}}{\lambda_o^{1/4}} = -\Gamma^{e}_{imag}$$

$$(3.162)$$

so that odd modes of scale $L < L_c$ are growing exponentially while those of longer scales $L > L_c$ are exponentially damped with

$$\Gamma^{o}_{real,+} = \frac{3}{2}K_c^{1/2}$$

$$\Gamma^{o}_{real,-} = \frac{4}{9}K_c^{1/2}$$

$$(3.163)$$

and $K_+^o = \left(\frac{3}{2}\right)^2 K_+^e$. The dynamo action is again oscillatory.

The result 3.152 may be traced to the general symmetry of our underlying equations 3.41 and 3.42. The product $\gamma \chi$ which is a measure of the overall dynamo strength to dissipation strength is for our analysis found to be positive. If $\gamma \chi < 0$ then $U(\hat{z}) = U(-\hat{z})$ implies $P(\hat{z}) = P(-\hat{z})$; and $U(\hat{z}) = -U(-\hat{z})$ implies $P(\hat{z}) = -P(-\hat{z})$. In our system, it may then be shown that what were even mode dispersion relations for $\gamma \chi > 0$ become odd mode dispersion relations when $\gamma \chi < 0$. This kind of behaviour has been noted by Moffat (1978) p. 230 for the study of $\alpha \omega^1$

dynamos. In his discussion, χ plays the role of $\gamma\chi$ and in a disc system containing two thin regions of dynamo action we quote:

"so that if a dipole oscillatory mode exists for $\chi = \chi_0$ say, then a quadropole oscillatory mode with the same (complex) growth rate p exists for $\chi = -\chi_0$."
The result 3.152 is an expression of this basic symmetry property.

The fact that our solutions necessarily have an oscillatory character may be traced to our approximation that our mean velocity field was taken to be toroidal. As Moffat points out (p. 213), this is a property of $\alpha\omega'$ dynamos and when the poloidal velocity fields are non-zero we may expect a frequency shift of $\underline{U}_P \cdot \underline{K}$ to occur for a mode of the mean field of wavenumber $\underline{K}$. If γ_{imag} is the frequency when $U_P = 0$, the new frequency is $\gamma'_{imag} = \gamma_{imag} - \underline{U}_P \cdot \underline{K}$.

Since our main poloidal flow is radial, we expect that the effects of such a flow will be negligible provided that the drift time scale $t_D = r/u^r$ is much longer than the characteristic time over which the mean field changes. With $t_B \gg t_K$ in our analysis, this requires $t_K \ll t_B \ll t_D$.

Putting all our results together we find that the time dependence for our solutions is given by

$$\exp\left\{ \pm \frac{3}{2} (0.41) M_t \frac{t}{t_K} \left[2k\left(1 - \frac{k^{1/2}}{k_c^{1/2}}\right) + i \frac{2}{\sqrt{3}} \frac{k^{3/2}}{\lambda_0^{1/4}} \right] \right\}$$

where + is for even modes and - for odd modes and where $t_k = r^{3/2}/(GM_x)^{1/2}$ is the Keplerian time.

Focussing on $k = k_+ = \frac{4}{9} k_c$ for even modes (i.e the mode whose growth rate is the quickest) corresponding to the scale L_+ we have

$$\exp\left\{ 0.41 \ M_t \ \frac{t}{t_k} \left[\frac{4}{9} k_c + i \frac{2\sqrt{2}}{3} \frac{k_c^{3/2}}{\lambda_o^{1/4}} \right] \right\}$$

This shows that the oscillation frequency is a factor $k_c^{1/2}/\lambda_o^{1/4} \ll 1$ smaller than the inverse growth time scale of the field. The growth time of the fields depends on M_t and k_c, the entire process being scaled by the Keplerian time scale. Now the exact value of k_c depends very much on the exact value of M_t. However, we may introduce the parameter δ such that $L = z_o/\delta$ with $\delta \ll 1$. Since $k = \delta^2/\lambda_o^{3/2}$ with this parameter, we have $k_c = \delta_c^2/\lambda_o^{3/2}$ where

$$\delta_c \equiv (12)^{1/2} \lambda_o \Big/ \left| \tan \frac{3\sqrt{3}}{8} \lambda_o \right| \ll 1$$

Using the dependence of λ_o on M_t we find that the even mode with scale $L_+ = z_o/\delta_c$ grows exponentially as

$$\exp\left\{ 0.2 \left(M_t \delta_c \right)^2 t/t_k \right\}$$

Consequently, the smaller the value of the turbulent Mach number M_t, the longer is the growth time of the field, the relevant time constant being

$$t_B^e = t_k \Big/ (0.2) \left(M_t \delta_c \right)^2 \tag{3.164}$$

Thus, the most rapidly growing even mode K_+ will occur with $M_t^e = 0.19$, with δ_c being a measure of $\left| M_t^c - M_{t,1}^e \right|$, and

$$t_B^e \approx \frac{138}{\delta_c^2} t_K \qquad (3.165)$$

For the odd modes, the most rapidly growing mode is $K = K_+^0 = \frac{9}{4} K_c$ corresponding to the scale $L_+ = \frac{2}{3} L_c = \frac{4}{9} L_+^e$. In this case however, the largest value of M_t is $M_{t,1}^0 = 0.04$ so that the exponential growth occurs with a typical time of

$$t_B^0 \approx \frac{446}{\delta_c^2} t_K \qquad (3.166)$$

These results clearly show that the most rapidly growing mode is the even mode of wavenumber $K_+^{1/2} = \frac{2}{3} K_c^{1/2}$. We note that the exact amplification rate is sensitive to the exact value of M_t. The build up of the field occurs on time scales $t_B \approx 100 t_K$ which is of the order of seconds to tens of seconds in the inner regions of the disc where $t_K \approx 10^{-2}$ s and approaches the drift time scale. The results show that the longer the length scale of the mode, the longer the time required to build up the amplitude by dynamo action.

We leave to chapter 4 the analysis of how such growing fields ultimately equilibriate to some steady value.

Chapter 4

Implications For Accretion Disc Models

1. Introduction

In this chapter, we bring together the various ideas investigated in chapters 2 and 3 and examine the effect of our analysis on accretion disc structure.

We first turn our attention to the equilibrium value of the mean large-scale magnetic field, and investigate what type of stresses are set up by such a field. Section 2 is devoted to this analysis and it is shown that the mean, large-scale, (long time average) Maxwell stresses give rise to the same type of accretion disc as studied by Shakura and Sunyaev (1973).

In section 3, we try to assess the long time averaged effect the localized intense magnetic fluctuations will have on angular momentum transport and disc structure. Arguments are introduced which, although not completely rigorous because of a lack of detailed information about the spectrum of the the magnetic turbulence, nonetheless show that the Lightman and Eardly instability mentioned in the opening chapter may be suppressed. A consistent cool thin accretion disc (averaged over long enough time scales) can therefore be imagined. The source of the hard X-ray spectrum would then appear to be

associated with a collection of intense loops of magnetic field, emerging from the disc surfaces, and undergoing solar-type flares.

Section 4 is a rather crude analysis of the type of spectrum one could expect from the flaring regions discussed. Again, we make the analogy with solar flares and model the hard X-ray emission as arising from a rapid flash-phase of the flare, wherein bremsstrahlung emission arises from a non-thermal electron population (accelerated in the flare region) interacting with the denser gas towards the disc surface.

2. Equilibriation Of The Mean Magnetic Field And Consequences For Accretion Disc Structure.

In this section, we study the angular momentum transport (over long time scales) generated by the mean field B. In order to do this, some estimate of the ultimate equilibrium value of B must be made.

We have shown in Chapter 3 that initially weak magnetic disturbances of long enough scale will grow exponentially on time scales $100\, t_k$. It was assumed in this case that the flow was Keplerian. We now ask, what does this field do to the turbulence and/or the mean flow to limit its own growth.

Two possibilities come to mind. The mean field may act to alter the turbulence (reaction on micro-scale) when the field approaches equipartition energies (see Moffat (1972)).

Another point of view is that the large-scale field may be determined by rotational constraints acting directly on the large-scale flows, and may be insensitive to the detailed structure of the underlying turbulence responsible for magnetic regeneration (see Malkus and Proctor (1975), Proctor (1977), and a brief review by Moffat (1978) p. 303-307). Which mechanism predominates is a question which has no general answer yet, however, the latter point of view is the one of immediate interest in accretion processes.

The idea is that growing large-scale magnetic fields will give rise to large-scale Lorentz forces. These forces in turn generate a large scale velocity field. The magnitude of the induced velocity can be determined from the induction equation and its estimation is independent of the magnitude of B. The ultimate level of mean magnetic field energy is then determined by the magnetostrophic balance in which Lorentz forces and Coriolis forces are of the same order of magnitude (provided certain conditions are met). In this picture, we imagine the induced velocity field as arising as a result of angular momentum transport by the mean field, which is how we connect with the accretion problem.

Let us briefly discuss the Malkus and Proctor (1975) analysis for "α^2" dynamos. The idea is to assume that α in the mean induction is unaffected by the large-scale magnetic field. Defining the quantity

$$R_{\alpha_c} \equiv \frac{|\alpha_c|\, r}{\eta}$$

where α_c is the value of α for which excitation of the large scale mean field can occur. When $R_\alpha > R_{\alpha_c}$, the field grows exponentially until the Lorentz force back-reaction on the flows is significant. If $R_\alpha = R_{\alpha_c}(1+\epsilon)$ where $0 < \epsilon \ll 1$, it is possible for the growth of the field to be arrested by the appearance of a mean velocity distribution driven by the Lorentz force; all this occurring before modification of α by the mean field $\underline{B}$ is important. The mean velocity field will continue to grow until it can compensate for the Ohmic losses of the growing magnetic field. For the problem of rotating fluids in a sphere, the mean magnetic field level should then be roughly determined by the balance of Coriolis and Lorentz forces. The exact level of the mean magnetic field depends on $(R_\alpha - R_{\alpha_c})$.

The equations studied for "α^2" dynamos in the rotating frame of reference are (neglecting Reynolds stresses; we return to this point later)

$$\frac{\partial \underline{u}}{\partial t} + \underline{u} \cdot \nabla \underline{u} + 2 \underline{\Omega} \times \underline{u} = -\nabla P + \frac{1}{\rho} \underline{J} \times \underline{B} + \nu \nabla^2 \underline{B} \tag{4.1}$$

$$\frac{\partial \underline{B}}{\partial t} = \nabla \times (\alpha \underline{B}) + \nabla \times (\underline{u} \times \underline{B}) + \eta \nabla^2 \underline{B} \tag{4.2}$$

where $\alpha(\underline{x})$ is prescribed and with initial conditions

$$\underline{u}(\underline{x},0) = 0 \quad , \quad \underline{B}(\underline{x},0) = \underline{B}_0(\underline{x})$$

where $\underline{B}_o(\underline{x})$ is the eigenfunction in the problem when $\underline{U}=0$ and $R_\kappa = R_{\alpha_c}$. With $R_\kappa = R_{\alpha_c}(1+\epsilon)$, the mean field $\underline{B}$ initially grows exponentially and generates a velocity fied given by 4.1. The velocity field grows until it has significant effect in 4.2. The relevant magnitude of $\underline{U}$ when this stage is reached is found by comparing $\nabla \times (\underline{U} \times \underline{B})$ with $\eta \nabla^2 \underline{B}$ so that we expect $\underline{U}$ is of order

$$U_o \approx \eta / r \qquad\qquad (4.3)$$

In the situation where

$$E = \nu/\Omega r^2 \ll 1 \qquad ; \qquad E_M = \eta/\Omega r^2 \ll 1$$

the Coriolis forces in 4.1 are more important than the inertial forces (at least away from the boundary) so that the relevant magnitude of B is deduced from the balance of the Lorentz and Coriolis forces, and is of order

$$\frac{B_o^2}{4\pi} = \rho \Omega U_o r = \rho \Omega \eta \qquad\qquad (4.4)$$

where both the estimates for B_o and U_o should by multiplied by a function of ϵ .

We wish to make similar estimates for the "$\alpha\omega$'" dynamo studied in Chapter 3. For this problem, both α and $U^\phi \approx V_\kappa$ are prescribed. Previous arguments have shown that for thin discs the toroidal velocity is always Keplerian to good

approximation and that this comes about because the particles orbit in the powerful external gravitational field of the central black hole. The growing mean field $\underline{B}$ is imagined to give rise to a radial velocity U^r. The effective magnetic diffusivity in the problem is $\mathcal{M}_T$. We then estimate the order of magnitude of the induced velocity field as

$$|U^r| = \mathcal{M}_T / r \tag{4.5}$$

arising from the Lorentz force reaction on the disc. Neglecting the Reynolds stress for the moment, we then expect that the vertically averaged Maxwell stress $\langle B^\phi B^r \rangle / 4\pi$ is (see equation 1.7) over long time, steady state conditions

$$W^{\phi r} = \left\langle \frac{B^\phi B^r}{4\pi} \right\rangle = -\Sigma u^r u^\phi \tag{4.6}$$

Equation 4.6 is nothing new; however, the radial velocity U^r has been set by the mean induction equation (relation 4.5). This means that we now have a sufficient number of equations to compute the disc structure, assuming that the Maxwell stress from the mean field $\underline{B}$ dominate the Reynolds stress. Before we analyze this last assumption, we note that from the definition 3.35 for $\mathcal{M}_T$, that U^r is just

$$|U^r| = \frac{M_t^2 c_s^2}{u^\phi} \tag{4.7}$$

so that the Maxwell stress 4.6 becomes (assuming $\overset{r}{U}<0$ for radial inflow)

$$\left\langle \frac{B^{\phi}B^{r}}{4\pi} \right\rangle \approx M_t^2 \, \Sigma \, c_s^2 \tag{4.8}$$

We note that 4.8 expresses the Maxwell stress in terms of the pressure in the same fashion as the standard model outlined in Chapter 1, that is, except for our factor of M_t^2. Again, the equilibrium values for $|u^r|$ and $|B^{\phi}B^r|$ found above should be multiplied by functions of ϵ in order to arrive at exact values.

Assuming that the equilibrium field $\underline{B}$ has a similar structure as computed in Chapter 3 (the ultimate field has roughly the same structure as the linearized analysis derives, provided that it is below equipartition strength) we estimate from equations 3.126 and 3.127

$$B^r \approx \beta \, \lambda^{1/2} \, B^{\phi}$$

as the relation between the radial and azimuthal field components in the region $z \rightarrow z_0$. With $M_t \ll 1$, and using the definition 3.46 for β and 3.60 for λ we have

$$\langle B^r \rangle \approx M_t^{2/3} \langle B^{\phi} \rangle \tag{4.9}$$

where numerical factors from the z integration have been dropped and only the scaling with M_t retained. With relation

4.9, we find from 4.8

$$\underbrace{\langle B^2 \rangle}_{8\pi} \approx \underbrace{\langle B^{\phi 2} \rangle}_{8\pi} \approx M_t^{4/3} \Sigma c_s^2$$

which shows that the mean magnetic field energy in the limit $M_t \rightarrow 0$ is below equipartition with the thermal energy of the gas by a factor $M_t^{4/3}$.

Considering the Reynolds stress contribution to $W^{r\phi}$, we have already noted that the eddy viscosity model (see Chapter 1) gives $W^{r\phi} \approx M_t \Sigma c_s^2$. It is however also reasonable to estimate the Reynolds stress (vertically averaged) as

$$\langle \overline{\rho u'^\phi u'^r} \rangle \approx \Sigma \tilde{u}^2 = M_t^2 \Sigma c_s^2 \qquad (4.10)$$

The model 4.10 shows that a competition between the Reynolds stress and the Maxwell stress due to the mean field may be expected. The dominant stress is likely to be decided by the detailed vertical structure and the magnitude of ϵ . Here, we assume the Maxwell stress dominates.

This simple order of magnitude analysis shows that the mean field Maxwell stress gives rise to the same steady-state disc structure equations as given in Chapter 1. This arises because we have assumed that $\tilde{u} = M_t c_s$ in our calculations for M_T .

The discussion so far has ignored the contribution to the stress $W^{r\phi}$ made by the intense fluctuating fields we discussed

in Chapter 2. We regarded these intense, short-lived, spatially localized fluctuations as negligible as far as angular momentum transport averaged over long time scales was concerned. We examine this assumption in the following section.

3. The Long Time Averaged Effects Of The Magnetic Fluctuations

We examine the restrictions that can be put on M_t in the case where magnetic fluctuations as large as $\tilde{b}^2/8\pi\rho_0 \approx V_k^2$ occur. Using the result $\tilde{b}^2 = (M_T/\eta)B^2$ and the equilibrium value for B discussed in the previous section, we obtain

$$\frac{\langle \tilde{b}^2 \rangle}{8\pi} = \frac{M_T}{\eta} \frac{\langle B^2 \rangle}{8\pi} = \frac{M_T}{\eta} M_t^{4/3} \sum c_s^2 \qquad (4.11)$$

and for maximal fluctuations

$$\frac{\langle \tilde{b}^2 \rangle}{8\pi} \approx \sum V_k^2$$

we have

$$V_k^2 \approx \frac{M_T}{\eta} M_t^{4/3} c_s^2 \qquad (4.12)$$

Using the expression for M_T, this is

$$V_k^2 \approx M_t^{10/3} \frac{r}{\eta V_k} c_s^2$$

or with the magnetic Reynolds number $R_M = r V_k/\eta$ we have

$$M^{10/3} \approx \left(\frac{r}{z_0}\right)^4 R_M^{-1} \qquad (4.13)$$

where we have noted that $(z_o/r) \approx (C_s/V_K)$. Since we are dealing with very large magnetic Reynolds numbers, the result 4.13 shows that maximal fluctuations may occur in regimes where M_t is small. As an example, with $R_M \sim 10^{12}$ and with ranges for z_o/r appropriate for the disc of $10^{-1} \gtrsim z_o/r \gtrsim 10^{-2}$, we find that

$$10^{-2.4} \lesssim M_t \lesssim 10^{-1.2} \tag{4.14}$$

This is interesting in that our model for large fluctuations is consistent with an analysis where $M_t \ll 1$.

Let us more closely examine how large the local magnetic fluctuations can become. The densities ρ in the three regions of the standard accretion disc model are in terms of the dimensionless variables (see Shakura and Sunyaev)

$$m \equiv M_x / M_\odot$$

$$r_* \equiv r / r_i$$

$$\dot{m} \equiv \dot{M} / \dot{M}_{cr} \sim \left(\dot{M} / 3 \times 10^{-8} M_\odot \, yr^{-1} \right) \frac{1}{m}$$

(a) inner region: $(1 \leq r_* \leq 150)$

$$\rho_i \approx 7.2 \times 10^{-7} \, M_t^{-2} \, \dot{m}^{-2} \, m^{-1} \, r_*^{3/2} \tag{4.15}$$

(b) middle region: $(150 \leq r_* \leq 6,300)$

$$\rho_m \approx 7.0 \, M_t^{-14/10} \, \dot{m}^{2/5} \, m^{-7/10} \, r_*^{-33/20} \tag{4.16}$$

(c) outer region: $(6,300 \leq r_*)$

$$\rho_0 \approx 5.0 \times 10^1 \, M_t^{-14/10} \, \dot{m}^{11/20} \, m^{-7/10} \, r_*^{-15/8} \qquad (4.17)$$

where the critical accretion rate $\dot{M}_{cr}$ is determined from the Eddington limit. We note that the only difference between Shakura and Sunyaev, and the formulas we give is that they use M_t when we use M_t^2 (this is because $W^{r\phi} \approx M_t \, P$ for their eddy viscosity model and $W^{r\phi} \approx M_t^2 \, P$ from the mean field Maxwell stress).

A glance at the radial dependences of these densities shows shows that the maximum density occurs at $r_* \approx 150$; at the boundary of the inner and middle regions with $r_* \rightarrow 150$.

For the Cyg X-1 source, the black hole mass is 10 $M_\odot$ so $m \sim 10$ and since the luminosity is 10^{37} erg s^{-1}; $\dot{m} \sim 10^{-2}$.

Writing $V_k^2 = \dfrac{c^2}{3} \dfrac{1}{r_*}$, we find that for maximal fluctuations $\tilde{b}^2/8\pi = \rho_0 V_k^2$, that in the inner zone of the disc

$$\tilde{b}_i^2 = 5.4 \times 10^{18} \, r_*^{1/2} \, M_t^{-2}$$

If we take $r_* = 150$; we then find that

$$M_t \approx 0.26 \quad \Longleftrightarrow \quad \tilde{b}_i \approx 10^{10.5} \, Gauss \qquad (4.18)$$

We use the estimate of $10^{10.5}$ Gauss, because as shown in

Chapter 1, we found that such a field strength can explain the shot noise model in terms of solar-type flares.

The value for the turbulent Mach number of M=0.26 derived by the above arguments is in agreement with the eigenvalue of M =0.19 found in Chapter 3. We have used two entirely different approaches and come down to similar estimates for the value of M_t. This leads us to the view that at equilibrium, the overall structure of the disc is determined by the mean magnetic field (it provides the angular momentum transport) which sets the value for $M_t \approx 0.19$. This disc structure, in turn, will effect the magnitude of the magnetic fluctuations that can be expected. The shot-noise model can be accounted for by randomly (in time) occurring flares, which have maximum energies if originating in the region $r \approx 100 - 150 \, r_*$. Flares occur everywhere on the disc surfaces, but the energies emitted by flares in regions other than $r_* \approx 100 - 150 \, r_*$ will be to low to stand out above the overall background emission. We note that with M_t =0.19 say, the interpretation of millisecond bursts as flare events becomes difficult. We return to this point in section 4.

Before leaving this discussion, we note that if we take $\tilde{b} \approx 10^{10.5}$ Gauss, then the total energy contained in the field is

$$\left(\tilde{b}^2 / 8\pi \right) \, \ell^3 \approx 4 \times 10^{37} \, erg$$

Now this considerably overestimates the energy release of

10^{36} ergs per event. The explanation is that only about 3% of the total magnetic field energy is being converted into other forms of energy during every flare event. This compares favourably with the results of the experiments discussed in Chapter 1.

All of the discussion to this point has concentrated on a thin disc as the underlying model for our calculations. As mentioned in the opening chapter however, the assumption that $W^{r\phi} = M_t P$ where M_t is a constant was shown by Lightman and Eardley (1974) to lead to a secular instability of the inner (radiation dominated) zone of the standard thin disc model. We briefly discuss this instability and later show that the contribution made to the overall stress by an intermediate time average of $\overline{\sigma''^{r\phi}}$ can stabilize the inner zone, so that it is consistent to think of a cool thin accretion disc.

Making no assumptions about stationarity, the disc structure equations deliver the following equation for the evolution of the surface density

$$\frac{\partial \Sigma}{\partial t} = \frac{1}{r}\frac{\partial}{\partial r}\left\{ \left[\frac{d(u^\phi r)}{dr}\right]^{-1} \frac{\partial}{\partial r}\left[r^2 W^{r\phi}(\Sigma, r)\right]\right\} \qquad (4.19)$$

a result which follows from the continuity equation

$$\frac{\partial \Sigma}{\partial t} + \frac{1}{r}\frac{\partial}{\partial r}(r \Sigma u^r) = 0 \qquad (4.20)$$

and the conservation of angular momentum

$$\Sigma \, u^r u^\phi = -\frac{z}{r} \frac{\partial}{\partial r} \left(r^2 \, W^{r\phi} \right) \tag{4.21}$$

Now in the inner radiation pressure dominated zone of the disc, one can show that in the constant M_t model for the turbulence

$$W^{r\phi} \propto \left(M_t \, \Sigma \right)^{-1} \tag{4.22}$$

a result which follows from the independence of P_r (and the temperature T) on the density Σ in this inner region. If equation 4.22 is substituted into 4.19, there results a non-linear diffusion type equation for the surface density Σ that turns out to have a negative effective diffusion coefficient. Lightman (1974(a) and (b)) studied this equation both analytically and numerically and confirmed that the result of this negative diffusion coefficient is for material to "clump" into rings, with higher density zones getting higher in density and lower density zones getting lower. This clumping occurs on all wavelengths (secular) and on a time scale

$$t_{instab} \gtrsim \left(\frac{z_0}{r} \right)^2 t_D \approx M_t^{-2} \, t_\kappa \tag{4.22b}$$

where the last equality is a consequence of

$$t_D = \left(\frac{t_D}{t_\kappa} \right) t_\kappa = \left(\frac{u^\phi}{u^r} \right) t_\kappa = M_t^{-2} \left(\frac{z_0}{r} \right)^{-2} t_\kappa$$

where t_D is the drift time scale $t_D \equiv r/u^r$. Physically, with $W^{r\phi} \propto \Sigma^{-1}$ (for constant M_t) one has low stress in high-Σ regions and high stress in low-Σ regions so that matter is pushed into regions of low stress resulting in increasing density contrast and the formation of dense rings of gas. The wavelengths λ of these regions must be $\lambda > l_u$ because of turbulent mixing on smaller scales. This ring structure is not thermally stable and should heat rapidly, resulting in the swelling of the optically thick, radiation pressure dominated cool regime into a much hotter, gas pressure dominated, optically thin one. It is this observation which lead to the two temperature model dicussed in Chapter 1. Lightman and Eardley (1974) point out that if M_t is not a constant however, but falls at least as fast as Σ^{-1}, then a stationary, stable, thin cool disc is possible. This may be seen by substituting $M_t \propto \Sigma^{-n}$ ($n \geqslant 1$) into 4.21 and then into equation 4.18, where one finds then a positive effective diffusion coeficient. Physically, what is happening is that the efficiency of angular momentum transport is decreased so that the instability no longer occurs.

Now in the magnetically dominated disc we have been discussing, the Maxwell stress due to the mean field takes the form $M_t^2 P$ so that this long time averaged stress cannot alter the instability discussed in the previous paragraph. Let us however examine the Maxwell stress arising from the

fluctuating fields. We recall that from Chapter 2 we had the stress arising from the magnetic fluctuations

$$\overline{\sigma''\phi r} = \frac{u^r}{u^\phi} \tilde{b}^2$$

corresponding to the situation where $\tilde{b}^2 = \frac{M_T}{\eta} B^2$. Now over the hydrodynamic time scale r/u^ϕ we found that stationarity was not possible and so the above expression for $\overline{\sigma''\phi r}$ denotes fluctuations in the overall Maxwell stress occurring on short time scales and small length scales. Taking the vertical average and using the results 4.11 and 4.5 we find

$$\left\langle \overline{\sigma''\phi r} \right\rangle = \left(M_T^2 \quad \frac{M_t^{4/3}}{\eta} \frac{1}{r u^\phi} \right) \Sigma c_s^2 \qquad (4.23)$$

Now from the long time averaged structure of the disc, assuming steady state gives

$$\dot{M} = 2\pi \Sigma u^r r$$

which, in view of equation 4.5 shows that

$$M_T = \dot{M} / 2\pi \Sigma \qquad (4.24)$$

and hence, 4.23 may be written

$$\left\langle \overline{\sigma''\phi r} \right\rangle = I\!N_0 \; \Sigma c_s^2 \qquad (4.25)$$

where have defined an effective turbulent Mach number $I\!N_0$ as

$$I\!N_0 = \left(\frac{\dot{M}}{(2\pi)^2} \quad \frac{M_t^{4/3}}{\eta} \frac{1}{r u^\phi} \right) \cdot \frac{1}{\Sigma^2} \qquad (4.26)$$

In other words, the localized Maxwell stress fluctuations corresponding to our intense magnetic fluctuations can be characterized by a viscosity parameter or effective Mach number $\mathcal{M}_o$ which has a density dependence of Σ^{-2}. This is just the type of density dependence that would stabilize the inner disc region. However, this analysis must be taken one more step. We must average these fluctuations 4.25 in the Maxwell stress over longer length and time scales in order to determine what their average effect will be. The relevant scales for averaging are the length and time scales over which the instability discussed could arise, which are scales intermediate between the hydrodynamic time scale and turbulent eddy size on the one hand, and the very long time and length scales assumed for the stationary disc models we have discussed.

The most obvious effect of magnetic fluctuations is to cause density fluctuations, since we have noted that regions of intense field should drive down the density in that region making it buoyant. Now our dynamo parameter α depends on $\rho_o^{-1} \frac{\partial \rho_o}{\partial z}$ so that we expect random fluctuations in the magnetic field to be associated with random fluctuations in α. The averaging problem then is to regard α as having a randomly varying component, which we average over a time scale t_α

$$t_k \ll t_\alpha \ll t_D$$

and over a length scale of

$$\ell_u \ll \ell_\alpha \ll r$$

The analysis to follow, first investigated by Kraichnan (1976) shows that these intermediate time and length scale averages of the induction equation with random fluctuations of α results in a modification of η_T to a new value η_T^{eff}. Hence, our fluctuations over the intermediate scales listed above allow us to assess the effect of $\overline{\sigma^{\prime\prime} r}$ fluctuations over these scales.

We follow Kraichnan's analysis starting from the mean induction equation

$$\frac{\partial \underline{B}}{\partial t} = \nabla \times \left(\alpha \, \underline{B} + \underline{u} \times \underline{B} \right) + \eta_T \nabla^2 \underline{B} \qquad (4.27)$$

and consider the effect of spatial and temporal fluctuations of α over the scales t_α and l_α. To do this, a double averaging procedure over scales a_1 and a_2 satisfying

$$\ell_u \ll a_1 \ll \ell_\alpha \ll a_2 \ll r \qquad (4.28)$$

is introduced. Preliminary averaging over a gives rise to the induction equation 4.27. We treat α as having a randomly varying component which will be averaged over the scale a_2. The double overbar $\overline{\overline{}}$ will denote averaging over a_2 quantities that have already been averaged over a_1.

Splitting $\underline{B}$ and α into mean and fluctuating parts

$$\underline{B} = \underline{B}_0 + \underline{b}_1 \quad ; \quad \alpha = \alpha_0 + \alpha_1 \tag{4.29}$$

where

$$\overline{\underline{B}} = \underline{B}_0 \quad ; \quad \overline{\underline{b}_1} = 0$$

$$\overline{\alpha} = \alpha_0 \quad ; \quad \overline{\alpha_1} = 0 \tag{4.30}$$

one then finds

$$\frac{\partial \underline{B}_0}{\partial t} = \nabla \times \left(\alpha_0 \underline{B}_0 + \underline{U} \times \underline{B}_0 + \overline{\alpha_1 \underline{b}_1} \right) + \eta_T \nabla^2 \underline{B}_0 \tag{4.31}$$

$$\frac{\partial \underline{b}_1}{\partial t} = \nabla \times \left(\alpha_1 \underline{B}_0 + \alpha_0 \underline{b}_1 + \underline{U} \times \underline{b}_1 \right) + \eta_T \nabla^2 \underline{b}_1 + $$

$$+ \nabla \times \underline{G}_1 \tag{4.32}$$

where

$$\underline{G}_1 \equiv \alpha_1 \underline{b}_1 - \overline{\alpha_1 \underline{b}_1} \tag{4.33}$$

The term $\nabla \times \underline{G}_1$ in equation 4.32 may be neglected (first order smoothing) provided that

$$\epsilon_1 \equiv \widetilde{\alpha}_1 t_\alpha / l_\alpha \ll 1 \tag{4.34}$$

where $\widetilde{\alpha}_1 = \left(\overline{\alpha_1^2}\right)^{1/2}$ is the root mean square of the fluctuation α_1. We notice that the induction equation 4.27 has been modified by the appearance of a new term $\overline{\alpha_1 \underline{b}_1}$. We estimate this correlation in the same manner as done in Appendices A and B. Specifically, we Fourier transform equation 4.32 to solve for $\hat{\underline{b}}_1$ (the Fourier transform of $\underline{b}_1$), compute $\overline{\hat{\alpha}_1 \hat{\underline{b}}_1}$, and then inverse transform. This procedure is complicated by the presence of terms depending on the mean velocity $\underline{U}$ and α_0 (not considered by Kraichnan).

Moffat (1978, p. 177) sketches out the case for $\alpha_0 = \underline{U} = 0$ where one finds

$$(-i\omega + \eta_T k^2)\, \hat{\underline{b}}_1 = -i\, \underline{B}_0 \times \underline{k}\, \hat{\alpha}_1 + \hat{\alpha}_1 \nabla \times \underline{B}_0 \tag{4.35}$$

where $\underline{B}_0$ and $\nabla \times \underline{B}_0$ are treated as uniform over the length scale l_α. One then obtains

$$\overline{\alpha_1 \underline{b}_1} = -\underline{B}_0 \times \underline{Y} + X (\nabla \times \underline{B}_0) \tag{4.36}$$

where

$$X = \iint \frac{\eta_T k^2 \Phi_{\alpha_1}(\underline{k}, \omega)}{(\omega^2 + \eta_T^2 k^4)}\, d\underline{k}\, d\omega \qquad ; \qquad \underline{Y} = \iint \frac{\underline{k}\, \Phi_{\alpha_1}(\underline{k}, \omega)}{(\omega^2 + \eta_T^2 k^4)}\, d\underline{k}\, d\omega \tag{4.37}$$

and $\Phi_{\alpha_1}(\underline{k}, \omega)$ is the spectrum function of the field α_1.

Now let us compare the terms $\nabla \times (\alpha_0 \underline{b}_1)$ and $\nabla \times (\underline{U} \times \underline{b}_1)$ with $\eta_T \nabla^2 \underline{b}_1$ in equation 4.32. The dominant contribution from $\nabla \times (\alpha_0 \underline{b}_1)$ is of order $\alpha_0 \underline{b}_1 / l_\alpha$, so that the η_T term dominates if

$$1 \gg \frac{\alpha_0 l_\alpha}{\eta_T} \approx \frac{z}{z_0} \frac{l_\alpha}{z_0} \tag{4.38}$$

where the last inequality in 4.38 follows from the estimates 3.35 and 3.36. Now for small Mach numbers M_t we noted that $\ell_u/z_0 \approx M_t$ so it is consistent to estimate $\ell_\alpha \approx z_0$ in order for 4.38 to hold. So near the surface regions $z \sim z_0$ the two terms become comparable.

The term $\nabla \times (\underline{u} \times \underline{b}_1)$ is more difficult because U^ϕ can be large. However, using the same arguments as used in Chapter 2, terms involving $\underline{U}$ will not be important provided that b_1^r is small compared to b_1^ϕ. The important contribution from $\underline{U}$ is then the radial velocity U^r so that $\eta_T \nabla^2 \underline{B}_0$ dominates if

$$1 \gg \frac{u^r \ell_\alpha}{\eta_T} \approx \frac{\ell_\alpha}{r} \tag{4.39}$$

which is well satisfied. Consequently, for scales $\ell_\alpha \approx z_0 \gg \ell_u$ (only if $M_t \ll 1$), and regions $z < z_0$ with axisymmetric fluctuations α_1 and $\underline{b}_1$, the results 4.36 and 4.37 are still applicable and equation 4.31 becomes

$$\frac{\partial \underline{B}_0}{\partial t} = \nabla \times \left(\alpha_0 \underline{B} + (\underline{U} + \underline{Y}) \times \underline{B}_0 \right) + (\eta_T - X) \nabla^2 \underline{B}_0 \tag{4.40}$$

Equation 4.40, under the approximations listed in the previous paragraph, shows that the effect of the fluctuations α_1 give rise to a correction $\underline{Y}$ to the velocity field and modify the diffusivity of the field $\underline{B}_0$ to

$$\eta_T^{eff} = (\eta_T - X) < \eta_T \tag{4.41}$$

where the last inequality arises from the fact that $X > 0$. For

fluctuations α_1 independent of ϕ; equation 4.37 shows that $Y^\phi = 0$ ($\bar{\Phi}_{\alpha_1}$ independent of k^ϕ). Hence we expect corrections to the radial inflow velocity U^r to be the main effect of $\underline{Y}$.

The crucial point is to examine the magnitude of X. Moffat shows that when

$$\varepsilon_2 \equiv m_T t_\alpha / l_\alpha^2 \ll 1 \qquad (4.42)$$

then X may be estimated as

$$X \sim O (\tilde{\alpha}_1^2 t_\alpha) \qquad (4.43)$$

Now, we have already constrained l_α to be $l_\alpha \approx z_0$, so that with $m_T \approx M_t^2 z_0^2 / t_\kappa$, the inequality 4.42 gives

$$\varepsilon_2 \approx \frac{M_t^2 \, t_\alpha}{t_\kappa} \quad \ll 1 \qquad (4.44)$$

so that the time scale t_α is constrained

$$t_\alpha < M_t^{-2} \, t_\kappa \qquad (4.45)$$

which by 4.22b is

$$t_\alpha < t_{instab.} \qquad (4.46)$$

where t_{instab} was the time scale over which the Lightman and Eardley instability occurred.

Let us estimate $\tilde{\alpha}_1^2$ in terms of the density fluctuations we imagine arising from intense magnetic fluctuations $\tilde{b}$ (on a scale a_1). Since α depends on the density as $\rho_0^{-1} \frac{\partial \rho_0}{\partial z}$, we

estimate

$$\widetilde{\alpha}_{\iota} \approx \left(\widetilde{\rho}_{\iota} \,/\, \rho_{o} \right) \; \alpha_{o} \qquad\qquad (4.46)$$

where $\widetilde{\rho}_{\iota}$ is the root mean squared density fluctuation averaged out over scales l_{α} and t_{α}. Then

$$\frac{X}{M_{T}} \approx \frac{\widetilde{\alpha}_{\iota}^{2} t_{\alpha}}{M_{T}} = \left(\widetilde{\rho}_{\iota}/\rho_{o} \right)^{2} \frac{\alpha_{o}^{2} t_{\alpha}}{M_{T}} < \left(\frac{z}{z_{o}} \right)^{2} \left(\frac{\widetilde{\rho}_{\iota}}{\rho_{o}} \right)^{2} \qquad (4.47)$$

Strict observance of 4.44 guarantees that $X \ll M_{T}$, however, pushing the time scale t_{α} up to t_{in+tl} implies from 4.47 that the magnitude of the density fluctuations associated with our local magnetic fluctuations is all important.

From our discussion and using 4.41 together with 4.47 we find

$$M_{T} > M_{T}^{\bullet H} \geq M_{T} \left[1 - \left(\frac{z}{z_{o}} \right)^{2} \left(\frac{\widetilde{\rho}_{\iota}}{\rho_{o}} \right)^{2} \right] \qquad (4.48)$$

If we were to average over longer times t_{α}, we could expect that $\widetilde{\rho}_{\iota}/\rho_{o}$ approaches some constant value so that always $M_{T}^{\ell H} > 0$. This is only speculation however. The general problem remains that if $X > M_{T}$, a negative diffusivity of the mean field would result, and therfore , the concept of the fields $\underline{b}'$ and $\underline{B}$ existing on two widely separated scales is in doubt. In general, the magnitude of X probably depends sensitively on the detailed spectrum of the turbulence (see

Kraichnan (1976)).

We note from relations 4.5 and 4.24 that a decrease of m_T is associated with a decreased radial inflow U^r and an increased value of the surface density Σ. The correction to U^r is the term Y_r^r.

We may now return to the discussion of the Lightman and Eardley instability. In Chapter 2 we saw that the Maxwell stress arising from the fluctuations can be related to the magnitude of the long time averaged stress as $\overline{\left\langle \frac{b'^r b'^\phi}{4\pi} \right\rangle} = \left[\frac{\tilde{b}^2/4\pi \rho_o}{u^{\phi 2}} \right] W^{r\phi}$. On short time scales, the magnetic energy fluctuations can reach equipartition with the rotational energy density and thus their associated stress is of the same order of magnitude as $W^{r\phi}$. Over much longer length and time scales magneto-hydrostatic balance must be maintained so that $\left\langle \frac{\tilde{b}^2}{4\pi} \right\rangle \lesssim \Sigma c_s^2$ and consequently $\overline{\left\langle \frac{b'^r b'^\phi}{4\pi} \right\rangle} \ll W^{r\phi}$ on these scales.

We now note that $W^{r\phi} = M_t^2 \Sigma c_s^2$, with M_t constant and $\overline{\left\langle \frac{b'^r b'^\phi}{4\pi} \right\rangle} = \mathcal{M}_o^{eff} \Sigma c_s^2$ where $\mathcal{M}_o^{eff}$ depends on $(m_T^{eff})^2$. On the longest scales, we expect m_T^{eff} and hence $\mathcal{M}_o^{eff}$ to take its smallest value so that magneto-hydrostatic balance can be satisfied. However, on shorter scales t_α and l_α, it is apparent that $\mathcal{M}_o^{eff}$ can be of the same order as M_t^2. Since $\mathcal{M}_o^{eff} \propto \Sigma^{-2}$, the Lightman and Eardley instability will be defeated by the stress due to the fluctuating field.

These arguments show that a thin, cool accretion disc is consistent when the effects of magnetic fluctuations are considered. We expect to find a corona of intense magnetic field fluctuations of maximum strength $\hat{b} \approx 10^{10.5}$ Gauss overlying this disc. These fields will undergo

flaring processes, and we turn finally to a brief analysis of the X-ray emission that might be expected.

4. X-ray Spectra From Solar-Type Flares In-The Cyg X-1 Source

The observed power law X-ray spectrum of the Cyg X-1 source is usually interpreted as arising from a radially dependent temperature integrated over the disc surface. The model of Galeev et al (1979) imagines that a magnetically confined, hot corona of material is heated by reconnection of the looped coronal fields giving rise to thermal bremsstrahlung emission. Their mechanism explains the hard component of the X-ray spectrum with the soft photon flux (<10 kev) arising from the cool underlying accretion disc. We note that for an energy release of 10^{36} ergs in a "thermal" flare then

$$10^{36} = 3kT(nV)$$

where T is the temperature, n the plasma particle density and V the volume of the magnetically confined plasma. To get the lowest estimate for nV, we adopt a temperature of 1.8×10^{9} °K corresponding to the maximal X-ray energies of 150 kev and find the number of particles

$$nV \approx 1.38 \times 10^{42}$$

which for a maximum loop radius of $1 \approx 10^{7}$ cm, $V \approx 10^{21}$ cm^3 and so we

are talking about plasma densities

$$M \approx 10^{21} \, cm^{-3}$$

which is less than the particle density $M \approx 10^{22} \, cm^{-3}$ in the outer portion of the inner radiation dominated zone of the accretion disc. One criticism we have of the Galeev et al model is that with loops of dimension $l \approx 3 \times 10^{6}$ cm and fields $\bar{b} \sim 10^{8}$ Gauss, if 3×10^{35} ergs are to released in each flare event then virtually the entire magnetic field energy must be converted into thermal energy of the plasma, which is contrary to the observation that only about 5% of the magnetic energy is so converted. We feel therefore that their time scales are overestimated by 5 and their fields underestimated by a factor 20. However, their basic physical principles provide a consistent model for thermal heating of the coronal plasma due to flares.

There is a large amount of uncertainty in the analysis of the hard X-ray component (>10 kev) of the solar flare X-ray emission, as to whether thermal or non-thermal (power-law) populations of electrons are responsible for generating the observed power-law X-ray spectra (see Kane (1975) for a series of articles dealing with this question). It does seem clear that for solar flares bremsstrahlung is the dominant radiation mechanism.

Observations of solar flares of duration 100 s shows that

there is a flash phase lasting 1 s during which much of the hard X-ray emission is occurring. The theoretical work suggests that a non-thermal electron population may be responsible for hard X-ray emission during this initial short flash-phase of the overall flare.
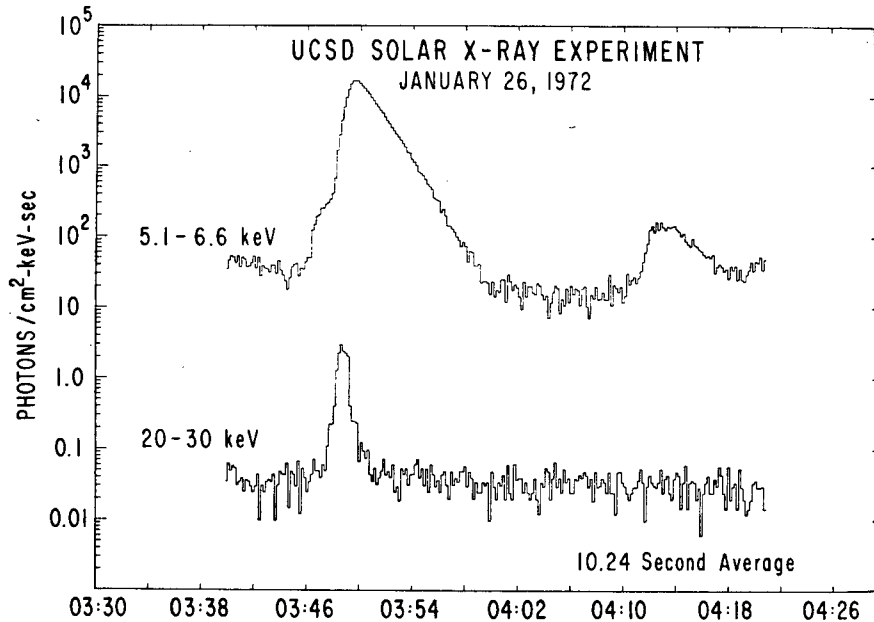
Datlowe et al (1974) have studied a sample of 123 hard solar X-ray bursts using the solar X-ray experiment on the OSO-7 satellite. During a typical event, the hard X-ray flux peaked earlier and decayed rapidly compared to the soft X-ray flux. This is clearly shown in Fig. 7 taken from their paper.

The hard and soft X-ray components of a flare exhibit very different behaviour. In addition, the OSO-7 data most commonly show a steady softening of the spectrum throughout the burst.

These authors find that there is a detectable time difference between the time interval in which the flare energy grows and the time interval over which hard X-ray producing non-thermal energy input takes place, suggesting that the soft (thermal) X-ray emission does not arise from energy input of the non-thermal electrons within the hot flare plasma itself.

Finally, for the solar bursts studied, the spectral indices ranged from 3.5 to 5.5.

Hard and soft X-ray flux from an SN flare at 03:46 UT on January 26, 1972. The upper trace gives the 5.1–6.6 keV channel of the soft X-ray detector, and is characteristic of the thermal X-ray flux. The lower trace gives the 20–30 keV channel of the hard X-ray detector, representative of the hard X-ray flux. Each point represents 10.24 s of data. Hard X-ray analysis was carried out from 3:47:31 to 3:49:24. The background was taken to be the flux from 04:00 to 04:08.

We shall therefore investigate what conditions are necessary in order that the hard X-rays from the Cyg X-1 source be interpreted as arising from non-thermal electron populations that are maintained in flares over some time $\Delta T_{flash} \ll \Delta T_{flare}$. We assume that:

(1) Each flare of total duration 10^{-1} s has an initial flash phase of duration $\Delta T_{flash} < 10^{-1}$ s during which the hard

component (>20 kev) of the X-ray emission occurs, liberating 10^{36} ergs of energy in this band.

(2) The spectral index for the X-ray photons of energy >20 kev is constant from flare to flare.

Both of these assumptions are crude because conditions at different flare sites on the accretion disc are apt to be different.

We follow the same procedures as used for solar flare work as outlined by Korchak (1976). Suppose that at each moment in time, the X-ray spectrum from an emitting region of volume V can be described by a power law form

$$\frac{dj}{d\varepsilon} = K_x \, \varepsilon^{-\delta} \quad \text{photons cm}^{-2} \text{ s}^{-1} \text{ kev}^{-1} \qquad (4.49)$$

for photon energies in some range $\varepsilon_1 \leq \varepsilon \leq \varepsilon_2$ and where δ is the "spectral index". Then assuming a differential cross-section appropriate for bremsstrahlung by Coulomb collisions, the instantaneous spectrum for the electrons may be written as

$$\frac{dN}{dE} = K_c \, E^{-(\delta-\frac{1}{2})} \quad \text{electrons kev}^{-1} \qquad (4.50)$$

where K_c may be determined in terms of K_x and the average gas density $\bar{n}$ in the emitting region, and which includes a factor R^2 where R is the distance from the source to the observer (R= 1A.U. For solar flares).

One must now go one more step and consider the relation between the electron spectrum in the emitting region (dN_e/dE) and the spectrum of the electrons in the source region. These two regions need not be the same, and in solar flares, the analysis suggests the source electrons are accelerated in the lower density regions higher in the atmosphere and move downward into denser regions closer to the stellar surface where the emission of X-rays occurs. If dN_e/dE is the instantaneous average spectrum already discussed, and dF_o/dE is the power of the source, then the relation between these two is given by a continuity equation which under quasi-static conditions may be solved to give

$$\frac{dF_o}{dE} = \frac{dN}{dE} \left(\frac{1}{\tau_c} + \frac{1}{\tau_e} \right) \tag{4.51}$$

where τ_c is the characteristic time for the loss of electrons due to Coulomb collisions of the electrons by the ambient gas of density $\bar{n}$ and τ_e is the characteristic time of escape from the emitting region.

The lifetime in the Coulomb collisions is given by

$$\tau_c = \frac{2 \times 10^8 E^{3/2}}{\bar{n} \, \delta} \quad s \tag{4.52}$$

where E is given in units of kev while the minimum estimate for the escape time is given by free escape,

$$\tau_{e, \, min} = \ell / v \tag{4.53}$$

where l is the linear dimension of the emitting region and v is the electron speed. When $T_e \ll T_c$, then the escape time is much smaller than the collision time and most of the electrons escape without colliding. This case is the so-called "thin target" approximation. Conversely , for $T_c \ll T_e$, the collision term dominates and most of the electrons lose their energy through collisions. This is the "thick-target" approximation and is obviously more efficient at producing X-rays. It has been noted by Brown (1975) that the thick target case may over-estimate the total number of electrons required for the X-ray emission by an order of magnitude. Korchak (1976) notes in his analysis that either of these cases are limiting approximations useful only for a qualitative analysis of a flare problem.

Let us first consider what conditions are required for the thick-target approximation. Here

$$T_c = 2 \times 10^8 E^{3/2} / \bar{n} \delta \ll T_{e,min} = \ell/v$$

Taking a typical electron energy of 50 kev say, with a dimension $1 \sim 10^6$ cm for the emitting region, and $\delta \approx 2$ say, we find that for the inequality 4.54 to be satisfied, the gas density in the thick-target must be $\bar{n} \gg 10^{14}$ cm^{-3}. With coronal atmospheres of about 10^{19}-10^{21} cm^{-3}, this could be well satisfied.

We restrict ourselves to the analysis of the thick-

target case for the moment. As Korchak points out, a lower electron energy cut-off E_1 kev must be introduced in order to estimate the total number of electrons and their total energy. It is possible to make and order of magnitude error in the theory because it is impossible to evaluate E_1 within the context of the theory itself.

Nevertheless, introducing the low energy cut-off for the electrons E_1 in the electron power-law spectrum, at a distance of 1A.U the total flux F_0 of electrons with an energy $E \geqslant E_1$ and their total power P for thick-target emission are given by (see Korchak)

$$F_o (E \geqslant E_1) = 3 \times 10^{33} \frac{(\delta-1) \; \Gamma(\delta-\frac{1}{2})}{\Gamma(\delta-1)} \quad K_x \; E_1^{-\delta} \quad s^{-1} \qquad (4.55)$$

$$P(E \geqslant E_1) = 5 \times 10^{24} \frac{\delta \; \Gamma(\delta-\frac{1}{2})}{\Gamma(\delta-1)} \quad K_x \; E_1^{1-\delta} \quad erg \; s^{-1} \qquad (4.56)$$

where E_1 is given in terms of kev and K_x is such that $K_x \, \varepsilon^{-\delta}$ has the units $cm^{-2} s^{-1} kev^{-1}$ with ε given in kev.

To specialize to Cyg X-1 conditions we first correct the results 4.55 and 4.56 by factors of $(R_{Cyg X-1}/R_{sun})^2$ where $R_{Cyg X-1} = 2.5 kpc = 5.15 \times 10^8$ A.U.

From the data of Dolan et al it seems two possibilities for the power law X-ray spectrum are possible.

(1) There is no break in the electron spectrum in the energy band 20-150 kev. In this case, from equations 1.2 and 1.3 we estimate

$$\delta \approx 2.0$$

$$E_0 = 28 \; keV \tag{4.57}$$

$$C = 7.7 \times 10^{-3} \; photons \; cm^{-2} \; s^{-1} \; keV^{-1}$$

which gives the value for K_x as

$$K_x \approx 6.04$$

Then for thick target bremsstrahlung, we find for Cyg X-1 flares

$$F_0 (E \geqslant E_1) \approx 4.25 \times 10^{51} \; E_1^{-2} \; s^{-1} \tag{4.58}$$

$$P (E \geqslant E_1) \approx 1.42 \times 10^{43} \; E_1^{-1} \; erg \; s^{-1} \tag{4.59}$$

Equation 4.59 gives the power contained in the non-relativistic electrons. If we want the entire hard X-ray emission per flare (>20kev) of $\approx 10^{36}$ ergs to arise from these non-thermal electrons, we require (note that the total emission per flare is 4×10^{36} ergs)

$$2 \times 10^{36} \; erg = \Delta T_{flash} \cdot P(E \geqslant E_1) \tag{4.60}$$

so that with a cut-off of $E_1 \approx 20$ kev;

$$\Delta T_{flash} \approx 3 \times 10^{-6} \; sec \tag{4.61}$$

which in turn implies that the total number of electrons required is

$$N_{e,tot} (E \geqslant E_1) = \Delta T_{flash} \cdot F_0 (E \geqslant E_1) \approx 3.18 \times 10^{43} \; electrons \tag{4.62}$$

There is one difficulty with these results. We have in Chapter 1 made a case for taking $l=10^6$ cm as the size of the magnetic fluctuations. We are imagining in our flare model that the flaring region is a neutral tube or sheet between two adjoining magnetic loops. Now the time for a light signal to propagate over 10^6 cm is

$$\tau_{light} = \ell / c = 3 \times 10^{-5} \; sec$$

Hence, case (1) violates causality considerations by an order of magnitude. If equation 4.56 is examined, it is seen that a higher spectral index ($\delta > 2$) is favourable for lengthening the flash time. This leads us to our second case.

(2) There is a break in the hard part of the X-ray spectrum at ~ 50 kev say. Dolan et al mention that a third of their spectra demonstrate the break with spectral indices of 2.5 or more for the higher energy domain.

We assume that the hard X-ray emission ($E > 50$ kev say) is the first radiation produced in the source, and that this emission has a spectral index of $\delta = 3.0$ say. As the flare continues, the lower energy (still hard) X-rays are produced but that these have a lower spectral index of $\delta = 2.0$ because the power law electron population is being degraded by inverse Compton scattering of cool disc photons. It is known that a power law electron population of spectral index Γ will give rise to an X-ray spectral index of $(\Gamma + 1)/2$ when Compton scattering occurs.

Thus, taking δ =3.0 as the photon index for $\mathcal{E}$ >50 kev say in spectra with an observed break in the 20-150 kev band, and adjusting K_x by a factor of 1.3 due to the change in slope of the spectrum (estimated from Fig. 3), we find that using E_i=20 kev gives

$$F_0 \approx 1.06 \times 10^{48} \quad s^{-1} \tag{4.63}$$

$$P = 5.25 \times 10^{40} \quad erg \; s^{-1} \tag{4.64}$$

from which using equation 4.60 we derive a flash time

$$\Delta T_{flash} \simeq 3.8 \times 10^{-5} \quad sec \tag{4.65}$$

and hence a total number of electrons per event of

$$N_{e,tot} = 4.24 \times 10^{43} \quad electrons \tag{4.66}$$

This flash time satisfies causality constraints.

Now with δ =3.0, for $\mathcal{E}$ >50 kev we assume that we have a single electron power law in the range 20-150 kev with spectral index

$$\Gamma_e = \delta - \tfrac{1}{2} = 2.5$$

Assuming that X-ray photons in the 20-50 kev range are emitted in the latter phases of the flash, one expects the electrons in this energy range to be degraded by inverse Compton scattering (we support this claim later). Thus, the

electrons with spectral index Γ_e =2.5 give rise to X-ray spectra for the 20-50 kev range with a spectral index of

$$\gamma = \left(\Gamma_e + 1\right)/2 = \left(2.5 + 1\right)/2 = 1.75$$

which is in agreement with the low state spectral index of 1.83±0.06 given by Dolan et al.

This model, involving a break in the X-ray spectrum due to the degradation of electrons in the latter phases of the flash by inverse Compton scattering, delivers a plausible picture of the flaring region. The idea that the spectrum of each flare steadily "softens" during the course of the flare seems to correspond with the solar flare results.

We note that the flash time of 4×10^{-5} s is much smaller than the escape time of 10^{-4} s so that a thick-target process must be assumed. Hence, the requirement $\tau_c < \Delta \tau_{flash}$ gives rise to (equation 4.52) a lower limit for the gas density of $\bar{n} > 1.8 \times 10^{15}$ cm^{-3}.

To make further progress we consider two possible extreme cases. We have noted that an upper limit on the coronal gas density was $\bar{n} \approx 10^{21}$ cm^{-3} while the lower limit is established by $\bar{n} \approx 1.8 \times 10^{15}$ cm^{-3} so that $\tau_c \leq \Delta \tau_{flash}$. Hence, we may consider 10^{15} cm$^{-3} < n_e < 10^{21}$ cm^{-3}. We consider the consequences of either extreme.

(1) $\underline{n}_e \approx \underline{10^{15}} \ \underline{cm}^{-3}$ ($\tau_c = \Delta \tau_{flash}$). Then from 4.66 we require a volume of 10^{28} cm^3 or $l \approx 10^9$ cm dimension of electrons to be

swept up in just one flare. This is clearly unrealistic since it approaches the radial extent of the disc itself.

(2) $n_e \approx 10^{21} cm^{-3}$ ($\tau_c \approx 10^{-5} \tau_{flash}$). Then if no reacceleration of electrons occurs, one requires a volume of $10^{22} cm^{-3}$ or $1 \sim 10^{7.3}$ cm. This is still large by an order of magnitude. However, with $n_e \sim 10^{21} cm^{-3}$ as the electron density, we see that the electrons are being accelerated and halted in the same spatial region. Under these conditions, Brown (1975) has suggested that the total number of electrons ($N_e \approx 10^{43}$) could be reduced if electrons were reaccelerated. The number of electrons required would then be reduced by a factor depending on how frequently electrons , already having undergone collision, could be reaccelerated. If this mechanism worked at high efficiency, then since $\tau_c / \Delta\tau_{flash} \approx 10^{-5}$, we would suppose that each electron would be reaccelerated a maximum of 10^{5} times. The total number of electrons now required is reduced to $N_{e.tot} \approx 10^{38}$ and with $n_e \approx 10^{21} cm^{-3}$, a volume of $10^{17} cm^{-3}$ is involved in each flash. An emission region consisting of a neutral tube of length 10^{6} cm then would have a radius of $\sim 10^{5}$ cm while a neutral sheet of area $10^{12} cm^{2}$ would have a thickness of 10^{5} cm.

We conclude that the electrons are most likely being accelerated in the the same region where emission occurs, and that with the electron density the same as the gas density of $\bar{n} \approx 10^{21} cm^{-3}$, an adequate fit to the date can be entertained.

We notice that the $10^{21} cm^{-3}$ coronal density is to occur in the region 100-150 r_* where we have already shown that the most powerful flares should originate.

This model for the spectrum should be regarded as crude because no physics of the acceleration mechanism has been produced. However, no comprehensive treatment as yet exists for solar flare mechanisms. It is interesting to note however that a collision time $10^{-10} s$ for $\bar{n} \approx 10^{21} cm^{-3}$ gives rise to a mean free path for electrons of 100kev energies say of $\lambda \approx 10^{-1} cm$. Now, as noted in Chapter 1, scaling arguments suggest that one may have electric fields equivalent to 10^{9} volts/cm so that over a mean free path of 10^{-1} cm, a particle could aquire $\sim 10^{3}$ kev energies. With a 100kev electron as our starting point, this suggests that if the electric fields are directly involved in some manner, then the acceleration mechanism operates at about a 10% efficiency for converting magnetic energy into particle acceleration. These considerations suggest that the combination of a high ambient gas density in the flaring region (compare to solar flares where $\bar{n} \sim 10^{10} cm^{-3}$ in the flaring region) together with an overall efficiency of <10% for pumping magnetic energy into particle acceleration , is responsible for limiting the bulk of the electrons to <150 kev energies, This explains the observed high energy cut-off at 150 kev.

Our model for the spectrum is then that randomly

occurring flares of 10/s lasting for 0.1s each emit total energies of order 10^{36} ergs. The dominant flares occur in a region 100-150 r_*. Each such flare is characterized by a double power law X-ray spectrum with $\delta \approx 2.0$ for the 20-50 kev range, and $\delta \approx 3.0$ for the 50-150 kev range. The hard X-ray emission (>20kev) of total energy 10 ergs per flare is modelled as arising in a very rapid flash phase of duration $\Delta\tau_{flash} \approx 4 \times 10^{-5}$ s during which the electron spectrum is taken to be a power law dependence, so that non-thermal bremsstrahlung is the dominant emission mechanism. The explanation of the double power law X-ray spectrum is that the electron population is progressively degraded by inverse Compton scattering of cool disc photons. In the final stages, thermal emission of soft photons is the predominant process. Such flares must have electron densities $n_e \approx 10^{21}$ electrons cm^{-3} for the thick target case.

The soft X-ray flux (E<20 kev) arises both from soft photons emitted by the flare after the flash phase, as well as the soft photon flux from the accretion disc itself.

Let us investigate the the efficiency of the inverse Compton process by which soft photons from the accretion disc scatter off the non-thermal electrons in the flash phase. Now the characteristic time for Compton cooling is of order (Tucker (1975))

$$\tau_{Compton} \approx \frac{3.08 \times 10^7}{U_{phot}.\, \gamma} \; s \qquad (4.67)$$

where U_{phot} is the energy density of the photon field and γ is the Lorentz factor for the electrons. From Shakura and Sunyaev, the photon energy density in the radiation dominated inner zone of the standard disc model is given by

$$U_{phot} \approx 2.1 \times 10^{15} \; M_t^{-2} \; m^{-1} \; r_*^{-3/2} \; erg \; cm^{-3} \qquad (4.68)$$

which, when substituted into equation 4.67, using $M_t = 0.19$ and m=10 gives

$$\tau_{Compton} \approx \frac{0.78 \times 10^{-8} \; r_*^{3/2}}{\gamma} \; s \qquad (4.69)$$

which specializing to the region $r_* \approx 100$ gives

$$\tau_{Compton} \approx \frac{0.78 \times 10^{-5}}{\gamma} \; s \qquad (4.70)$$

For mildly relativistic electrons ($\gamma = 3$), the Compton cooling time is of order of the flash duration $\tau_{comp} \lesssim \Delta\tau_{flash} \approx 10^{-6}$ s. We note that the radiation zone photon energy density is independent of $\dot{m}$ so that variations in $\dot{m}$ will not effect this result. We see that Compton scattering becomes dominant towards the end of the flash phase.

The photon energy density from the middle zone of the disc depends on $\dot{m}$ however. It is smaller than the energy density of the radiation dominated zone so that cool photons from this part of the disc would not be expected to alter the Compton time significantly. However, variations in $\dot{m}$ will effect the overall soft X-ray output of the source. This

explains the observation that the hard X-ray characteristics are virtually unaltered in either high or low states, whereas the soft photon flux certainly does change between these two states.

Finally, we consider the millisecond bursts. If these bursts are at all real, we suggest that they may be some sort of "naked" flash phase of a flare not accompanied by soft photon emission (see Canizares (1976)). We emphasize that rapid flash times are required for the model we have discussed. These flares occur well away from the event horizon. Rapid flash phenomena may very well explain any variations at millisecond and submillisecond time scales so that observations of such variations would not constitute a test of whether a rotating or non-rotating black- hole exists at the centre of an accretion disc.

Conclusions

The analysis of magnetohydrodynamics in a turbulent accretion disc using the methods of Mean Field Electrodynamics shows that magnetic fluctuations and mean magnetic fields are important on different time and length scales.

In Chapter 2, the analysis shows that if small correlation time scales $\tau_u < t_k$ are considered, then intense fluctuations of the magnetic field are possible on short $l_u \ll z_o$ length scales. On such time scales, the accretion disc cannot be stationary. If the mean properties of the fluctuations are considered over longer time and length scales, we find that because energy is being drained out of the turbulent fluctuations to support the fluctuating and mean magnetic fields, that buoyancy forces become more prominant a factor in damping out the turbulence, especially in the surface regions of the disc. The analysis of the velocity, temperature, and magnetic fluctuations shows that the mean magnetic field can determine how large such fluctuations will be. This question was furthur studied in Chapters 3 and 4.

In Chapter 3, we show that assuming a steady mean field, that matching a disc mean field to an external vacuum field reulted in an estimate for the turbulent Mach number of $M_t \approx 0.19$. If an underlying standard disc model is assumed, this would reduce to two the total number of parameters

required to fit the observations (assuming steady state). The toroidal field dominates in the disc and the favoured configuration is a mode of "dipole symmetry" for B_ϕ (and consequently "quadropole symmetry" for B_z). The vacuum field is expected to be very weak in comparison to the disc field in the limit of small Mach numbers. These results are all obtained by analytic means in the low Mach number limit. The central result of this Chapter 3 is the demonstration that a turbulent dynamo is possible in a "standard" cool accretion disc model. The "dipole symmetry" mode for B_ϕ is again the favoured configuration since for wavelengths larger than a critical wavelength (dependent on M_t) this mode has the fastest growth rate. The time scales for this growth are of order $100t_K$ in the limit that small deviations from equilibrium are considered.

The roles of the mean and fluctuating magnetic fields as far as accretion disc structure and observational consequences are found to be quite different, even though the two fields are interrelated as examined in Chapter 2. In Chapter 4, it was shown that on long length and time scales, that Maxwell stresses due to the mean field dominate those arising from the fluctuating fields, and that they provide a stress $W^{r\phi}$ of the same form as assumed for the analysis of the "standard " accretion disc model. On intermediate time scales however, the magnetic fluctuations contribute a stress which acts to

stabilize the accretion disc to "clumping" in the inner radiation dominated zone. Consequently, such standard models are consistant and the hard X-ray emission from the source must arise from either a hot corona or intense solar-type flares. Chapters 2 and 4 show that magnetic fluctuations are sufficiently strong to account for these phenomena and provide a physical basis for the shot noise model.

The interpretation of the hard X-ray component as arising from the "flash-phases" of solar type flares on the accretion disc shows that rapid flash times $\Delta t_{flash} \gtrsim 4 \times 10^{-5}$ s are expected. This means that sub-millisecond bursting of the Cyg X-1 source need have nothing to do with processes occurring near a black hole event horizon. Such rapid variations, if found, cannot reliably be used to discriminate between either a rotating or non-rotating black hole.

Many features of our analysis may be extended to other astrophysical phenomena. Immediate application to the galactic dynamo problem is possible. The idea that active galaxies may be powered by accretion discs around central massive black holes can be further tested by applying these methods to the system and determining the role of magnetic fields in such energy releasing processes. Double radio sources seem to require twin opposed beams of relativistic electrons to power them. Magnetic fields generated by accretion discs may have long range structure capable of collimating such beams.

Intense electric fields generated in flare events on an accretion disc may provide bursts of extremely relativistic electrons.

In general, we may state that because strong mean magnetic fields can be generated by dynamo action in a turbulent accretion disc, and that intense short lived magnetic fluctuations orders of magnitude above the mean field level can occur, that magnetic processes form a crucial element in any models for the Cyg X-1 source.

Bibliography

Abramowitz, M. and Stegun, I.A. 1968, _Handbook of Mathematical Functions_ (Dover)

Alme, M.L. and Wilson, J.R. 1976, Ap.J., _210_, 233

Bahcall, J.N. 1978, _Annual Review of Astronomy and Astrophysics_, Vol. 16, p. 241

Baum, P.J., Bratenahl, A. and White, R.S. 1973, Phys of Fluids, _16_, 226

Baum, P.J. and Bratenahl, A. 1976, Solar Physics, _47_, 331

Blandford, R.D. 1976, Mon. Not. R. Astr. Soc., _176_, 465

Blandford, R.D. and Znajek, R.L. 1977, Mon. Not. R. Astr. Soc., _179_, 433

Bleistein, N. and Handelsman, R. 1975, _Asymptotic Expansions of Integrals_ (Holt, Rinehart and Winston), Chap. 7

Blumenthal, G.R. and Tucker, W.H. 1972, Nature, _235_, 97

Boyer, S., Byraw, E., Chubb, T. and Friedman, H. 1965, Science, _142_, 394

Braginskii, S.I. 1965, JETP, _20_, 726

Bratenahl, A. and Yeates, C.M. 1970, Phys. of Fluids, _13_, 2696

Canizares, C.R. 1976, Ap.J. Letters, _207_, L101

Datlowe, D.W., Elcan, M.J. and Hudson, H.S. 1974, Solar Phys., _39_, 155

Eardley, D.M. and Lightman, A.P. 1975, Ap.J., _200_, 187

Flannery, B. 1975, Ap.J., _201_, 661

Galeev, A.A., Rosner, R. and Vianna, G.S. 1979, Ap.J., _229_, 318

Giacconi, R., Gursky, H. Paolini, F.R. and Rossi, B.B. 1962, Phys. Rev. Letters, _9_, 439

Gilman, P.A. 1970, Ap.J., 162, 1019

Gradshteyn, I.S. and Ryzhik, I. 1965, Table of Integrals, Series, and Products (Academic Press)

Ichimaru, S. 1977, Ap.J., 214, 840

Kane, S.R. 1975, Solar Gamma-, X-, and EUV Radiation ; I.A.U. Symposium No. 68 (D. Reidel)

Kellogg, E.M. 1975, Ap.J., 197, 689

Korchak, A.A. 1976, Sov. Astron., 20, 211

Kraichnan, R.H. 1976, J. Fluid Mech., 75, 657

Krause, F. and Roberts, P.H. 1973, Ap. J., 181, 977

Krause, F. and Roberts, P.H. 1976, J. Math. Phys., 17, 1808

Landau, L.D. and Lifshitz, E.M. 1959, Fluid Mechanics (Pergamon Press), Chap. 2

Liang, E.P.T. and Price, R.H. 1977, Ap.J., 218, 247

Lightman, A.P. 1974a, Ap.J., 194, 419

Lightman, A.P. 1974b, Ap.J., 194, 429

Lightman, A.P. and Eardley, D.M. 1974, Ap.J. Letters, 187, L1

Lovelace, R.V.E. 1976, Nature, 262, 649

Malkus, W.V.R. and Proctor, M.R.E. 1975, J. Fluid Mech., 67, 417

Moffat, H.K. 1972, J. Fluid Mech., 53, 385

Moffat, H.K. 1978, Magnetic Field Generation in Electrically Conducting Fluids (Cambridge)

Novikov, I.D. and Thorne, K.S. 1973, in Black Holes ; Les Houches Summer School of Theoretical Physics (1972), (ed. C. DeWitt and B.S. DeWitt), p. 345

Oda, M., Gorenstein, P., Gursky, H., Kellogg, E., Schreier, E., Tannenbaum, H. and Giacconi, R. 1971, Ap.J. Letters, 166, L1

Oda, M. 1977, Space Sci. Rev., 20, 757

Parker, E.N. 1955a, Ap.J., 121 , 491

Parker, E.N. 1955b, Ap.J., 122 , 293

Parker, E.N. 1971, Ap.J., 163 , 225

Pouquet, A., Frisch, U. and Leorat, J. 1976, J. Fluid Mech., 77 , 321

Prendergast, K.H. 1960, Ap.J., 132 , 162

Pringle, J.P. and Rees, M.J. 1972, Astron. Astrophys., 21 , 1

Proctor, M.R.E. 1977, J. Fluid Mech., 80 , 769

Roberts, P.H. 1971, in Mathematical Problems in the Geophysical Sciences (ed. W.H.Reid), p. 129

Roberts, P.H.and Soward, A.M. 1975, Astron. Nachr., 296 , 49

Rothschild, R.E., Boldt, E.A., Holt, S.S. and Serlemitsos, P.J.1974, Ap.J. Letters, 189 , L13

Rothschild, R.E., Boldt, E.A., Holt, S.S. and Serlemitsos, P.J. 1977, Ap.J., 213 , 818

Sanford, P.W., Ives, J.C., Bell-Burnell, S.J., Mason, K.O. and Murdin, P. 1975, Nature, 256 , 109

Shakura, N.I. and Sunyaev, R.A. 1973, Astron. Astrophys., 24 , 337

Shakura, N.I., Sunyaev, R.A. and Zilitinkevich, S.S. 1978, Astron. Astrophys., 62 , 179

Shapiro, L.S., Lightman, A.P. and Eardley, D.M. 1976, Ap.J., 204 , 187

Steenbeck, M., Krause, F. and Rädler, K.H. 1966, Z. Naturforsch., 21a , 1285 (English translation: Roberts and Stix (1971), Tech. Note 60, NCAR, Boulder, Colorado)

Stewart, J.M. 1976, Astron. Astrophys., 49 , 39

Sweet, P.A. 1969, Annual Review of Astronomy and Astrophysics , Vol. 7, p. 149

Tennekes, H. and Lumley, J.L. 1972, A First Course in Turbulence (MIT)

Terrell, N.J. 1972, Ap.J. Letters, _174_ , L35

Tucker, W.H. 1975, _Radiation Processes in Astrophysics_ (MIT),
    p. 165

Weisskopf, M.C. and Sutherland, P.G. 1978, Ap.J., _221_ , 228

Whitham, G.B. 1974, _Linear and Non-Linear Waves_ (John Wiley
    and Sons)

Znajek, R.L. 1978, Mon. Not. R. Astr. Soc., _185_ , 833

Appendix A

Mean Field Electrodynamics

A.1 Basic Ideas

We refer the reader to the excellent reviews by Moffat (1978, Chapter 7) and Roberts (1971). Introducing the decomposition of the magnetic and velocity fields

$$\underline{b} = \underline{B} + \underline{b}' \qquad ; \qquad \overline{\underline{b}'} = 0 \tag{A.1}$$

$$\underline{u} = \underline{U} + \underline{u}' \qquad ; \qquad \overline{\underline{u}'} = 0$$

the mean and fluctuating parts of the induction equation are

$$\frac{\partial \underline{B}}{\partial t} = \nabla \times (\underline{u} \times \underline{B} + \underline{\mathcal{E}}) + \eta \nabla^2 \underline{B} \tag{A.2}$$

$$\frac{\partial \underline{b}'}{\partial t} = \nabla \times (\underline{u} \times \underline{b}' + \underline{u}' \times \underline{B} + \underline{\mathcal{G}}') + \eta \nabla^2 \underline{b}' \tag{A.3}$$

where a mean electromotive force

$$\underline{\mathcal{E}} = \overline{\underline{u}' \times \underline{b}'} \tag{A.4}$$

is seen to arise due to the correlation of the fluctuating velocity and magnetic fields and

$$\underline{\mathcal{G}}' \equiv \underline{u}' \times \underline{b}' - \overline{\underline{u}' \times \underline{b}'} \tag{A.5}$$

It is the objective of mean field electrodynamics to express $\underline{\mathcal{E}}$ as a linear functional of $\underline{B}$. Then A.2 is a closed equation for $\underline{B}$ which may be studied in isolation from $\underline{b}'$.

We first note that the computation of $\underline{\varepsilon}$ is simplest when

$$\underline{G}' \approx 0 \qquad\qquad (A.6)$$

known as the first order smoothing approximation. If l_u is the correlation length of the turbulent fluctuations and τ_u the correlation time, this term is small when as an example,

$$\epsilon_2 \equiv \tilde{u}\,\tau_u / l_u \ll 1 \qquad\qquad (A.7)$$

We consider the consequences of A.7 more in section A.2. With $\underline{G}' \approx 0$, and writing equation A.3 as

$$\frac{\partial \underline{b}'}{\partial t} + \left(\underline{u}.\nabla \underline{b}' - \underline{b}'.\nabla \underline{u} \right) - \eta \nabla^2 \underline{b}' = \nabla \times \left(\underline{u}' \times \underline{B} \right) \qquad (A.8)$$

we see that the fluctuating field $\underline{b}'$ is being created from $\underline{B}$ by $\underline{u}'$. Hence the correlation between $\underline{u}'$ and $\underline{b}'$ reduces to determining the correlation tensor of $\underline{u}'$. Solving A.8 in terms of a Green's function $G_{ij}(\underline{x},t;\underline{x}',t')$ (the boundaries should have negligible effect in evaluating $\underline{\varepsilon}$ since correlations over l_u are the only important considerations)

$$b_i'(\underline{x},t) = \int_{-\infty}^{t} dt' \int_{-\infty}^{\infty} d\underline{x}'\; G_{ik}(\underline{x},t;\underline{x}',t')\, \varepsilon_{k\alpha\beta} \frac{\partial}{\partial x_\alpha'} \left[\varepsilon_{\beta\ell m} u_\ell'(\underline{x}',t') B_m(\underline{x}',t') \right]$$

$$(A.9)$$

$$\approx -\varepsilon_{k\alpha\beta}\, \varepsilon_{\ell m\beta} \int_{-\infty}^{t} dt' \int_{-\infty}^{\infty} d\underline{x}'\; \frac{\partial G_{ik}(\underline{x},t;\underline{x}',t')}{\partial x_\alpha'}\; u_\ell'(\underline{x}',t')\, B_m(\underline{x}',t')$$

Using A.9, the definition A.4 then gives

$$\varepsilon_i(\underline{x},t) = \varepsilon_{ijn}\, \varepsilon_{k\alpha\beta}\, \varepsilon_{\ell m\beta} \int_{-\infty}^{t} dt' \int_{-\infty}^{\infty} d\underline{x}'\; \frac{\partial G_{jk}(\underline{x},t;\underline{x}',t')}{\partial x_\alpha'}\; Q_{n\ell}(\underline{x},t;\underline{x}',t')\, B_m(\underline{x}',t')$$

$$(A.10)$$

where the correlation tensor $Q_{ml}(\underline{x}, t; \underline{x}', t')$ is

$$Q_{ml}(\underline{x}, t; \underline{x}', t') = \overline{u'_m(\underline{x}, t)\, u'_l(\underline{x}', t')} \qquad (A.11)$$

When the ensemble average in equation A.11 depends on $\underline{x}$ but not t, the turbulence is " <u>statistically steady</u> " and in this case

$$Q_{ml}(\underline{x}, t; \underline{x}', t') = Q_{ml}(\underline{x}, \underline{x}'; t - t')$$

If the ensemble average does not depend on x, the turbulence is " <u>homogeneous</u> " so that for a steady, homogeneous turbulence

$$Q_{ml}(\underline{x}, t; \underline{x}', t') = Q_{ml}(\underline{x} - \underline{x}'; t - t')$$

In a steady turbulence, the ensemble average may be replaced by a time average over any one member of the ensemble, and for a homogeneous turbulence, the ensemble average may be replaced by a spatial average.

If the statistical properties of the turbulence are independent of the orientation of the co-ordinate frame (at a point) the turbulence is " <u>isotropic</u> " and if the properties are independent of whether the frame is right or left handed it is " <u>mirror symmetric</u> "

Returning to equation A.10 we see that if we expand $B(\underline{x}', t')$ in a power series about $\underline{x}$, that is $\underline{B} \approx \underline{B}(\underline{x}) + (\underline{x} - \underline{x}') \cdot \nabla \underline{B}(\underline{x})$ then because Q_{ml} vanishes with $|\underline{s}| = |\underline{x} - \underline{x}'|$ the dominant terms should arise from the lowest derivatives. Hence, the general form for $\mathcal{E}_i$ to first order in the spatial derivatives is

$$\mathcal{E}_i = a_{ij} B_j + b_{ijk} \frac{\partial B_j}{\partial x_k} \qquad (A.13)$$

where the tensors a_{ij} and b_{ijk} depend on $\underline{U}$ and on the statistical properties of $\underline{u}'$ but not on $\underline{B}$.

The exact specification of a_{ij} and b_{ijk} for a given case involves intricate calculation but very general conclusions can be drawn from the form of equation A.13. Since $\underline{\mathcal{E}}$ is a polar vector and $\underline{B}$ is an axial vector, we require that both a_{ij} and b_{ijk} be axial.

As an example, if $\underline{U}=0$ and the turbulence is steady, homogeneous, and isotropic; then the only isotropic skew tensors of degree two and three are

$$a_{ij} = \alpha \, \delta_{ij} \qquad\qquad (A.14)$$

$$b_{ijk} = \eta_T \, \varepsilon_{ijk}$$

where α is a pseudoscalar (dot product of a polar and an axial vector) and η_T is a scalar.

In this case A.13 becomes

$$\underline{\mathcal{E}} = \alpha \, \underline{B} - \eta_T \, \nabla \times \underline{B} \qquad\qquad (A.15)$$

$$\rightarrow \text{Ohm's Law:} \qquad \underline{J} = \sigma_{eff} \, (\underline{E} + \alpha \, \underline{B}) \qquad\qquad (A.16)$$

$$\sigma_{eff} \equiv \left(c^2 / 4\pi \right) \left[\frac{1}{\eta_T} + \frac{1}{\eta} \right]$$

In a mirror symmetric turbulence all associated pseudoscalars must vanish. Hence, if we have a non-mirror symmetric turbulence, an electromotive force proportional to $\underline{B}$ arises (known as the 'α-effect') which is a type of term capable of the regeneration of the mean field.

The term $-\mathcal{M}_T \nabla \times \underline{B}$ makes the total diffusivity appearing in the mean induction equation equal to $\mathcal{M}_T^{eff} = \mathcal{M}_T + \eta$. Mean Field Electrodynamics therefore delivers a turbulent diffusivity for the mean field $\underline{B}$ which in the high conductivity limit $\ell_u^2 \tau_u / \eta \gg 1$ dominates the ambient diffusivity. In this limit therefore, the mean field in a turbulent conductor cannot be imagined to be "frozen-in" to the plasma.

The important question is what causes a lack of mirror symmetry. The smaller the size of some turbulent eddy, the greater the tendency towards isotropy. Hence, as far as the small eddies are concerned, we can imagine that as a first approximation, the turbulence is homogeneous, isotropic, and mirror-symmetric. Deviations from this state will be small and will depend on $\underline{\lambda}$; the direction of anisotropy. Anisotropy exists if we have a local rotation $\underline{\Omega}$ or the presence of a density gradient $\underline{g}$ in the problem. Summing up, we imagine that our turbulent fluctuations can be written

$$\underline{u}' = \underline{u}'_0 + \underline{u}'_1$$

where $\underline{u}'_0$ is an isotropic, homogeneous, and mirror-symmetric turbulence with small deviations $\underline{u}'_1$ depending on the presence of some anisotropy in the problem. For the presence of both local rotation and a density gradient, one may show that $\alpha = \alpha (\underline{\Omega} \cdot \underline{g})$ (which is a pseudoscalar). The small, non-mirror symmetric contribution $\underline{u}'_1$ is responsible for generating the α - effect.

A.2 The First Order Smoothing Approximation

Krause and Roberts (1976) showed that in the first order smoothing approximation (equation A.6, satisfied by the inequality A.7 as an example), it is still possible to have large magnetic fluctuations compared to the mean magnetic field amplitude if one is in the high conductivity limit

$$\frac{\tilde{u}^2 \tau_u}{\eta} \equiv \frac{\eta_T}{\eta} \gg 1 \qquad (A.17)$$

where $\tilde{u}^2$ is the mean squared velocity fluctuation and τ_u is a time scale typical of the fluctuation $\underline{b}'$. The reason for this result is that in computing $\underline{\varepsilon}$, it is only the part $\underline{b}'_{corr}$, the part of $\underline{b}'$ that is correlated with $\underline{u}'$ that is important and this part is of order

$$\underline{b}'_{corr} \approx \epsilon_z \underline{B} \qquad (A.18)$$

Ignoring the effects of the mean flow, they solve equation A.3 by a Green's function technique obtaining (see equations 6 and 10 in their paper)

$$\overline{u'_i(t) \, b'_j(t+\tau)} = \int_{-\infty}^{t} d\tau' \int_{-\infty}^{\infty} d\xi' \, G(\tau-\tau') \, \varepsilon_{jk\ell} \, \varepsilon_{\ell mn} \, \nabla'_k \left[Q_{im}(\tau') \, B_n(t+\tau') \right] \qquad (A.19)$$

$$b'_i(t) \, b'_j(t+\tau) = \int_{-\infty}^{\tau} d\tau' \int_{-\infty}^{\infty} d\xi' \, G(\tau-\tau') \, \varepsilon_{jk\ell} \, \varepsilon_{\ell mn} \, \nabla'_k \left[\overline{b'_i(t) \, u'_m(t+\tau')} \, B_n(t+\tau') \right] \qquad (A.20)$$

where the velocity correlation $Q(\tau')$ is defined by A.11 and the Green's function G is

$$G(\tau) \equiv (4\pi\eta\tau)^{-3/2} \exp\left(-\xi^2/4\eta\tau\right) \qquad (A.21)$$

appropriate for the diffusion operator.

For equation A.19; in the high conductivity limit $\ell_u^2/\tau_u \gg \eta$ so that for $0 < \tau_u < \ell_u^2/\eta$, the Green's function is basically a δ function. Equation A.19 can then be approximated as

$$\overline{u_i'(t)\, b_j'(t+\tau)} \approx \frac{\tau_u \tilde{u}^2}{\ell_u} B \equiv \epsilon_2 \tilde{u} B \ll \tilde{u} B \qquad (A.22)$$

which shows that the first order smoothing assumption is giving the result A.18.

In this high conductivity limit however, equation A.20 for the magnitude of the mean squared magnetic fluctuations shows that because $\overline{u_i'(t)\, b_j'(t+\tau)}$ is correlated for a time $T \approx \ell^2/\eta \gg \tau_u$, then the estimate of A.20 is

$$\overline{b'^2} \approx \frac{\tilde{u}^2 \tau_u}{\eta} B^2 \equiv \frac{\eta_T}{\eta} B^2 \gg B^2 \qquad (A.23)$$

It is this result which is crucial to the theory we investigate in the text.

A.3 Formalism For Computing Various Correlations Arising In Mean Field Electrodynamics

The approach we employ to calculate α, η_T etc was

developed by Roberts and Soward (1975). Here we summarize some of the results that they worked out and which we shall need for our own calculations. Introducing the concept of a large scale on which the mean velocity, magnetic etc fields vary and a microscale for a description of the turbulence, it is convenient to introduce mean and relative co-ordinates for two points $\underline{x}_1$ and $\underline{x}_2$ as

$$\underline{X} \equiv \tfrac{1}{2}(\underline{x}_1 + \underline{x}_2) \; ; \quad \underline{x} \equiv (\underline{x}_1 - \underline{x}_2) \; ; \quad T \equiv \tfrac{1}{2}(t_1 + t_2) \; ; \quad t \equiv t_2 - t_1 \qquad (A.24)$$

in terms of which the two-point, two-time correlation functions such as

$$\underline{\Phi}_{ij}(\underline{x}_1, t_1; \underline{x}_2, t_2) = \overline{u_i'(\underline{x}_1, t_1)\, u_j'(\underline{x}_2, t_2)}$$

may be expressed as

$$\Phi_{ij}(\underline{X}, T; \underline{x}, t) = \overline{u_i'(\underline{X} + \tfrac{1}{2}\underline{x}, T + \tfrac{1}{2}t)\, u_j'(\underline{X} - \tfrac{1}{2}\underline{x}, T - \tfrac{1}{2}t)} \qquad (A.25)$$

The turbulence is steady if

$$\overline{\Phi}_{ij}(\underline{X}, T; \underline{x}, t) = \overline{\Phi}_{ij}(\underline{X}, T; \underline{x}, -t)$$

and locally mirror symmetric if

$$\Phi_{ij}(\underline{X}, T; \underline{x}, t) = \Phi_{ij}(\underline{X}, T; -\underline{x}, t)$$

The method used by these authors relys on a double Fourier transformation and expansion method whereby the Fourier transform with respect to $\underline{x}$ of A.26 is

$$\hat{\Phi}_{ij}(\underline{X}, t; \underline{k}, \omega)$$

and the Fourier transform for the mean variables $\underline{X}$, T

$$\tilde{\Phi}_{ij} (\underline{K}, \underline{\Omega}; \underline{k}, \omega)$$

The idea is to regard variations of mean quantities as negligible over scales l_u and times τ_u which characterize the turbulence. Hence, the induction equation for the fluctuation is first Fourier transformed, the various correlations computed in $\underline{K} - \underline{\Omega}; \underline{k} - \omega$ space, and then an expansion of the results carried out in powers of $\underline{K}$ (that is a power series in large scale derivative $\partial/\partial\underline{X}$). The results are then transformed back so that the various coefficients in the problem will be integrals over the microscale spectrum $\underline{k}$, and ω. The idea of separation of scales is obviously central to the whole process.

As an example, the calculation of $\underline{\mathcal{E}}$ proceeds by taking the Fourier transform of equation A.3 to find

$$\hat{b}_i'(\underline{k},\omega) = \varepsilon_{ijk}\,\varepsilon_{klm}\; i\,k_j \int \hat{u}_\ell'(\underline{k}-\underline{k}',\omega)\, B_m(\underline{k}')d\underline{k}' \;\Delta(\omega+i\eta k^2)$$

$$(A.26)$$

where $\Delta(\omega)$ is defined as

$$\Delta(\omega) \equiv \left[\exp(i\omega t) - 1 \right] / i\omega \qquad (A.27)$$

so that in the high conductivity limit

$$\Delta(\omega+i\eta k^2) \sim \Delta(\omega) \qquad (A.28)$$

which, as $t \to \infty$ goes to

$$\Delta(\omega) \to \pi\delta(\omega) + i/\omega \qquad (A.29)$$

We may now compute $\tilde{\mathcal{E}}_i$ using equation A.26 as

$$\tilde{\mathcal{E}}_i = \varepsilon_{i\alpha\beta}\, \varepsilon_{\beta j k}\, \varepsilon_{k\ell m} \left[-i \left(\ell_j - \tfrac{1}{2} K_j \right) \Delta^* \left(\omega - i\eta \left(\underline{\ell} - \tfrac{1}{2}\underline{K} \right)^2 \right) \times \right.$$

$$\times \int \hat{u}'_\alpha \left(\underline{\ell} + \tfrac{1}{2}\underline{K}, \omega \right) \hat{u}'_\ell \left(-\underline{\ell} + \tfrac{1}{2}\underline{K} - \underline{k}', \omega \right) B_m(\underline{k}')\, d\underline{k}' \qquad (A.30)$$

This result is expanded in power of $\underline{K}$ and converted into $\underline{X}$-space.

In the case of homogeneous turbulence

$$\overline{\hat{u}'_\alpha \left(\underline{\ell} + \tfrac{1}{2}\underline{K}, \omega \right) \hat{u}'_\ell \left(-\underline{\ell} + \tfrac{1}{2}\underline{K} - \underline{k}', -\omega \right)} = \delta(\underline{K} - \underline{k}')\, \hat{\phi}_{\alpha\ell} \left(\underline{\ell} + \tfrac{1}{2}\underline{k}', \omega \right) \qquad (A.31)$$

so that

$$\tilde{\mathcal{E}}_{i\,homog.} = i\, \varepsilon_{i\alpha\beta}\, \varepsilon_{\beta j k}\, \varepsilon_{k\ell m} \left(\ell'_j - K_j \right) \hat{\phi}_{\alpha\ell}(\underline{\ell}', \omega)\, B_m(\underline{K})\, \Delta(-\omega) \qquad (A.32)$$

where $\underline{\ell}' = \underline{\ell} + \tfrac{1}{2}\underline{K}$. Inverting this result with respect to $\underline{K}$ and integrating over all $\underline{\ell}'$ and ω then gives

$$\overline{(\underline{u}' \times \underline{b}')}_i = \varepsilon_{i\alpha\beta}\, \varepsilon_{\beta j k}\, \varepsilon_{k\ell m} \left\{ \frac{\partial B_m}{\partial X_j}\, I^{(1)}_{\alpha\ell} - B_m\, I^{(2)}_{j\alpha\ell} \right\} \qquad (A.33)$$

where

$$I^{(1)}_{\alpha\ell} \equiv \iint \hat{\phi}_{\alpha\ell}(\underline{\ell}, \omega)\, \Delta(-\omega)\, d\underline{\ell}\, d\omega \qquad (A.34)$$

$$I^{(2)}_{j\alpha\ell} \equiv \iint i\, \ell_j\, \hat{\phi}_{\alpha\ell}(\underline{\ell}, \omega)\, \Delta(-\omega)\, d\underline{\ell}\, d\omega \qquad (A.35)$$

We digress slightly to point out that for isotropic

turbulence, the correlation tensor $\hat{\Phi}_{\alpha\ell}$ will contain a mirror symmetric part and and a non-mirror symmetric part. To lowest order in $\partial/\partial \underline{x}$ the form of $\hat{\Phi}_{\alpha\ell}$ is

$$\hat{\Phi}_{\alpha\ell} = \hat{\Phi}_{\alpha\ell}^{M.S.} + \hat{\Phi}_{\alpha\ell}^{H}$$

$$= \hat{\Phi} \, P_{ij}(\underline{k}) - \frac{i}{2k^2} \hat{H} \, \varepsilon_{ijk} k_k \qquad (A.36)$$

where $\hat{\Phi}$ is the Fourier transform of $\overline{\underline{u}'.\underline{u}'}$ and is the spectrum of the turbulent intensity while $\hat{H}$ is the helicity spectrum, which is the Fourier transform of $\overline{\underline{u}'.\nabla \times \underline{u}'}$. In addition, the tensor $P_{ij}(\underline{k})$ is defined as

$$P_{ij}(\underline{k}) \equiv \delta_{ij} - \frac{k_i k_j}{k^2} \qquad (A.37)$$

Substitution of A.36 into the expressions A.35 and A.34 results in the reduction of A.33 to

$$\underline{\mathcal{E}} = \overline{\underline{u}' \times \underline{b}'} = -\eta_T \nabla \times \underline{B} + \alpha \underline{B} \qquad (A.38)$$

where the positive definite turbulent diffusivity η_T is

$$\eta_T \equiv \frac{8\pi^2}{3} \int \hat{\Phi}(k,0) \, k^2 \, dk \qquad (A.39)$$

and the parameter α (dimensions of velocity) is related to the helicity

$$\alpha \equiv -\frac{8\pi^2}{3} \int \hat{H}(k,0) \, k^2 \, dk \qquad (A.40)$$

(equations A.38 - A.40 are results 3.51 - 3.53 in the Roberts

and Soward paper).

We shall require equations A.26 and A.33 for the analysis in Appendix B. We must specify how the helicity is to arise in our shear flow, and include the effects of density gradients in the problem.

We first write down the effects of local rotation in generating helicity. For us the local rotation comes about through the antisymmetric part of the local strain. Consider first the effect of rotation. In the rotating frame, the velocity fluctuation obeys

$$\frac{\partial \underline{u}'}{\partial t} + \underline{u}' \cdot \nabla \underline{u}' + 2 \underline{\Omega}_* \times \underline{u}' = - \nabla p' + \nu \nabla^2 \underline{u}' \tag{A.41}$$

Suppose that the turbulence is imagined to be predominantly isotropic and mirror symmetric ($\underline{u}_o'$) with the rotation $2\underline{\Omega}_*$ introducing a small deviation $\underline{u}_1'$ to this state. In the limit $\widetilde{u}_o \tau_u / \ell_u \ll 1$ the inertial term in A.41 is ignorable and $\nu / \Omega_* \ell_u^2 \ll 1$ is well satisfied so that

$$\frac{\partial \underline{u}_1'}{\partial t} = - \nabla p' - 2 \underline{\Omega}_* \times \underline{u}_o' \tag{A.42}$$

Fourier transforming A.42, and finding the correlation

$$\hat{\Phi}_{ij}^{(1)} = \hat{\psi}_{ij} + \hat{\psi}_{ij}^*$$

$$\hat{\psi}_{ij} = \overline{u_i^{(1)'}(\underline{k} + \tfrac{1}{2}\underline{K}, \omega) \, u_j^{(0)'}(-\underline{k} + \tfrac{1}{2}\underline{K}, -\omega)} \tag{A.43}$$

one may show that expansion to O(K) and inverse transforming that

$$\hat{\tilde{\Phi}}^{(1)}_{ij} = \hat{\tilde{\Phi}}_{ij}$$

where the helicity is

$$\hat{H}_{rot}(\underline{X},T; \underline{k},\omega) = 4i(\underline{k}\cdot\underline{\Omega}_*)\; \hat{\tilde{\phi}}^{(0)}\left[\Delta(\omega) - \Delta^*(\omega)\right] +$$

$$+ 2\Omega_{*q}\, P_{qs}\; \frac{\partial\hat{\tilde{\phi}}^{(0)}}{\partial X_s}\left[\Delta(\omega) + \Delta^*(\omega)\right] \tag{A.44}$$

We notice that the vorticity of the mean flow is $2\,\underline{\Omega}_* = \underline{\Omega}$.

Roberts and Soward show that if instead of pure rotation, we have a mean flow with a non-zero strain on the long scales, then the antisymmetric part of this strain tensor

$$\underline{\Omega}_* = \tfrac{1}{2}\underline{\Omega} = \tfrac{1}{2}\nabla\times\underline{u}$$

will generate helicity $\hat{H}_{a.s.}$ given by exactly 1/2 the result found in A.44. This is physically sensible because the vorticity $\nabla\times\underline{u}$ of the mean flow is acting as a local rotation. Thus

$$\hat{H}_{a.s} = \tfrac{1}{2}\hat{H}_{rot}. \tag{A.45}$$

Finally, these authors note that the effects of compressibility may be taken into account by replacing all gradients $\partial\hat{\tilde{\phi}}^{(0)}/\partial X_s$ of $\hat{\tilde{\phi}}^{(0)}$ by

$$\frac{\partial\hat{\tilde{\phi}}^{(0)}}{\partial X_s} \longrightarrow \frac{1}{\rho^2}\frac{\partial}{\partial X_s}(\rho^2\,\hat{\tilde{\phi}}^{(0)}) \tag{A.46}$$

If we do not include derivatives of $\hat{\Phi}^{(o)}$ as important, then the mirror symmetric part of the isotropic turbulence is to first order in the density gradient

$$\hat{\Phi}_{ij}^{m.s.} = \hat{\Phi}^{(o)} \left(P_{ij}(\underline{k}) + \frac{i}{k} \frac{1}{\rho} \frac{\partial \rho}{\partial x_p} \left[k_i \, \delta_{jp} - k_j \, \delta_{ip} \right] \right) \qquad (A.47)$$

(see equation 3.38 of Roberts and Soward) while the helicity A.44 we will use may be corrected by using A.46 and ignoring the gradient of $\hat{\mathcal{E}}^{(o)}$.

We close by noting with these authors that neglect of the effects of local rotation (to zeroth order) on the turbulence requires

$$Q = \tilde{u} \, T_u / l_u \gg T_u \, \Omega \quad \Longrightarrow \quad (T_u \ll t_\kappa) \qquad (A.48)$$

Also in the analysis of the velocity spectrum, the requirement

$$\hat{\Phi}^{(o)}(\underline{k}, \omega) \approx O(\omega^2) \qquad \text{as} \quad \omega \to 0 \qquad (A.49)$$

is used; a behaviour which has usually been accepted in the dynamical theory of turbulence.

Appendix B

The Calculation Of Correlations Between Velocity And Magnetic Field Fluctuations

B.1 The Calculation Of $\xi = \overline{u' \times b'}$

We assume in this calculation that the helicity is generated by the antisymmetric part of the mean strain $\frac{1}{2} \nabla \times \underline{u}$. We shall include the effect of density gradients $\rho_0^{-1} \nabla \rho_0$ and will assume that for our purposes the turbulence is homogenous over the scales that the density varies. Hence, we ignore gradients of the turbulent intensity $\nabla \hat{\Phi}$.

With $\underline{\Omega} \equiv \nabla \times \underline{u}$ and with the assumptions above, we have to first order in $\rho_0^{-1} \nabla \rho_0$ (see equations A.36 and A.47)

$$\hat{\Phi}^{(0)}_{k\ell} = \left\{ P_{k\ell} + \frac{i}{k^2} (k_k \delta_{\ell p} - k_\ell \delta_{kp}) \rho_0^{-1} \frac{\partial \rho_0}{\partial X_p} \right\} \hat{\Phi}^{(0)} - \frac{i}{2k^2} \varepsilon_{sk\ell} k_s \hat{H}^{(0)} \tag{B.1}$$

with the helicity (see equation A.44)

$$\hat{H}^{(0)} = \left\{ i (\underline{k} \cdot \underline{\Omega}) [\Delta(\omega) - \Delta^*(\omega)] + \Omega_q P_{qs} \rho_0^{-1} \frac{\partial \rho_0}{\partial X_s} [\Delta(\omega) + \Delta^*(\omega)] \right\} \hat{\Phi}^{(0)} \tag{B.2}$$

Substituting B.2 into B.1, we use equation A.33 for the

calculation of $\mathcal{E}_i = \overline{u' \times b'}_i$ assuming that we may approximate the turbulence as homogeneous to zeroth order. We shall keep terms up to first order in $\partial/\partial X_s$. Noting that only when an even number of direction cosines $\hat{l}_m$ appear in the integration over $\underline{l}$ do we get a non-zero result, we find

$$
\begin{aligned}
\mathcal{E}_i = \varepsilon_{i\alpha\beta}\, \varepsilon_{\beta j k}\, \varepsilon_{k \ell m} \Bigg\{ & \iint P_{\alpha \ell}\, \Delta(-\omega)\, \vec{\Phi}^{(o)}\, d\underline{l}\, d\omega \quad \frac{\partial B_m}{\partial X_j} + \\
& + \varepsilon_{s\alpha\ell} \iint \hat{l}_s\, \hat{l}_r\, \Delta(-\omega)\, [\Delta(\omega) - \Delta^*(\omega)]\, \vec{\Phi}^{(o)}\, d\underline{l}\, d\omega\, \frac{\partial B_m}{\partial X_j}\, \frac{L_r}{2} + \\
& + \iint \hat{l}_j\, [\hat{l}_\alpha\, \delta_{\ell t} - \hat{l}_\ell\, \delta_{\alpha t}]\, \Delta(-\omega)\, \vec{\Phi}^{(o)}\, d\underline{l}\, d\omega \quad L_t^{-1}\, B_m - \\
& - \varepsilon_{s\alpha\ell} \iint \hat{l}_j\, \hat{l}_s\, P_{rt}\, \Delta(-\omega)\, [\Delta(\omega) + \Delta^*(\omega)]\, \vec{\Phi}^{(o)}\, d\underline{l}\, d\omega \quad L_t^{-1}\, B_m\, \frac{L_r}{2}
\end{aligned}
$$

$$
\underline{L}^{-1} \equiv \rho_o^{-1}\, \nabla\rho_o \qquad ; \qquad \hat{l}_\beta = l_\beta / l
$$

$$(B.3)$$

Performing the integration over $\underline{l}$ using

$$
\int d\underline{l} = \int d\Omega \int dl\, l^2
$$

with the identities

$$
\int \hat{l}_i\, \hat{l}_j\, d\Omega = \frac{4\pi}{3}\, \delta_{ij}
$$

$$(B.5)$$

$$
\iint \hat{l}_i\, \hat{l}_j\, \hat{l}_\ell\, \hat{l}_m\, d\Omega = \frac{4\pi}{15}\, \left(\delta_{ij}\, \delta_{\ell m} + \delta_{i\ell}\, \delta_{jm} + \delta_{im}\, \delta_{j\ell} \right) \qquad (B.6)
$$

equation B.3 reduces to

$$\mathcal{E}_i = (\varepsilon_{i\alpha l}\,\delta_{jm} - \varepsilon_{i\alpha m}\,\delta_{jl}) \left\{ \begin{array}{l} I_1 \quad \delta_{\alpha l} \quad \dfrac{\partial B_m}{\partial X_j} \quad + \\[2em] + \; I_2 \; \varepsilon_{s\alpha l} \quad \dfrac{\partial B_m}{\partial X_j} \; \dfrac{l_s}{4} \quad + \\[2em] + \; I_3 \left(\delta_{\alpha j}\,\delta_{lt} - \delta_{jl}\,\delta_{\alpha t}\right)\, L_t^{-1}\, B_m \; - \\[2em] - \; I_4 \; \varepsilon_{s\alpha l} \left(4\,\delta_{js}\,\delta_{rt} - \delta_{jr}\,\delta_{st} - \delta_{jt}\,\delta_{sr}\right)_x \\[1em] \qquad \times \; L_t^{-1}\, B_m\, \dfrac{\Omega_r}{2} \end{array} \right. \tag{B.7}$$

where the integrals I_m are

$$I_1 \equiv \frac{8\pi}{3} \int\limits_{-\infty}^{\infty}\int\limits_{0}^{\infty} d\omega\, dk\; k^2\, \Delta(-\omega)\; \hat{\Phi}^{(0)}(k,\omega) \tag{B.8}$$

$$I_2 \equiv \frac{4\pi}{3} \int\limits_{-\infty}^{\infty}\int\limits_{0}^{\infty} d\omega\, dk\; k^2\, \Delta(-\omega)\left[\Delta(\omega) - \Delta^*(\omega)\right]\, \hat{\Phi}^{(0)}(k,\omega) \tag{B.9}$$

$$I_3 \equiv I_1 / 2 \tag{B.10}$$

$$I_4 \equiv \frac{4\pi}{15} \int\limits_{-\infty}^{\infty}\int\limits_{0}^{\infty} d\omega\, dk\; k^2\, \Delta(-\omega)\left[\Delta(\omega) + \Delta^*(\omega)\right]\, \hat{\Phi}^{(0)}(k,\omega) \tag{B.11}$$

and where we have employed the identity

$$\varepsilon_{\beta jk} \, \varepsilon_{\ell mk} = \delta_{\beta\ell} \, \delta_{jm} - \delta_{\beta m} \, \delta_{j\ell} \qquad\qquad (B.12)$$

Summing over the indices, the third term in B.7 vanishes leaving

$$\underline{E} = -I_1 \, \nabla \times \underline{B} + \frac{I_2}{4} \left(\nabla B_s \right) \underline{\ell}_s +$$

$$+ \left(2 I_4 \right) \left\{ -2 \left(\underline{L}^{-1} \cdot \underline{\ell} \right) \underline{B} + \left(\frac{\underline{L}^{-1} \cdot \underline{B}}{2} \right) \underline{\ell} + \left(\frac{\underline{B} \cdot \underline{\ell}}{2} \right) \underline{L}^{-1} \right\}$$

$$(B.13)$$

We now turn to the simplification of the integrals I_1, I_2, and I_4. Using the relation A.27 for $\Delta(\omega)$, and taking the high conductivity limits one obtains

$$\lim_{t \to \infty} \Delta(-\omega) = \pi \delta(\omega) - i/\omega$$

$$\lim_{t \to \infty} \Delta(-\omega) \left[\Delta(\omega) - \Delta^*(\omega) \right] = \frac{3}{\omega^2} - \frac{\pi}{\omega} i \left[2 \delta(\omega) - 2 \delta(2\omega) - \delta(-\omega) \right]$$

$$\lim_{t \to \infty} \Delta(-\omega) \left[\Delta(\omega) + \Delta^*(\omega) \right] = \frac{1}{\omega^2} + \frac{\pi}{\omega} i \left[\delta(\omega) + \delta(-\omega) - 2 \delta(2\omega) \right]$$

$$(B.14)$$

Taking the real parts we find

$$m_T = Re \left\{ I_1 \right\} = \frac{8\pi^2}{3} \int_0^\infty \hat{\bar{\Phi}}^{(0)}(k,0) \, k^2 \, dk \qquad\qquad (B.15)$$

$$\beta = 2 Re \left\{ I_4 \right\} = \frac{16\pi}{15} \int_0^\infty \int_0^\infty \frac{\hat{\bar{\Phi}}^{(0)}(k,\omega)}{\omega^2} \, k^2 \, dk \, d\omega \qquad (B.16)$$

$$I_2 = 15 \, I_4 = \frac{15}{2} \beta \qquad\qquad (B.17)$$

Assuming that $\hat{\vec{\Phi}}^{(0)}(\ell,\omega) \approx \hat{\vec{\ell}}^{(0)}(\ell,0)\,\omega^2$ as $\omega \to 0$, we have roughly

$$\beta \approx \frac{16\pi/15}{8\pi^2/3}\,M_T\,\tilde{\tau}_u = \frac{2}{5\pi}\,M_T\,\tilde{\tau}_u \qquad (B.18)$$

For the toroidal velocity field

$$\underline{U} \approx (0,\,U_\phi,\,0) \qquad ;\qquad U_\phi \sim V_k \qquad (B.19)$$

we have

$$\underline{\Omega} = (0,\,0,\,\Omega_z) \qquad ;\qquad \Omega_z = \frac{V_k}{2r} \qquad (B.20)$$

so that equation B.13 becomes

$$\underline{\mathcal{E}} = -M_T\,\nabla \times \underline{B} \;+\; \frac{15}{8}\beta\left(\nabla B_z\right)\Omega_z \;+$$

$$+\;\beta\left\{ \left(-2\,L_z^{-1}\,\Omega_z\right)\underline{B} \;+\; \left(\frac{L^{-1}\cdot\underline{B}}{2}\right)\underline{\Omega} \;+\; \left(\frac{B_z\,\Omega_z}{2}\right)\underline{L}^{-1}\right\}$$

$$(B.21)$$

Equations B.21 show that a term of the form $\alpha\,\underline{B}$ appears in the expression for $\underline{\mathcal{E}}$. Hence, defining

$$\alpha(r,z) \equiv -\frac{2\beta\,\Omega_z}{L_z} = -2\left(\frac{2}{5\pi}\right)\frac{M_T\,\tilde{\tau}_u}{L_z}\,\Omega_z \qquad (B.22)$$

gives

$$\underline{\mathcal{E}} = -M_T\,\nabla \times \underline{B} \;+\; \alpha\left\{ \underline{B} \;-\; \frac{L_z}{4}\,\frac{(L^{-1}\cdot\underline{B})}{\Omega_z}\,\underline{\Omega} \;-\; \frac{(L_z\,B_z)}{4}\,\underline{L}^{-1} \;-\; \frac{15}{16}\,L_z\,(\nabla B_z)\right\} \qquad (B.23)$$

Expressing B.23 in cylindrical polar co-ordinates, with

the assumption of axisymmetry and defining the ratio

$$\epsilon \equiv L_z / L_r \qquad\qquad (B.24)$$

gives rise to equations 3.10 to 3.12 in Chapter 3.

B.2 The Calculation Of $\overline{\underline{u}' \times (\nabla \times \underline{b}')} \equiv F$

Beginning with formula A.26 for $\hat{\underline{b}}'$ and noting that $\nabla \times \underline{b} \to i\underline{k} \times \underline{b}$ in the Fourier domain we find

$$\tilde{F}_i = \varepsilon_{i\alpha\beta}\, \varepsilon_{\beta\gamma\delta}\, \varepsilon_{\delta j k}\, \varepsilon_{k\ell m}\, (-i)\left(k_j - \tfrac{1}{2}K_j\right)(-i)\left(k_\gamma - \tfrac{1}{2}K_\gamma\right) \times$$

$$\times \int \overline{\hat{u}'_\alpha\left(\underline{k}+\tfrac{1}{2}\underline{K},\omega\right)\, \hat{u}'_\ell\left(-\underline{k}+\tfrac{1}{2}\underline{K}-\underline{k}',-\omega\right)}\; B_m(\underline{k}')\, d\underline{k}'\; \Delta(-\omega)$$

$$(B.25)$$

which, with the assumed homogeneity (to zeroth order), of the turbulence leads to (see steps leading to A.33)

$$\tilde{F}_i = -\varepsilon_{i\alpha\beta}\, \varepsilon_{\beta\gamma\delta}\, \varepsilon_{\delta j k}\, \varepsilon_{k\ell m}\, \left(k'_j - K_j\right)\left(k'_\gamma - K_\gamma\right)\, \hat{\Phi}^{(0)}_{\alpha\ell}(\underline{k}',\omega)\, B_m(\underline{K})\, \Delta(-\omega)$$

$$(B.26)$$

Integrating over $\underline{k}'$ and ω and inverting with respect to $\underline{K}$, we have in analogy with equation B.7

$$\overline{\left(\underline{u}' \times (\nabla \times \underline{b}')\right)}_i = \varepsilon_{i\alpha\beta}\, \varepsilon_{\beta\gamma\delta}\, \varepsilon_{\delta j k}\, \varepsilon_{k\ell m}\left\{ -\iint k'_j k'_\gamma\, \hat{\Phi}^{(0)}_{\alpha\ell}\, \Delta(-\omega)\, d\underline{k}'\, d\omega\; B_m \right.$$

$$+ i\iint k'_j\, \hat{\Phi}^{(0)}_{\alpha\ell}\, \Delta(-\omega)\, d\underline{k}'\, d\omega\; \frac{\partial B_m}{\partial X_\gamma} +$$

$$\left. + i\iint k'_\gamma\, \hat{\Phi}^{(0)}_{\alpha\ell}\, \Delta(-\omega)\, d\underline{k}'\, d\omega\; \frac{\partial B_m}{\partial X_j} \right.$$

$$(B.27)$$

If we now substitute equations B.1 and B.2 for $\hat{\Phi}^{(o)}_{\alpha\ell}$ into B.27 and keep terms to first order in $\partial/\partial X_s$, we find that the last two terms in B.27 make no contribution. The first term in B.27 contains the product $k'_j k'_\gamma$, so integration over $d\underline{k}'$ only gives non-zero results for those parts of $\hat{\Phi}^{(o)}_{\alpha\ell}$ containing an even number of factors k'_t. Hence, using identity B.12 twice, we find

$$\overline{\left(\underline{u}' \times (\nabla \times \underline{b}')\right)_i} = -Bm \left\{ \iint d\underline{k}\, d\omega\, k^2 \left[\hat{k}_i \hat{k}_m \hat{\Phi}^{(o)}_{\ell\ell} + \hat{k}_\alpha \hat{k}_\ell \hat{\Phi}^{(o)}_{\alpha\ell} \delta_{im} - \hat{k}_i \hat{k}_\ell \hat{\Phi}^{(o)}_{m\ell} - \right] \Delta(-\omega) \right. $$
$$\left. - \hat{k}_\alpha \hat{k}_\ell \hat{\Phi}^{(o)}_{\alpha i} \right\}$$

$$= -Bm \iint d\underline{k}\, d\omega\, k^2\, \hat{k}_i \hat{k}_m\, 2\hat{\Phi}^{(o)}(\underline{k},\omega)\, \Delta(-\omega)$$

$$(\text{B.28})$$

where we note that

$$k_s P_{st} = 0 \qquad ; \qquad \varepsilon_{srt} k_r k_t = 0 \qquad ; \qquad P_{\ell\ell} = 2$$

Integrating B.28 over $d\underline{k}$ and using B.5 then gives

$$\overline{\left(\underline{u}' \times (\nabla \times \underline{b}')\right)} \approx -\frac{8\pi}{3} \int_0^\infty k^4 \hat{\Phi}(k,o)\, dk\, \underline{B} \approx -\frac{M_T}{\ell_u^2}\, \underline{B} \qquad (\text{B.29})$$

We calculate the quantity $\overline{\underline{\varepsilon}' \cdot \underline{j}'}$ from Chapter 2 using the identity

$$4\pi\, \underline{\varepsilon}' \cdot \underline{j}' \equiv (\underline{u}' \times \underline{B}) \cdot \nabla \times \underline{b}' = -\underline{u}' \times (\nabla \times \underline{b}') \cdot \underline{B} \qquad (\text{B.30})$$

so that

$$\overline{\underline{\varepsilon}' \cdot \underline{j}'} \approx \frac{M_T}{\ell_u^2}\, \frac{B^2}{4\pi} \qquad (\text{B.31})$$

where we have used the result B.29. Evidently $\overline{\varepsilon' \cdot j'}$ is positive which shows that the interpretation of this term as a loss term for $\tilde{u}^2$ and a source term for $\tilde{b}^2$ is valid.

Turning to the estimation of $\underline{\varepsilon} \cdot \underline{J}$ we have using B.23

$$\underline{\varepsilon} \cdot \underline{J} = \frac{1}{4\pi} \overline{(\underline{u'} \times \underline{b'})} \cdot \nabla \times \underline{B} \approx \frac{1}{4\pi} \left\{ \alpha \, \underline{B} \cdot \nabla \times \underline{B} - \mu_T (\nabla \times \underline{B})^2 \right\} \quad (B.32)$$

Unlike the $\overline{\varepsilon' \cdot j'}$ term, the magnitude of $\underline{\varepsilon} \cdot \underline{J}$ depends on the comparison of the α term with repect to effects due to the dissipation μ_T. Using equation B.22 we have

$$\alpha \approx -\frac{\mu_T}{L_z} \left(\frac{\tau_u}{t_\kappa} \right)$$

so that

$$\underline{\varepsilon} \cdot \underline{J} \approx \left(\frac{\mu_T}{-L_z} \frac{\tau_u}{t_\kappa} \left(-\frac{1}{L_z^B} \right) - \frac{\mu_T}{(L_z^B)^2} \right) \frac{B^2}{4\pi} \quad (B.33)$$

Now, for our small correlation time limit, we set $\tau_u \leq t_\kappa$, so that the crude order of magnitude estimate B.33 becomes

$$\underline{\varepsilon} \cdot \underline{J} \approx \frac{\mu_T}{(L_z^B)^2} \frac{B^2}{4\pi} \left\{ \frac{L_z^B}{L_z} - 1 \right\} \quad (B.34)$$

Appendix C

The Integral Representation For U(ẑ)

C.1 The Solution Of Equation 3.53 For U(ẑ)

Given the equation $\mathcal{L}(\psi) = 0$, the representation

$$\psi = \int K(z,t)\, \nu(t)\, dt \qquad (c.1)$$

results in

$$\mathcal{L}(\psi) = \int \mathcal{L}_z\left(K(z,t)\right)\, \nu(t)\, dt = 0 \qquad (c.2)$$

Choice of an appropriate kernel $K(z,t)$ such that

$$\mathcal{L}_z(K) = M_t(K) \qquad (c.3)$$

where M_t is some new differential operator in t, gives

$$\mathcal{L}(\psi) = \int M_t\left(K(z,t)\right)\, \nu(t)\, dt = 0 \qquad (c.4)$$

Integration by parts transfers the differential operations from $K(z,t)$ to $\nu(t)$ resulting in

$$\mathcal{L}(\psi) = \int K(z,t)\, \tilde{M}_t\left(\nu(t)\right)\, dt + P(\nu, K) \qquad (c.5)$$

where $\widetilde{M_t}$ is the adjoint operator to M_t and $P(v, K)$ is the so-called bilinear concomitant. Obviously if $v(t)$ satisfies

$$\widetilde{M_t}(v) = 0$$

and the path of integration is chosen such that $P(v, K)$ vanishes at the end points, then the differential equation is satisfied.

It may readily be shown that if

$$M_t(K) = \alpha(t) \frac{d}{dt}K + \beta(t) K \tag{c.6}$$

then

$$\widetilde{M_t}(v) = -\frac{d}{dt}(\alpha v) + \beta v \tag{c.7}$$

and

$$P(v, K) = \alpha v K \tag{c.8}$$

The reader may refer to Morse and Feshbach (1953) for more detail.

We now apply this to the solution of equation 3.53. The choice of the Laplace kernel

$$K(\hat{z}, t) = e^{\hat{z}t}$$

is motivated by the observation that

$$\frac{d}{d\hat{z}}(e^{\hat{z}t}) = \hat{z} e^{\hat{z}t} = \frac{d}{dt}(e^{\hat{z}t}) \tag{c.9}$$

so that use of this kernel will require only a first order differential equation in t to be solved to find $\nu(t)$. Thus with

$$\mathcal{L}_{\hat{z}} \equiv \left\{ \frac{d^4}{d\hat{z}^4} - 2\kappa \frac{d^2}{d\hat{z}^2} - \hat{z}\frac{d}{d\hat{z}} + (\kappa^2 - 1) \right\} \tag{c.10}$$

we find

$$\mathcal{L}_{\hat{z}}(e^{\hat{z}t}) = \left[t^4 - 2\kappa t^2 - \hat{z}t + (\kappa^2 - 1) \right] e^{\hat{z}t} \tag{c.11}$$

Employing the relation C.9 then gives

$$\mathcal{L}_{\hat{z}}(e^{\hat{z}t}) = M_t(e^{\hat{z}t})$$

where

$$M_t(e^{\hat{z}t}) = \left\{ -t\frac{d}{dt} + \left[t^4 - 2\kappa t^2 + (\kappa^2 - 1) \right] \right\} e^{\hat{z}t} \tag{c.12}$$

Comparing C.12 with C.6 we see that with

$$\alpha(t) = -t$$
$$\beta(t) = \left[t^4 - 2\kappa t^2 + (\kappa^2 - 1) \right] \tag{c.13}$$

we find the equation for ν as

$$\widetilde{M}_t(\nu) = \frac{d}{dt}(t\nu) + \left[t^4 - 2\kappa t^2 + (\kappa^2 - 1) \right]\nu = 0 \tag{c.14}$$

Differentiating we have

$$\frac{d\nu}{dt} + \left[t^3 - 2\kappa t + \frac{\kappa^2}{t} \right]\nu = 0 \tag{c.15}$$

whose solution is

$$\mathcal{V} = \frac{e^{-\left[t^4/4 - \kappa t^2\right]}}{t^{\kappa^2}} \qquad (c.16)$$

Hence, with the Laplace kernel and $\mathcal{V}$ given by C.16, $U(\hat{z})$ takes the form

$$U(\hat{z}) = \int_C \frac{e^{-t^4/4 + \kappa t^2 + \hat{z} t}}{t^{\kappa^2}} \, dt \qquad (c.17)$$

where the contours C are chosen such that $P(\mathcal{V}, \kappa)$ vanishes at the end-points of integration.

C.2 Relations Between Solutions $U(\hat{z})$

We begin with the integral relations defined by equation 3.58 for κ and $\hat{z}$ real with $\kappa < 1$, and for the contours C_m sketched in Fig. 6

We deform the various contours so that they run along the co-ordinate axes of the relevant quadrant of the complex-t plane. As an example, $U_1(\hat{z})$ is

$$U_1(\kappa, \hat{z}) = \int_{i\infty}^{0} \frac{exp\left(-t^4/4 + \kappa t^2 + \hat{z} t\right)}{t^{\kappa^2}} \, dt \quad + \quad \int_{0}^{\infty} \frac{exp\left(-t^4/4 + \kappa t^2 + \hat{z} t\right)}{t^{\kappa^2}} \, dt$$

$$(c.19)$$

Let us define the integral

$$I(\kappa, \hat{z}) = \int_{0}^{\infty} \frac{exp\left(-t^4/4 + \kappa t^2 + \hat{z} t\right)}{t^{\kappa^2}} \, dt \qquad (c.20)$$

Using this definition, and changing variables; in the first integral of C.19 as $t \rightarrow e^{i\pi/2} \tau$ we find that $U_1(\hat{z})$ can be written as

$$U_1(\kappa, \hat{z}) = I(\kappa, \hat{z}) - e^{i\pi/2(1-\kappa^2)} I(-\kappa, i\hat{z}) \qquad (c.21)$$

Similar deformations of the other contours defining the solutions U_2, U_3, U_4 leads to

$$U_2(\kappa, \hat{z}) = -I(\kappa, \hat{z}) + e^{-i\pi/2(1-\kappa^2)} I(-\kappa, -i\hat{z}) \qquad (c.22)$$

$$U_3(\kappa, \hat{z}) = e^{-\pi i(1-\kappa^2)} I(\kappa, -\hat{z}) - e^{-i\pi/2(1-\kappa^2)} I(-\kappa, -i\hat{z}) \qquad (c.23)$$

$$U_4(\kappa, \hat{z}) = -e^{-\pi i(1-\kappa^2)} I(\kappa, -\hat{z}) + e^{-3\pi i/2(1-\kappa^2)} I(-\kappa, i\hat{z}) \qquad (c.24)$$

Summing the four soltuions given by C.21 to C.24 gives

$$\sum_{m=1}^{4} U_m(\kappa, \hat{z}) = \left(e^{2\pi i \kappa^2} - 1\right) e^{+i\pi/2(1-\kappa^2)} I(-\kappa, i\hat{z}) \qquad (c.25)$$

This sum is non-zero for $\kappa^2 \neq m$ where m is any integer. In this case, our four solutions are linearly independent. The factor $\left(e^{2\pi i \kappa^2} - 1\right)$ is expected to arise in the case where we evaluate a function on a contour that runs around a branch cut in the complex plane.

Comparing the representation C.21 for U_1 with C.23 for U_3 we see that

$$U_1(\kappa, \hat{z}) = e^{+\pi i (1-\kappa^2)} U_3(\kappa, -\hat{z}) \qquad (c.26)$$

Similar comparison of C.27 with C.24 shows that

$$U_2(\kappa, \hat{z}) = e^{+\pi i (1-\kappa^2)} U_4(\kappa, -\hat{z}) \qquad (c.27)$$

Then from C.26, rearrangement gives

$$U_3(\kappa, \hat{z}) = e^{-\pi i (1-\kappa^2)} U_1(\kappa, -\hat{z}) \qquad (c.28)$$

and from C.27

$$U_4(\kappa, \hat{z}) = e^{-\pi i (1-\kappa^2)} U_2(\kappa, -\hat{z}) \qquad (c.29)$$

The set of relations C.26 to C.29 gives the relation between solutions for $\hat{z} > 0$ and $\hat{z} < 0$, and comprise the set of symmetry relations mentioned in the text.

It may also be shown that (P.H. Roberts, private communication)

$$U_1(\kappa, \hat{z}) = e^{\pi i /_2 (1-\kappa^2)} U_2(-\kappa, i\hat{z}) \qquad (C.30)$$

a result which follows from C.21 and C.22. We also have

$$U_3(\kappa, \hat{z}) = e^{\pi i /_2 (1-\kappa^2)} U_4(-\kappa, i\hat{z}) \qquad (C.31)$$

as seen from C.23 and C.24. The four symmetry relations C.26, C.27, C.30 and C.31 allow the linear independence of the solutions corresponding to the four contours C_n (n=1,...,4) to be established.

Appendix D

Asymptotic Analysis Of $U(\hat{z})$

D.1 Asymptotic Form For The Solutions $U(z)$

Taking equation 3.62 as our starting point, we expand the function

$$\psi(\tau) \equiv \lambda f(\tau) + \lambda^{1/2} \kappa \, g(\tau)$$

as a Taylor series about a saddle point τ_0 giving

$$\psi(\tau) \approx \left(\tfrac{1}{2} \lambda f''(\tau_0) \right) (\tau - \tau_0)^2 + \left(\lambda^{1/2} \kappa \, g'(\tau_0) \right) (\tau - \tau_0) \qquad (D.1)$$

where, since τ_0 is a saddle point; $f'(\tau_0) = 0$. With $g(\tau) \equiv \tau^2$ there is a term

$$\left(\lambda^{1/2} \kappa \, g''(\tau_0) \right) (\tau - \tau_0)^2$$

which we have ignored with respect to

$$\left(\tfrac{\lambda}{2} f''(\tau_0) \right) (\tau - \tau_0)^2$$

which is valid in the limit

$$\frac{\kappa}{\lambda^{1/2}} \ll 1 \qquad (D.2)$$

Hence, in the limit $\lambda \to \infty$, the representation 3.62 becomes

$$U_n \approx \lambda^{(1-\kappa^2)/4} \, \chi(\kappa, \tau_0) \, \exp\left[\lambda f(\tau_0) + \lambda^{1/2} \kappa \, g(\tau_0) \right] \ell_n \qquad (D.3)$$

where

$$\ell_n \equiv \int_{C_n} \exp\left\{ \left(\tfrac{1}{2} \lambda f''(\tau_0) \right) (\tau - \tau_0)^2 + \left(\lambda^{1/2} \kappa \, g'(\tau_0) \right) (\tau - \tau_0) \right\} d\tau$$

$$(D.4)$$

and C_M' is the contour deformed to run through the saddle point τ_0.

Defining the new real variable

$$-\frac{1}{2}\xi^2 \equiv \frac{1}{2} f''(\tau_0) (\tau-\tau_0)^2 \tag{D.5}$$

where $(\tau-\tau_0) \equiv r e^{i\alpha}$ (r real) and α chosen such that

$$f''(\tau_0) e^{2\alpha i}$$

is real and negative, one may write the integral ℓ as (in the limit $\lambda \to \infty$)

$$\ell = \frac{e^{i\alpha}}{|\lambda f''(\tau_0)|^{1/2}} \int_{-\infty}^{\infty} exp\left\{ -\frac{\xi^2}{2} + \frac{\kappa g'(\tau_0)}{|f''(\tau_0)|^{1/2}} \xi \right\} d\xi \tag{D.6}$$

which on completing the square for the integral so it takes the form

$$\int_{-\infty}^{\infty} exp\left(-u^2/2 \right) du = \sqrt{2\pi}$$

gives

$$U_M(\kappa,\vec{z}) = \left(2\pi \Big/ |\lambda f''(\tau_0)| \right)^{1/2} \lambda^{(1-\kappa^2)/4} \chi(\kappa,\tau_0) exp\left[\lambda f(\tau_0) + \lambda^{1/2}\kappa g(\tau_0) \right] \times$$

$$\times \; e^{i\alpha} \; exp\left(\frac{\kappa^2 (g'(\tau_0))^2}{f''(\tau_0)} \right) \tag{D.7}$$

Noting that

$$\left(g'(\tau)\right)^2 = 4\tau^2 \qquad ; \qquad f''(\tau) = -3\tau^2$$

equation D.7 then reduces to the result given in equation 3.65 where the term $\lambda^{\frac{1}{2}} \kappa \ g(\tau_0)$ is negligible with respect to $\lambda f(\tau_0)$ in the limit D.2. The angle $\propto$ is the direction of steepest descent from the saddle point.

D.2 Saddle Points, Critical Points, And Directions Of Steepest Descent

To evaluate the saddle points of the problem, we set

$$f'(\tau_0) = 0 \qquad (D.8)$$

where $f(\tau) \equiv -\tau^4/4 \pm \tau$ and where the + sign is for $\hat{z}>0$ and the $-$ sign for $\hat{z}<0$. Hence the saddle points satisfy

$$\tau_0^3 = \pm 1 \qquad (D.9)$$

so that for $\hat{z}>0$; the three saddle points are at

$$\tau_0 = +1 \qquad ; \qquad e^{\pm 2\pi/3 \ i} \qquad (D.10)$$

and for $\hat{z}<0$; the saddle points are at

$$\tau_0 = -1 \qquad ; \qquad e^{\pm \pi/3 \ i} \qquad (D.11)$$

With these values for τ_0 , $f(\tau_0)$ and $f''(\tau_0)$ are then computed. The angle $\propto$ (double valued) is then computed as mentioned in section D.1. These results are gathered into Table 9.

Table 9. Saddle Points Of $F(\tau)$

|	τ_0	$f(\tau_0)$	$f''(\tau_0)$	α
$z > 0$	$+1$	$3/4$	-3	0 , π
	$e^{+2\pi i/3}$	$-\frac{3}{8} + i\frac{3\sqrt{3}}{8}$	$-3\,e^{+4\pi i/3}$	$-2\pi/3$, $+\pi/3$
	$e^{-2\pi i/3}$	$-\frac{3}{8} - i\frac{3\sqrt{3}}{8}$	$-3\,e^{-4\pi i/3}$	$2\pi/3$, $5\pi/3$
$z < 0$	-1	$3/4$	-3	0 , π
	$e^{+\pi i/3}$	$-\frac{3}{8} - \frac{3\sqrt{3}}{8}i$	$-3\,e^{+2\pi i/3}$	$-\pi/3$, $+2\pi/3$
	$e^{-\pi i/3}$	$-\frac{3}{8} + \frac{3\sqrt{3}}{8}i$	$-3\,e^{-2\pi i/3}$	$+\pi/3$, $+4\pi/3$

The function $\chi(\tau) \equiv \tau^{-k^2}$ has a critical point at $\tau_c = 0$. We must then assess the path of steepest descent from this point as well. Now $f(\tau_c) = 0$ and $f'(\tau_c) = 1$. Consulting Table 7.1 of Bleistein and Handelsman (1975), the steepest path in this case is

$$\hat{z} > 0 : \quad \alpha = \pi$$

$$\hat{z} < 0 : \quad \alpha = 0$$

This reference provides an excellent discussion of the method of steepest descents. We diagram the saddle points γ_0, critical point γ_c, and the directions of steepest descent (arrows) for both $\hat{z}>0$ and $\hat{z}<0$ in Fig. 8. We have placed the branch cut on the positive imaginary axis for convenience so as not to interfere with the saddle points at ± 1.

Fig. 8. Directions Of Steepest Descent

$\hat{z} > 0$

$\hat{z} < 0$
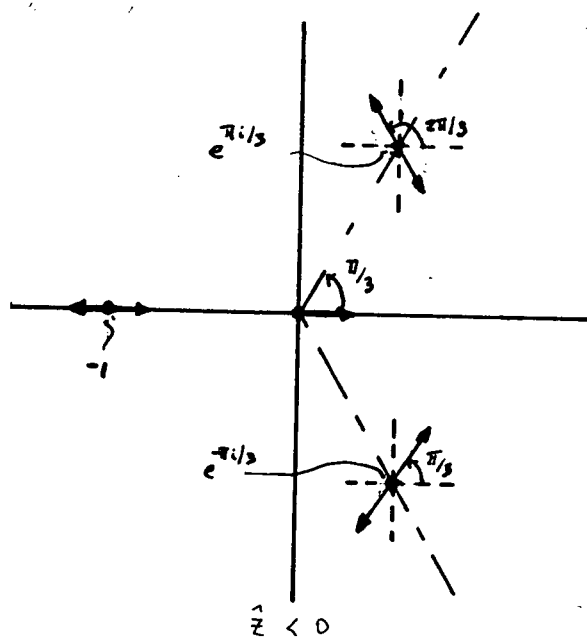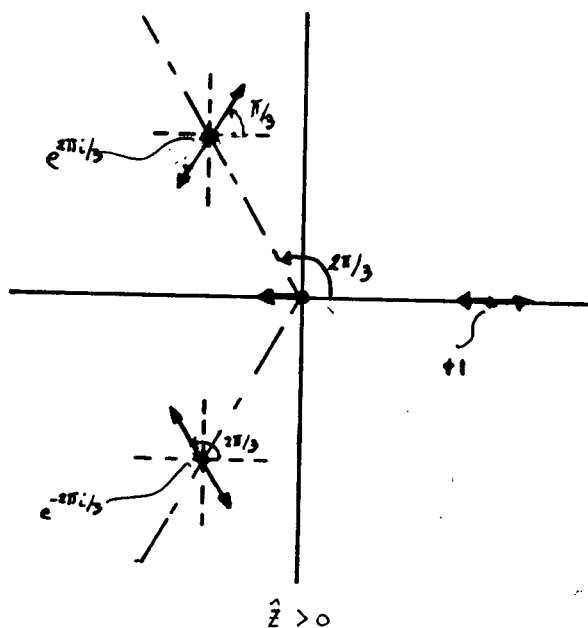
D.3 <u>Paths</u> <u>Of</u> <u>Steepest</u> <u>Descent</u>

If we write

$$\tau = x + iy \; ; \qquad f(\tau) = u(x,y) + iv(x,y) \qquad (D.12)$$

it may be shown (see Bleistein and Handelsman) that curves
of steepest descent and ascent from any point $\tau_0 = x + iy$ are
those curves defined by

$$\text{Im}\left\{ f(\tau) \right\} \equiv v(x,y) = v(x_0, y_0) \qquad (D.13)$$

To pick out the descent paths (two from each saddle point, in
opposite directions), we use the directions computed in Table
9 for each saddle point.

From the definition of $f(\tau)$ and from Table 9, equation
D.13 then gives, for $\tau_0 = \pm 1$ (+ sign for z>0, - sign for z<0);

$$y\left\{ \pm 1 - x(x^2 - y^2) \right\} = 0 \qquad (D.14)$$

for $\tau_0 = e^{\pm 2\pi i/3}$ (both for z>0):

$$y\left\{ +1 - x(x^2 - y^2) \right\} = \pm 3\sqrt{3}/8 \qquad (D.15)$$

and for $\tau_0 = \pm e^{\pi i/3}$ (both for z<0):

$$y\left\{ -1 - x(x^2 - y^2) \right\} = \mp 3\sqrt{3}/8 \qquad (D.16)$$

It is not necessary to have a detailed knowledge of y(x)
at every point, however the general properties of the paths of
steepest descent are required for the analysis in section D.4

From equation D.14 it follows that y satisfies either of

(a) $\quad y = 0 \qquad$ (b) $\quad y^2 = x^2 \mp \frac{1}{x} \qquad$ (D.17)

Now from the results of Table 9, we know that the directions $\alpha = 0, \pi$ correspond to steepest descent paths from these saddle points. Hence, the curve y=0 corresponds to the steepest descent paths from these saddle points. The curve $y^2 = x^2 \mp \frac{1}{x}$ then corresponds to steepest ascent paths from these points. In the limit $x \to \infty$; y=±x so that these are the asymptotes for the ascent paths. In addition, for $\tau_0 = +1$, x⩾1 and $\tau_0 = -1$, x⩽-1.

Writing equation D.15 in the form

$$\left(x y^2 + 1 - x^3 \right) \mp \frac{3\sqrt{3}}{8} y^{-1} = 0 \qquad (D.18)$$

we see that in the limit x→0, D.18 may be satisfied by

$$y \approx (-x)^{-1/2} \quad ; \quad x < 0$$

Rearranging equation D.14 in the form

$$y^3 + \left(\frac{1}{x} - x^2 \right) y \mp \frac{3\sqrt{3}}{8} x^{-1} = 0 \qquad (D.19)$$

shows that in the limit $x \to -\infty$; again

$$y = 0 \quad ; \quad y^2 = x^2$$

Now the directions y=±x are out of the zones of convergence

for our integral representations, so that the limit y=0 for x → ∞ must be the behaviour of the steepest descent curve.

This same kind of reasoning may be applied to equation D.16 where the restriction x>0 must be made for solutions to exist.

The results of this analysis are illustrated in Fig. 9 for the case z>0 and z<0. The descent paths are labelled D_m in solid line and ascent paths in dotted lines.

Fig. 9. Paths Of Steepest Descent

$z \geq 0$

$z < 0$
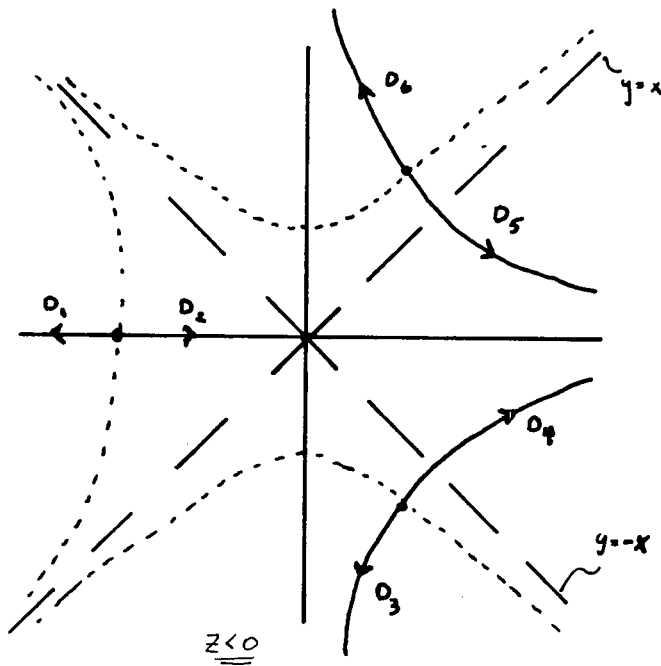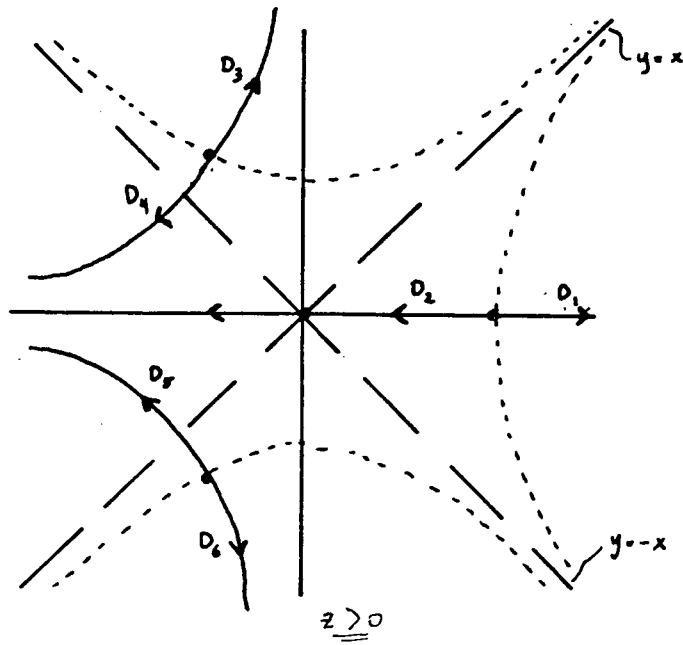
D.4 Final Results For Asymptotic Expansion Of The Solutions $U_n(\kappa,\hat{z})$

In this section, the asymptotic form for each solution $U_n(\kappa,\hat{z})$ is determined by deforming the contour C_n onto one or more paths of steepest descent, and assessing the contribution from each of the saddle points or critical points that are picked up. Only the dominant contributions will be kept. We shall do the analysis for $z > 0$ since similar considerations apply for the $z < 0$ case.

(1) $U_4(\kappa,\hat{z})$

The contour C_4 is deformable into the contour (see Figures 9(a) and 6)

$$C_4 = D_3 - D_4 \qquad (D.20)$$

Hence, only the contribution from the saddle point at $\tau_0 = e^{+2\pi i/3}$ is picked up. Using formula 3.65 we then have

$$U_4(\kappa,\hat{z}) \approx \sqrt{\tfrac{2\pi}{3}} \; e^{-2\pi\kappa^2 i/3} \; e^{-\tfrac{4}{3}\kappa^2} \; \frac{1}{\lambda^{(1+\kappa^2)/4}} \; exp\left(\lambda\left[-\tfrac{3}{8}+i\tfrac{3\sqrt{3}}{8}\right]\right) \times$$

$$\times \left\{ -e^{-2\pi i/3} + e^{\pi i/3} \right\} \qquad (D.21)$$

$$= -2\sqrt{\tfrac{2\pi}{3}} \; e^{-\tfrac{2\pi}{3}(\kappa^2+1)i} \; e^{-\tfrac{4}{3}\kappa^2} \; exp\left(\lambda\left[-\tfrac{3}{8}+i\tfrac{3\sqrt{3}}{8}\right]\right) \Big/ \lambda^{(1+\kappa^2)/4}$$

(2) $U_3(\kappa,\hat{z})$

The contour C_3 may be deformed onto

$$C_3 = D_5 - D_6$$

so that the saddle point at $T_0 = e^{-2\pi i/3}$ is picked up. We then have

$$U_3(\kappa, \hat{z}) \approx \sqrt{\frac{2\pi}{3}} \; e^{+2\pi i \kappa^2/3} \; e^{-\frac{4}{3}\kappa^2} \; \exp\left(\lambda\left[-\frac{3}{8} - i\frac{3\sqrt{3}}{8}\right]\right) \; \frac{1}{\lambda^{(1+\kappa^2)/4}} \; \times$$

$$\times \; \left\{ e^{2\pi i/3} - e^{5\pi i/3} \right\}$$

$$= 2\sqrt{\frac{2\pi}{3}} \; e^{\frac{2\pi}{3}(\kappa^2+1)i} \; e^{-\frac{4}{3}\kappa^2} \; \exp\left(\lambda\left[-\frac{3}{8} - i\frac{3\sqrt{3}}{8}\right]\right) \Big/ \lambda^{(1+\kappa^2)/4}$$

$$\text{(D.23)}$$

(3) $\underline{U}_2(\kappa, \hat{z})$

The contour C_2 is deformable onto

$$C_2 = -D_1 + D_2 - D_5 + D_6 \qquad\qquad \text{(D.24)}$$

so that contributions from the saddle point at $T_0 = +1$, the critical point $T_c = 0$, and the saddle point $T_0 = e^{-2\pi i/3}$ are picked up. However, the saddle point at $T_0 = +1$ contributes the factor $e^{\frac{3}{4}\lambda}$ which is exponentially growing, whereas the $T_c = 0$ has no exponential factor and $T_0 = e^{-2\pi i/3}$ contributes an exponentially damped factor $e^{-\frac{3}{8}\lambda}$. Hence, to very good accuracy the contribution from $T_0 = +1$ is the only factor we need consider and we have

$$U_2(\kappa, \hat{z}) \approx -2\sqrt{\frac{2\pi}{3}} \; e^{-\frac{4}{3}\kappa^2} \; \exp\left(\frac{3}{4}\lambda\right) \Big/ \lambda^{(1+\kappa^2)/4} \qquad \text{(D.25)}$$

(4) $\underline{U}_1(\kappa, \hat{z})$

Here we note that the contour C_1 lies entirely to the

right of our branch cut whereas the contour $D_1 - D_2 - D_3 + D_4$ runs to the left of the branch cut. The dominant contribution is still from $T_0 = +1$ for the same reasons as discussed for U_2. Hence we find

$$U_1(\kappa, \hat{z}) = +2\sqrt{\frac{2\pi}{3}} \ e^{-\frac{4}{3}\kappa^2} \ \exp\left(\frac{3}{4}\lambda\right) \Big/ \lambda^{(1+\kappa^2)/4} \qquad (D.26)$$

These results are summarized in Chapter 3 by equations 3.66 and 3.67 and Table 4.

Appendix E

Expansions Of $U_m(\kappa, \hat{z})$ About $z=0$

Taking the function $U_1(\kappa, \hat{z})$ as an example we had U_1 as $(z>0)$

$$U_1(\kappa, \hat{z}) = I(\kappa, \hat{z}) - e^{i\frac{\pi}{2}(1-\kappa^2)} I(-\kappa, i\hat{z})$$

from equation C.21 where the integral $I(\kappa, \hat{z})$ was given by C.20. Expanding I as a power series in $\hat{z}$ about $\hat{z}=0$ we have

$$I(\kappa, \hat{z}) = \sum_{m=1}^{\infty} \frac{\hat{z}^m}{m!} a_m(\kappa) \qquad (E.1)$$

where

$$a_m(\kappa) \equiv \int_0^\infty t^m \frac{\exp(-t^4/4 + \kappa t^2)}{t^{\kappa^2}} dt \qquad (E.2)$$

Changing variables in E.2 to $\tau = t^2$, defining $\nu_m = (m+1-\kappa^2)/2$ one gets

$$a_m(\kappa) = \frac{1}{2} \int_0^\infty \tau^{\nu_m - 1} \exp(-\tau^2/4 + \kappa\tau) d\tau \qquad (E.3)$$

Using the identity 3.76 given in Chapter 3, $a_m(\kappa)$ then becomes

$$a_m(\kappa) = \frac{(2)^{\nu_m/2}}{2} \Gamma(\nu_m) \exp(\frac{\kappa^2}{2}) D_{-\nu_m}(\sqrt{2}\,\kappa) \qquad (E.4)$$

where D_{ν_m} is the parabolic cylinder function.

Doing the same expansion for $I(-\kappa, i\hat{z})$ and substituting everything back into the expression for $U_1(\kappa, z)$ we find

$$U_1(\kappa, \hat{z}) = \frac{\exp(\kappa^2/2)}{2} \sum_{m=0}^{\infty} (2)^{\nu_m/2} \frac{\Gamma(\nu_m)}{m!} \left[D_{-\nu_m}(\sqrt{2}\,\kappa) - e^{i\pi\nu_m} D_{-\nu_m}(-\sqrt{2}\,\kappa) \right] \hat{z}^m$$

$$(E.5)$$

The coefficents in the expansion E.5 may be simplified using the identity

$$D_\nu(x) - e^{-\nu\pi i} D_\nu(-x) = \frac{\sqrt{2\pi}}{\Gamma(-\nu)} e^{-i(\nu+1)\pi/2} D_{-\nu-1}(ix) \qquad (E.6)$$

which may be found in Gradshteyn and Ryzhik (1965), p.1066, formula 9.248.2. Using formula E.6, the the expansion E.5 becomes ($\hat{z} > 0$)

$$U_1(\kappa, \hat{z}) = \sqrt{\frac{\pi}{2}} \exp(\kappa^2/2)\, e^{-\pi i/2} \sum_{m=0}^{\infty} (2)^{\nu_m/2} \frac{e^{i\nu_m\pi/2}}{m!} D_{\nu_m-1}(i\sqrt{2}\,\kappa)\, \hat{z}^m$$

$$(E.7)$$

Similar expansions are arrived at by starting with formulas C.22, C.23 and C.24 for U_2, U_3, and U_4 respectively.

Derivatives of E.7 are easily found, as well as the limit $\hat{z} \to 0^+$. As an example

$$U_1(\kappa, 0^+) = \sqrt{\frac{\pi}{2}} \exp(\kappa^2/2)\, e^{-i\pi/2}\, 2^{\nu_0/2}\, e^{i\nu_0\pi/2} D_{\nu_0-1}(i\sqrt{2}\,\kappa) \qquad (E.8)$$

which is shown by equation 3.78.

The expansions for $z<0$ are found by using the results above (for $\hat{z}>0$) and applying the symmetry relations C.26 – C.29 in order to get the $\hat{z}<0$ expansions.